Winter 1-31-1994

Machining of silicon wafers with an abrasive water jet cutter

Frank J. Marciniak
New Jersey Institute of Technology

ABSTRACT

Machining of Silicon Wafers with an Abrasive Water Jet Cutter

by
Frank J. Marciniak

This thesis consists of a study of the effects of abrasive water jet cutting on brittle silicon substrates. In total, 26 different cuts were made in a single crystal silicon substrate with an abrasive water jet cutter under different conditions of water flow, water pressure, and abrasive flow rate. These cuts were analyzed for surface roughness, and microstructure.

The roughness measurements were compared in order to determine the best possible cutting conditions. The cut with the best roughness of 0.000170 inches was obtained under cutting conditions of 30 KSI water pressure, 1 inch/minute cutting speed, and an abrasive flow rate of 56 grams/minute.

Other trends in the data show the optimum cutting speed to be between 1 and 2 inches/ minute. The water pressure of 30 KSI achieved better results than the 50 KSI presures under similar cutting conditions . At both 50KSI and 30 KSI, low abrasive flow rates result in better roughness values.

MACHINING OF SILICON WAFERS WITH AN ABRASIVE WATER JET CUTTER

by
FRANK J. MARCINIAK

A Thesis
Submitted to the Faculty of
New Jersey Institute of Technology
in Partial Fulfillment of the Requirements for the Degree of
Master of Science in Manufacturing Systems Engineering

Manufacturing Engineering Division

January 1994

APPROVAL PAGE

Machining of Silicon Wafers
With an Abrasive Water Jet Cutter

FRANK J. MARCINIAK

Dr. E. S. Geskin, Thesis Advisor — Date
Professor of Mechanical Engineering, NJIT

Dr. N. M. Ravindra, Committee Member — Date
Associate Professor of Microelectronics
Department of Physics, NJIT

Dr. Raj. S. Sodhi, Committee Member — Date
Associate Professor of Mechanical Engineering
and Director of Manufacturing Engineering Programs, NJIT

BIOGRAPHICAL SKETCH

Author: Frank J. Marciniak

Degree: Master of Science
in Manufacturing Systems Engineering

Date: January, 1994

Undergraduate and Graduate Education

- Master of Science in Manufacturing Systems Engineering,
  New Jersey Institute of Technology,
  Newark, NJ, 1994

- Bachelor of Science in Ceramic Engineering,
  Rutgers University,
  College of Engineering,
  New Brunswick, New Jersey, 1989

Major: Manufacturing Systems Engineering

ACKNOWLEDGMENT

I wish to express my deepest gratitude to Dr. Ernest Geskin, Professor, Mechanical Engineering Department of New Jersey Institute of Technology for his valuable guidance throughout this investigation. I would also like to thank Dr. N.M. Ravindra, Associate Professor, Physics Department of New Jersey Institute of Technology, for his continuous supervision and support during my work.

I would also like to thank Leon Tourietzky for his help and tutoring in the operation of the laboratory equipment.

TABLE OF CONTENTS

TABLE OF CONTENTS
(CONTINUED)

LIST OF TABLES

LIST OF TABLES
(CONTINUED)

TABLE PAGE

LIST OF FIGURES

LIST OF FIGURES
(CONTINUED)

CHAPTER 1

INTRODUCTION

There are two different reasons for studying the effects of machining on ceramic materials. They are scientific and economical. The scientific aspect is a search for knowledge and understanding of the materials being studied. The economical aspect is an effort to improve the process of machining and cutting in order to realize lower costs, higher quality, and improved productivity. These goals can be accomplished through knowledge of the machining and finishing processes, the resultant characteristics of the surface, and the effect on the properties of the materials.

The three major types of solid materials are metals, organics, and ceramics. A lack of understanding of any one of these areas leaves a major gap in the scientific understanding of materials. The study of ceramic materials in terms of structure, defects, and properties is a unique challenge. Machining of ceramic materials is important to many engineers whose areas of specialization may be far from this area because of its importance in determining the character of the surface of ceramic materials and the important resulting properties such as mechanical and electrical. These properties are very important in the processing of electronic materials due to the continuous miniaturization of electronics.

The economic motivation takes into account two important factors. The first is the effect of machining practices on the cost of components. Machining costs tend to be a large part of the cost of ceramic components. Therefore, improved ceramic machining can play a significant role in cost reduction.

The second factor is the increasing demands of technology. Better performance is demanded of most ceramic bodies, especially in the electronics area. This is true both from a mechanical and an electrical standpoint. Many applications for ceramics put a higher demand on the materials than they have in the past. They require materials with higher strengths or more resistance to wear. In the electronics applications, they require good electrical properties with very tight tolerances.

Because the economic and scientific motivations are interdependent, the economic gains that can be accomplished from advanced machining techniques will only come from scientific advances. The ability to machine ceramics is in itself a challenge. There are many different machining methods available for these brittle materials. They range from traditional machining with a cutting tool and grinders and polishers to nontraditional methods such as abrasive water jet cutting to laser cutting.

The interaction between a cutting method and the workpiece is a very complex phenomenon. Each method has certain characteristics that differentiate them from the other methods. These characteristics also affect the final outcome of the workpiece cuts. The same types of cutting methods have been applied to other non-ceramic materials such as metals and polymers. Ceramics, however, present additional challenges that are not present in these other materials. One challenge is the general absence of macro-scopic ductility to prevent fracture in the materials(1). There is also a much broader range of structure and bonding and related intrinsic properties such as hardness, conductivity, and elastic modulus. Also, there is a broader range of microstructures. Additionally, ceramic bodies have been produced with finer grain sizes than are commonly used in most metals. They can even be made of single crystals such as in the case of single crystal silicon used in the manufacture of electronic substrates.

Because of these differences, and a lower quantity of research being performed on these materials over the years, less is known about ceramics. Many fewer important details are known about ceramics than about metals.

The rewards that can be gained from studying ceramic machining are the scientific understanding of materials, and the economic gains of more easily produced, and more reliable components. It is hopeful that an understanding of the process of removal and the character of the resulting surface can be attained. Understanding this can increase our knowledge of the surface dependent properties and provide us with the ability to improve upon these properties. These advances could lead to the development of new machining methods, and possibly new machining tools, designed specifically for ceramics. But, in all likelihood, they will result in either new, or at least broader, applications of ceramics.

The use of non-traditional machining could contribute to better machining techniques and increased productivity. There should also be a greater choice between traditional mechanical machining and non traditional methods than there currently is.

The purpose of using non traditional machining methods is to obtain a final ceramic body that has specific, highly accurate dimensions, with desirable surface qualities, thereby eliminating undesirable surface characteristics. The requirements needed to create a mirror finish on a silicon substrate are very demanding. Machining to these tight tolerances with a high degree of repeatability is a very difficult task.

CHAPTER 2

NON-TRADITIONAL MACHINING METHODS

There are many methods of non-traditional machining that have come of age recently. Because of the more complex shapes and cutting requirements, new machining methods had to be developed. The creation of new materials has also urged these developments. Materials such as ceramics, composites, and some metals can be difficult to machine due to their high hardness, brittleness, poor thermal properties, chemical reactivity with the cutting tool, or inhomogeneous microstructures. In some cases, the only way to effectively machine such materials is with non traditional methods.

Generally, non-traditional methods are considered to be manufacturing processes adopted in the last 50 years that use common energy forms in new ways or that apply forms of energy never used before. Non-traditional processes are subdivided according to the form of energy that is being used: mechanical, electrical, thermal and chemical. They are summed up in table 2-1.

Mechanical methods of non-traditional processes harness direct mechanical abrasive action to remove material. Mechanical processes are usually used in materials that are difficult to machine with traditional techniques because of hardness, toughness or brittleness. Ceramics, composites, and organics tend to be good materials for mechanical machining because they are not electrically conductive, and because they may be damaged when thermal processes are applied.

Electrical methods of non-traditional processes are limited to electrically conductive materials in their application. These methods can be used to cut difficult to machine materials, as well as other materials that require complex shapes. Complex shapes can be produced with a single pass of the tool.

TABLE 2-1 NON-TRADITIONAL MACHINING METHODS (2)

MECHANICAL	ABRASIVE JET MACHINING (AJM)
	ABRASIVE FLOW MACHINING (AFM)
	WATER JET MACHINING (WJM)
	ABRASIVE WATER JET MACHINING (AWJM)
	ULTRASONIC MACHINING (USM)
ELECTRICAL	ELECTROCHEMICAL MACHINING (ECM)
	ELECTROCHEMICAL GRINDING (ECG)
	ELECTROCHEMICAL DISCHARGE GRINDING (ECDG)
	ELECTROSTREAM DRILLING (ESD)
	CAPILLARY DRILLING (CD)
	SHAPED TUBE ELECTROLYTE MACHINING (STEM)
THERMAL	ELECTRICAL DISCHARGE MACHINING (EDM)
	ELECTRICAL DISCHARGE WIRE MACHINING (EDWM)
	ELECTRICAL DISCHARGE GRINDING (EDG)
	ELECTRON BEAM MACHINING (EBM)
	LASER BEAM MACHINING (LBM)
	THERMAL ENERGY METHOD (TEM)
CHEMICAL	CHEMICAL MILLING (CM)
	PHOTOCHEMICAL MACHINING (PCM)

2.1 Mechanical Non-Traditional Machining Methods

Thermal methods of non-traditional machining processes use heat energy to remove material. These processes are usually unaffected by the materials physical properties and are often applied to extremely hard workpiece materials. Because of the thermal process, materials that are used for critical applications may require the removal of the heat affected zone.

Chemical methods of machining use chemical reactions to remove material. Because material is removed by chemical reaction, there are no forces acting on the workpiece (3). This allows parts to be machined without concern for distortion or damage. Also, because the machining takes place on all areas of the workpiece, it can be highly efficient and fast.

Abrasive Jet Machining is a process that removes material from a workpiece through the use of abrasive particles entrained in a high velocity gas stream. It is similar to sandblasting, except that it uses smaller sized abrasives (10-50 micron) and a more finely controlled delivery system. Abrasive Jet Machining is used to cut, clean, peen, deburr, deflash, or etch glass, ceramics, or hard metals (4).

Abrasive Flow Machining finishes surfaces and edges by extruding viscous abrasive media through or across the workpiece. Abrasion occurs only where the flow of the media occurs, with other areas remaining unaffected. This method can be used to process many inaccessible passages on a workpiece simultaneously. It is used to deburr and polish surfaces and edges in a variety of materials from aerospace components to medical components (5).

Water Jet Machining uses a high velocity water stream as a cutting tool. This is limited to softer, less brittle materials. Abrasive water jet machining uses fine abrasive solids in the water jet stream to cut harder, denser materials such as glass, and ceramics (6).

Ultrasonic Machining utilizes the vibration of a tool at approximately 20 kHz to machine hard, brittle materials. It consists of two methods: ultrasonic impact grinding, and rotary ultrasonic machining. In ultrasonic impact grinding, an abrasive slurry flows through the gap between the workpiece and the vibrating tool. As the tool moves on the downstroke with the vibration, the particles are accelerated. The impact of the particles on the material cause chipping and erosion of the workpiece. In rotary ultrasonic machining, a rotating core drill is vibrated at 20 kHz. A liquid coolant is forced through the bore of the tube to cool and flush away the removed material (7).

2.2 Electrical Non-Traditional Machining Methods

Electrochemical Machining is the controlled removal of material through anodic dissolution in an electrolytic cell where the workpiece is the anode, and the tool is the cathode. The electrolyte is pumped through the gap between the tool and the workpiece, while direct current is passed through the cell at low voltage. This dissolves the material from the surface of the workpiece (8).

Electrochemical grinding is similar to electrochemical machining except that it uses a grinding wheel in place of the contouring tool. It is used to machine difficult to machine materials (9).

Electrochemical Discharge Grinding uses a positively charged workpiece, a highly conductive electrolyte, and alternating or pulsed direct current (10). The intermittent spark discharges remove the material from the workpiece surface.

Electrostream and capillary drilling are electrochemical machining processes that are used to cut holes that are too deep to be cut by electrical discharge machining and too narrow to be drilled by shaped tube electrolytic machining (11)

Shaped Tube Electrolytic Machining is a modified electrochemical machining process that is used to drill holes with a large depth to diameter ratio. It uses an acid electrolyte to dissolve the removed material so that it does not clog the hole. It is limited in usage to corrosion resistant materials (12).

2.3 Thermal Non-Traditional Machining Methods

Electrical Discharge Machining is a process that removes material with sparks (13). A shaped electrode is used to make a cavity that is the mirror image of the electrode. In this method, DC electrical power is supplied to the circuit in pulses to create the sparks. The sparks travel through the dielectric fluid at a controlled distance (14). With each spark, material is removed by vaporization and melting. This method is useful for machining conductive materials that have complex shapes (15).

Electric Discharge Wire Machining is similar to Electric Discharge Machining except that it uses a travelling wire to cut the workpiece (16).

Electric Discharge Grinding is similar to electric discharge machining except that the electrode is a rotating graphite wheel and the workpiece moves on a servo-controlled worktable (17).

Electron Beam Machining uses a high velocity beam of electrons to strike an object and cause rapid melting and vaporization of the material, leaving a hole in the workpiece (18).

Laser Beam machining uses an intensely focussed monochromatic light to remove, melt, or thermally modify a material (19). Laser beam machining provides rapid material removal with an easily controlled, non contact, non wearing tool. It can be used for drilling, welding, marking, and heat treating of a variety of materials. The effectiveness of laser beam machining depends upon the reflectivity, absorption, thermal conductivity, specific heat, and heat of vaporization of the material (20). A variety of lasers from

CO_2 to YAG lasers that employ different wavelengths of light and energy intensities can be used depending upon the application and type of material being worked on (21).

Thermal Energy Method is used for deburring of parts by the use of intense heat. It is fast and removes all burrs on a workpiece simultaneously (22).

2.4 Chemical Non-Traditional Machining Methods

Chemical Milling is a form of controlled chemical etching. The process removes material from the whole part, or specific areas of the part if masks are used. It works by applying a chemically resistant mask to the workpiece. The mask is scribed and removed in the areas that are to be etched. An etchant is then used to remove material through a chemical reaction with the material. It can be used to create very intricate and close tolerance patterns on the surface of the workpiece (23).

Photochemical Milling is an etching process that uses a photoresist to define the locations where etching will take place. It is used to provide intricate, close tolerance patterns on a variety of flat materials (24)

2.5 The Future of Non-Traditional Machining Methods

Non-traditional machining methods are slowly gaining in popularity. These methods are ensured to play an increasingly important role because of their steadily increasing capabilities, as well as their benefits of being computer controlled processes. Most non-traditional methods are computer controlled. This insures process reliability and repeatability. They can also be adaptively controlled by the use of many types of in-process sensors. This allows the process to be changed while running without changing the hard tools by changing the process parameters in the computer. The ability to detect and correct these situations automatically insures the increasing use of non-traditional processes in unattended machining cells and automated factories.

2.6 Abrasive Waterjet Process Description

This study is expected to give some insight into the effects of abrasive water jet machining on silicon substrates. Water jet machining is a non-traditional cutting technique that employs a high velocity water stream that is entrained on its target by use of a nozzle that focuses the water stream to cut the target material.

An abrasive water jet incorporates fine solid abrasive particles into the water jet stream. These particles act as cutting agents. This is extremely effective in the cutting of hard, brittle materials that otherwise would shatter under the stress of a simple water jet stream that contained no abrasives.

In abrasive water jet machining, the solid particles absorb the kinetic energy from the water jet stream. When these particles impinge upon the sample, the energy is transferred from the particles to the surface of the sample.

This creates many small fractures in the sample surface. When these fractures cross, material is loosened and thereby removed from the surface.

2.7 Advantages of Abrasive Waterjet Cutting

There are some disadvantages to using some of the conventional cutting methods or even the non traditional cutting methods. Some of these techniques produce dust particles, heat affected zones in the material, or put high mechanical stresses on the material that can cause warpage.

Water jet cutting can be an affective tool in eliminating these problems as well as in providing some additional advantages over other cutting methods.

Water jet machines are capable of cutting a variety of materials without a major change in system components.

Water jet cutting can be used to cut a wide range of materials without requiring a substantial change in system components. In most cases, the only changes that need to be done are a change in nozzle size, cutting speed, or water pressure (25).

Because it is computer controlled, it is easily integrated with automated systems.

Water jet cutting cuts without heat, which prevents thermal distortion and structural changes in the target material.

Work hardening of materials is eliminated.

Tooling costs are reduced because of the minimal force that is imparted to the workpiece by the unit.

Airborne dust is eliminated, creating better working conditions.

The unit is computer controlled, making it easy to program cutting sequences and store them for future use.

Water jet cutters have omnidirectional cutting capabilities with the ability to do circular cuts, drill, and change directions during cutting.

2.8 Waterjet Cutting Theory

Water jet cutting consists of accelerating water in a circular nozzle up to a velocity of 750 m/s and focussing the jet stream on a target. It is an energy conversion process in which the water pressure is converted into kinetic energy by accelerating the water in a focussing nozzle. The fluid velocity is related to water pressure by the Bernoulli equation for incompressible fluid flow:

$$v=SQRT(2p/s)$$ where p=pressure in psi

s=average fluid density.

Based on the Bernoulli equation for incompressible fluid flow, the volumetric flow rate of the water is related to the diameter of the orifice size by the equation

$$Q=(pi/4)*D^2*Cd*V$$

where Q=flow of water (gpm)

D=Diameter of sapphire nozzle (inch)

V=velocity of fluid (fps)

This can get very complex with abrasive jet cutting.

There are three different velocities and flow rates that can be determined. They are for the abrasive, the fluid, and the air that is sucked into the stream as it exits the nozzle (26).

The flow rate and the pressure of the water jet have different effects on cutting. The flow rate affects the rate of material removal. The pressure determines the kinetic energy of the jet stream molecules, and therefore its ability to cut the target material. Higher strength materials have higher molecular bonding forces. Therefore, higher strength materials require higher kinetic energy (higher pressure) jet streams in order to be cut effectively.

As the jet hits the surface of the workpiece, the velocity of the stream drops. This creates a high pressure zone on the surface of the workpiece. If this pressure is sufficient, the material in the impingement zone will move, and the jet will penetrate into the workpiece.

If the stresses created in the impingement zone are less than the deformation threshold, cutting will not take place.

In abrasive jet cutting, solid abrasive particles are added to the jet stream through a carbide mixing tube. The abrasives are sucked into the jet stream by the vacuum created by the high velocity stream. This creates a high velocity water-particles stream. This stream reaches the sample surface at high velocity. When the particle collide with the sample surface, they are decelerated. This results in a high pressure zone that is much higher than that of a conventional waterjet stream by itself. This creates stresses on the material that exceed the strength of the material. When this strength is exceeded, small particles are removed from the workpiece surface. The effects on the material are limited to the small areas where the individual particles strike the surface (27).

The cutting of materials depends upon the ductility of the materials being cut. In ductile materials, erosion takes place through the penetration of the solid particles through the material. As the particles penetrate, they move the material that is in their path. In brittle materials, the impact of a particle on the surface results in microcracking of the surface. This microcracking takes place in the form of radial and lateral cracking. The lateral cracking (cracking parallel to the material surface) causes the material to be loosened and eventually removed from the surface (28).

The surface topography of the material is affected by the individual particles that strike the surface as well as the integrity of the stream as a whole (29). The individual particles control the micro topography of the surface, while the state of the water flow controls the macro topography.

2.9 Waterjet System Theory

Abrasive Water Jet Cutting has many system variables that can affect the cutting performance of the unit. These variables can be broken down into several categories. They are hydraulic parameters, nozzle parameters, abrasive parameters, cutting parameters, and workpiece parameters.

The hydraulic parameters affect the kinetic energy of the fluid as it passes the through the nozzle assembly. These are fluid pressure, hydraulic power, and type of fluid (30).

The nozzle parameters affect the energy conversion and abrasive mixing process. They are nozzle diameter, carbide tube diameter, length of carbide tube, and angle of convergence.

The abrasive parameters are type of abrasive, size of abrasive, shape of abrasive, and abrasive feed rate.

The cutting parameters are distance form nozzle to workpiece, traverse speed, and angle of cutting.

The quality of cut is also affected by the type of material that is being worked on. The workpiece parameters are material hardness and brittleness.

The results of the cutting process can be looked at in several different ways for some important output characteristics. They are depth of cut, surface roughness, kerf width, surface flaws, and subsurface microcracking (31)

CHAPTER 3

SUBSTRATE MATERIALS

Electronic ceramics play an important role in the microelectronics industry. They act as both substrate material as well as material for the circuits themselves.

In terms of substrates, materials play a key role in the reliability and operation of microelectronic circuits. They provide a means of physical support for the assembly of the devices. They provide a base for the electrical connection patterns and film resistors. They provide a mechanism for conducting thermal energy away from the circuit. Substrates must have the proper mix of mechanical, electrical, chemical and thermal properties in order to be able to provide a good basis for reliable microelectronics (32).

Some of these properties are the following. Substrates must have high electrical resistivity in order to prevent the conduction of electricity between closely spaced circuit lines. Volume resistivities should be greater than 10^{14} ohm-cm. Surface insulation resistance should be greater then 10^{9} ohms. The materials should have low porosity and high purity. This is to avoid moisture buildup, contamination, electron arcing, and atomic migration. Substrate materials must have good thermal conductivity in order to dissipate heat generated by the circuits. They must have thermal expansion coefficients that match the attached devices in order to minimize stress and fracture of the components during operation of the device. They must be able to withstand the high temperatures involved in processing of the thin films (800-1000 degrees C). They must be able to withstand chemical etchants that are used in the processing of the thin film materials. They must also have very smooth surfaces in order to obtain the precision and stability that is necessary in very small thin films (33).

Silicon is a good material for electronic substrates. Like other group IV insulators and semiconductors, it crystallizes in the diamond cubic lattice structure. Each silicon atom has four bonds, one to each of its four nearest neighbors (34).

Crystals are made up of regular repeating orders of atoms. The planes of the crystal structure are defined by their Miller Indices. These indices, h,k,l are the reciprocals of the intercepts of the planes with the x, y, and z axes. A plane is denoted by the symbol (hkl). A family of planes can be denoted by a bracketed symbol {hkl}. The Indices are the smallest integers having the same ratio. These indices can also be used to define direction. In cubic crystals, the direction perpendicular to a given plane has the same miller indices as the plane, denoted by a bracketed symbol [hkl]. A family of directions is denoted by <hkl>. For example, the x axis is the [100] direction, and the three coordinate axes are the <100> directions. The body directions are the <111> directions.

The atoms in a single silicon crystal are stacked in a regular, repeating order. In the [111] direction, there is a regular repeating order of atomic planes (35). Any disturbance in this repeating order is considered to be a defect.

Defects can take two different forms. They can be point defects, or extended defects. Point defects are imperfections that occur at a lattice point and do not distort the crystal over a long distance. Extended defects that have a larger effect on the crystal, usually repeating itself over many spacings or affecting the stacking order of the crystal. Vacancies and atomic impurities are examples of point defects. Vacancies can occur when an atom is located in the wrong position, or is not present at all. Impurities can take the place of silicon atoms in the structure or can occupy interstitial sites in the structure.

Some important impurities in Silicon crystals are oxygen, carbon, and hydrogen. Oxygen affects the mechanical properties (strength) of the crystal. Carbon does not adversely affect silicon crystals, but it may play a role in oxygen interactions in the crystals. Hydrogen is a very rapid diffuser into a silicon crystal (36). Any impurities or defects at the surface of the crystal can affect the quality of the film that will eventually be formed on it.

The extended defects are dislocations and slip, and stacking faults. Dislocation and slip occur when the stresses in the structure cause a part of the crystal to deform and slip across another part. These dislocations may move through the crystal along the direction of the shearing force.

Stacking faults occur either in layer growth, or by oxidation. If Silicon dioxide is present, it takes up more space than silicon atoms in the structure. This causes an excess of Silicon interstices. If enough stress is created, stacking faults form.

Plastic deformation of silicon wafers usually occurs at high temperatures during device fabrication. It can also occur at low temperatures during microhardness measurements, scribing or other machining methods.

Plastic deformation occurs by slip between {111} planes in a <110> direction. With this mechanism, slip can be propagated from small surface damage deeply into the wafer during high temperature processing. Plastic flow due to excessive stress from thermal shock can occur at low temperatures.

Fracture can occur in silicon crystals. Because of its brittle nature, fracture is more common in single crystal silicon than plastic deformation at low temperatures. the easiest direction for fracture is along the <111> directions, or in {100} planes, along <110> directions (37).

Integrated circuits, and discrete solid state devices are manufactured on single crystal silicon wafers. In order to obtain high reliability and good performance from the final product, it is important that the starting wafers be of reproducible high quality. This is to ensure that the small high resolution patterns that are formed on the wafer surface are uniform. The front surface must be smooth and flat. The electrical and chemical properties of the wafer must be tightly controlled. The preparation of the starting silicon wafer is important in achieving a high quality electronic device (38).

Traditional wafer preparation starts with the cutting of large single crystal silicon ingots into thin wafers. The final wafer must have at least one side that is clean, flat and defect free (39).

Typical wafer preparation encompasses the following steps. First, the crystal must be cropped to remove the seed and tong ends of crystal as well as any out of specification portions. The crystal is then ground down to reduce the diameter to the specified tolerance with a diamond grinding wheel. Flat areas are ground lengthwise along the crystal to serve as identification of the wafer type and axis orientation. The crystal is etched to remove any defects that were created in the grinding operation. Thin wafers are then cut from the ingot using a diamond blade. The cut wafers are heat treated to eliminate oxygen donors, normalizing resistivity. The edges are ground with a diamond wheel to remove the square corners created in diamond cutting. Grinding or lapping of the surface is done to smooth out the surface of the wafers. Etching is then done to remove the damaged surface layers from the cutting, lapping, and edge profiling operations. Polishing is then done to create a defect free mirror surface. The surface is then cleaned to remove contaminants and prepare the wafer for the fabrication line.

This process requires the removal of silicon material by mechanical and chemical means. The mechanical means are sawing, lapping, and grinding. using abrasives such as diamond, SiC, or Al_2O_3. There is no plastic flow associated with abrasive machining of silicon. Because of the hard, brittle nature of silicon, the penetration of abrasive particles establishes a field of damage in the form of cracks extending into the material from the surface. This leaves a rough surface and subsurface damage that consists of microcracks, dislocations, and stresses (40). The grit size controls the roughness and the speed of material removal.

Flats are ground into the material according to the crystal orientation and the dopant type. The orientation of the flats makes it easy to identify the crystal orientation (111 or 100) and the material (n or p type) (41).

In a wafering operation, a blade with diamond particles embedded in it is forced into the silicon crystal at pressures that exceed the compressive strength of the crystal. Microcracks form ahead of the cutting blade due to high stress fields. These cracks propagate into the crystal mainly along lattice planes. When the cracks intersect, material is released. Microcracks also propagate laterally into the material. This damage is called sawing damage. This damage can be increased due to blade runout and machine vibration. These microcracks, if they run deep enough into the subsurface are responsible for problems such as exit chips, cracks and breakage.

Acceptable wafer quality can be achieved with this method only if constant attention is paid to the blade, the machine and the process parameters. Blade cutting of wafers can also result in bowing of the wafers. As the blade vibrates and moves laterally while cutting, it deviates from a straight path through the material. This occurs when the greatest cutting forces are applied at the surfaces of the cut.

CHAPTER 4

EXPERIMENTAL EQUIPMENT

4.1 The Scanning Electron Microscope

4.1.1 Scanning Electron Microscope Theory

The scanning electron microscope (SEM) works by forming a wide beam of electrons and condensing it into a fine beam that is approximately 200 angstroms across. This beam sweeps across the sample in a series of step-like passes. When this happens, electrons strike the sample surface, knocking loose showers of electrons that are part of the specimen. These electrons are called secondary electrons. These secondary electrons hit a signal detector. This signal detector amplifies a signal and sends it to a CRT screen or a photographic camera so that it can be viewed (42).

An SEM consists of three groups of components: The electron optical column with its associated electronics, the vacuum system with specimen chamber and stage, and the signal detector and display system.

4.1.2 The Electron Optical Column

The electron column consists of an electron gun and 2 to 4 electron lenses. An electron beam from the electron source flows through the lenses, which serve to demagnify and condense the beam diameter. This brings the final point of the beam to a spot size of under 250 angstroms. The final lens assembly contains two sets if magnetic scanning coils which cause the beam to be deflected in a rastor-like pattern over the specimen surface. Three other elements in the electron optical column are: a set of apertures to help define the angular aperture subtended by the beam at the specimen and to avoid contamination at the lens surfaces, an astigmate which is a set of coils that eliminates any astigmatisms that may be present in the system, and a set of plates that superimpose modulation on the electron beam.

4.1.3 SEM Vacuum Pumping System

A vacuum pumping system removes air from the chamber and provides acceptable vacuum in the system to insure proper imaging. The specimen stage is designed so that the specimen can be rotated and tilted to allow the operator to view the sample at the proper angle and sample position.

When the electron beam bombards the sample surface, the electrons interact with the sample, giving off primary electrons, which are reflected electrons form the electron beam, secondary electrons, which are electrons that are knocked loose from the sample atoms, beam induced conduction, and cathodoluminescence (43). These signals are picked up by a signal detector, amplified, and sent to a CRT for image display. The CRT image scans are synchronized with the electron beam scans to acquire a useable image at the CRT.

4.2 The Videometrix Econoscope

The Matrix Videometrix Econoscope is a fully automatic, 3-axis video system. It uses non-contact techniques to provide rapid dimensional verification of complete parts or specific features of a part.

4.2.1 The Videometrix Econoscope Hardware

The econosope consists of a PC, a 3-axis positioning control system, and a digital image processor and a part monitor section. It uses a menu driven software package that allows it to be operated easily by the user.

The econoscope is intended to be used for part inspection. The final inspection results can be compiled into statistical data and used for SPC.

The system uses a Hewlett Packard series 200 PC with a Hewlett Packard Winchester hard disk as well as a Hewlett Packard Thinkjet Printer. It utilizes a joystick for manual stage and lens movement.

The inspection station is the actual measuring device of the system. It provides the mechanical means of making measurements through the use an X and Y axis stage, and a Z stage. These stages are controlled with electric stepper motors and precision lead screws that move the stage along the individual axes. The stage movements can be defined as data points in relation to the zero point. These data points can be used to define part features.

The stage can be moved manually with a joystick, and the points manually recorded. Or, when inspecting a part, the stage movements fall under control of the computer, and the part is defined automatically with the computer storing the data points.

The image gathering is performed by using a video camera along with a microscope. The microscope consists of 5x, 10x and 20x lenses which enhance feature identification and definition. The video camera processes the image and supplies the raw video to the Digital Image Processor. The Digital Image Processor uses a moveable measurement window that appears on the screen to analyze images for precision measurements. The field of view is digitized into a 480 by 512 pixel matrix at maximum window size. The digitized image is processed by the computer, which determines the output that is desired once the features are analyzed.

The Econoscope takes measurements in both standard and metric units. The measuring capacity is a sample of size X: 6 in., Y: 6 in., and Z: 6 in.. The system resolution is X-axis: 4 microinches, Y-axis: 4 microinches, and Z-axis: 4 microinches. Straightness resolution is: .0002 in.. Squareness resolution is: .0002 in.. System measuring accuracy is: +- .0003 in..

4.2.2 The Videometrix Econoscope Software

The Videometrix software has different modes of operation they include Manual Measurement, Part Definition, Output Definition, Run part and Stat Pak.

Manual Measurement is useful in defining dimensions such as X, Y, and Z measurements, diameter, and radius measurements, angles, flatness, and straightness.

Part definition is used to define part dimensions, save these dimensions on file, and recall them again for reference in checking the quality of subsequent parts by verifying dimensions and features of these additional parts.

The Output Definition mode is used to mathematically reconstruct the part from the data points captured within the Part Definition module and output the results.

The Run Part module provides a computerized statistical analysis of the data gathered by the system. The data is compiled and output in the form of tabular and graphical printouts.

There is also a program called TOPO. This software allows the user to gather and view information on the surface contour of a part. It is broken down into Two processes: Inspect and Graphics.

The Inspect process is used to gather data. The user defines the area that is being observed by programming in the number of focus points that will be gathered, the length and width of the area being observed, lens magnification, the size of the Digital Image Processor window, and the intensity of the surface lighting. The Econoscope focuses on each focus point and gives a reading for the Z value. When the Z values are collected for each focus point in the entire collection of data points, a graphics printout of the surface can be viewed.

The Graphics process is used to view the collected points on the CRT screen or on a hard copy printout. Different viewing angles of the final data, as well as a listing of the collected data points can be obtained (44).

4.3 Abrasive Waterjet Cutting System

Abrasive water jet cutting and water jet cutting can offer some advantages over other types of machining, depending on the application it is being used for. Some of the advantages are cost savings, the production of little or no dust during cutting, the elimination of thermal distortions by cutting without heat, and the elimination of internal stresses that may damage the workpiece. The cutting of complicated shapes becomes easy with water jet cutting due to the omnidirectional nature of the cutter. Additional advantages could be low noise, fast cutting speed, and smooth cutting surface, depending on the application.

The abrasive water jet cutter used in this study is made by the Ingersoll-Rand Company. It has four major components: the water preparation unit, the water distribution system, the work station, and the catcher and drainage system.

4.3.1 Abrasive Waterjet Cutter Water Preparation Unit

The purpose of the water preparation unit is to feed pure water into the system and to pressurize the water. First, the water is fed into the system using a low pressure booster pump (180 psi.). This water is treated using a series of low pressure filters and softeners. This is done to remove dissolved solids from the water that would otherwise precipitate out at high pressures and destroy the nozzle orifice.

A hydraulic unit contains an oil intensifier (pump) that is a double acting piston type pump. It has two separate circuits, one for oil, and one for water. The oil is pressurized against a large diameter piston by an intensifier pump that develops pressures of 1500 to 3000 psi. This piston is connected to a smaller diameter piston that pressurizes the water. This setup results in a step up in pressure from the large piston to the small piston in a ratio that is equal the ratio of the size of the size of the large piston to the small piston. With this principle, water pressures of 50 to 60 KSI can be created.

A series of check valves allows the water to enter the high pressure cylinder on the suction stroke and leave on the discharge stroke. The booster pump assures a continuous flow into the suction side of the high pressure cylinders.

The high pressure water from both sides of the intensifier is discharged into an accumulator where the pressure gets stabilized. The accumulator provides uniform discharge pressure and flow to the cutting nozzle.

4.3.2 Abrasive Waterjet Cutter Distribution System

High pressure tubing, swivels, flexible joints and fittings are used to connect the accumulator to the work station.

4.3.3 Abrasive Waterjet Cutter Workstation

The workstation is the place where the cutting operation is performed. It consists of a nozzle assembly, an abrasive feeder, a traverse mechanism, and a catcher.

The nozzle assembly is the place where the water pressure is converted into kinetic energy by accelerating the water to a velocity of between 2000 and 3000 fps.

In a pure water jet cutting system, the nozzle is made of sapphire with a small orifice of diameter between .004 in. and .014 in. Abrasive water jet cutting systems employ the same nozzle as in a pure water jet cutting system along with a secondary nozzle, called a carbide tube, that is made of tungsten carbide to resist wear from the abrasives.

Abrasives are fed into the jet stream by use of a vibratory feeder that controls their flow rate. An applied voltage to the vibratory tray causes the abrasive to flow out of the tray into an abrasive tube. Flow is controlled by adjusting the voltage. The effect of vibration on the flow rate varies with type and size of the abrasive.

Abrasives enter the water stream from a side port between the sapphire nozzle and the carbide tube. The suction from the water stream draws the abrasives into the water stream. The abrasive particles are accelerated and the kinetic energy is transferred to the abrasive particles from the water (45).

In order to perform effective cutting with the jet, either the jet or the workpiece has to be able to move.

In this system. the movement of the cutter is controlled by a two and one half axis robotic workcell with an Alan Bradley 8200 controller. The positioning accuracy of the nozzle with the controller is +/- .005 in. with a repeatability of +/- .005 in..

4.3.4 Abrasive Waterjet Cutter Catcher and Drainage System

The catcher is designed to contain the water jet stream and abrasives after they exit the workpiece. This ensures that the system operates safely, and so that the waste material can be disposed of properly.

4.3.5 Abrasive Waterjet Cutter Controller

The Ingersoll Rand Two and One Half Axis Water Jet Cutter is controlled by an Allen Bradley Series B 8400 MP/ Bandit IV revision F Firmware Controller.

The AB controller consists of a CPU (Central Processor Unit), a CRT (Cathode Ray Tube), a keyboard, and controls for machine operation. The CPU is the computer module that processes system information and directs axis movement. The CRT allows the user to monitor and control the machine functions. The keyboard is used to enter data for part programs as well as access software functions. The control functions are for emergency stop, spindle speed adjustment, feedrate, and other machine functions.

The controller can be operated from a Manual operate mode or an Auto operate mode.

The Manual operate mode allows manual movement of the axes to take place. Machine Home, Jog Handwheel, Jog Continuous, Jog Incremental, allow the axes to be moved by direct control from the keys.

This mode also allows other operations by using Manual Data Input (MDI). MDI allows the user to input a single desired data block for immediate execution by the controller.

The Auto Operate mode can be used to run a program. When this mode is used, a program must be properly written, tested and debugged so that it can be properly executed. Programming is accomplished by using the softkeys on the keyboard to get into the Job Setup page. From here, the user can enter the number of a program to be executed or he can enter zero to load a program from an external device.

The commands that are important.for Job Setup are the following. Inch/ Metric allows the user to display the measurement units for all dimensions such as axis displays, feedrates, and offsets in either inch or metric units. The Block Delete command is used to stop the execution of a block of commands or an individual command. The Optional Stop command will halt the execution of the program at that point in order to allow other functions, such as tool changes, to be performed. The program will restart again and continue on only when the cycle start button is pushed. The Tool Offset command is used to allow for differences in tool size when programming. The operator can program arm motion into the controller without having to take into account tool length. With the proper Tool Offset code, the tool size is automatically factored into the programming sequence.

The program edit softkey is used to enter a new program or edit a program that is already in storage. The Insert command key is used to enter characters and blocks of data. The Delete command key is used to remove characters or blocks of data from the program.

M codes are commands that control toolhead functions such as flow rate and pressure. G codes are used to control arm movements such as drilling and cutting motions (46)

CHAPTER 5

EXPERIMENTAL PROCEDURES

The experiment was performed on a polished single crystal silicon wafer that is two inches in diameter. The machining was performed using the two and one half axis water jet cutter with silicon carbide abrasive particles.

Single crystal silicon is a very strong, yet brittle material that requires careful handling in order to insure that it will not fracture during the cutting process. In order to prevent the thin, brittle ceramic wafer from cracking and shattering, the sample was placed on a flat plastic material that was used as a backing for support. It was secured to the backing material to prevent movement of the wafer. In order to try to minimize damage to the polished surface away from the cuts by stray particles from the abrasive waterjet stream and to get a square edged cut, transparent plastic tape was placed on the polished side of the wafer. This insures that only the surface of the area being cut will be affected by the cutting jet stream. Any abrasive particles that sprayed out into a wider area away from the immediate jet stream were prevented from hitting the surface of the sample by the tape.

Initially, an attempt was made to cut the wafers with the two and one half axis water jet cutter using only a high pressure water stream with no abrasive particles. Upon attempted cutting of the wafer with this method, the wafer cracked in half along the crystal planes. It was then decided that the machine would have to be set up for abrasive jet cutting. The system was set up with a carbide tube and 120 grit abrasive particles.

With abrasive water jet cutting, the wafer was cut under varying conditions of cutting stream pressure, cutting speed, and abrasive flow rate. Initially, 13 different cuts were made with the abrasive water jet cutter. These cutting conditions are summed up in table 5-1.

TABLE 5-1 FIRST SET OF ABRASIVE WATER JET CUTTING CONDITIONS FOR SILICON WAFER

CUT NUMBER	ABRASIVE FLOW RATE (GPM)	PRESSURE (KSI)	ABRASIVE NUMBER	NOZZLE NUMBER	TRAVERSE SPEED (IN/MIN)	CARBIDE NUMBER
CA01A	229	50	120	10	5	30
CA02A	229	50	120	10	3	30
CA03A	229	50	120	10	2	30
CA04A	229	50	120	10	1	30
CA05A	229	33	120	10	3	30
CA06B	229	33	120	10	2	30
CA07A	229	33	120	10	1	30
CA08A	185	33	120	10	1	30
CA09A	185	33	120	10	2	30
CA10A	185	33	120	10	3	30
CA11H	185	50	120	10	3	30
CA12A	185	50	120	10	2	30
CA13A	185	50	120	10	1	30

These cuts were analyzed using the SEM at 50X and 500X magnifications in order to try to get an idea of the micorostructural damage that took place during cutting. The Videometrix microscope was used to measure the surface roughness characteristics of the sample for the different cuts.

Additional cuts were then made with the abrasive water jet cutter in order to try to get a smoother cut that would better match that or surpass that of diamond cutting. These cuts also were made under varying conditions of abrasive flow rate, cutting speed, and water pressure. These cutting conditions are summed up in table 5-2 and table 5-3.

TABLE 5-2 SECOND SET OF ABRASIVE WATER JET CUTTING CONDITIONS FOR SILICON WAFER

CUT NUMBER	ABRASIVE FLOW RATE (GPM)	PRESSURE (KSI)	ABRASIVE NUMBER	NOZZLE NUMBER	TRAVERSE SPEED (IN/MIN)	CARBIDE NUMBER
CB1B	82.06	50	120	7	2	30
CB2B	144.8	50	120	7	2	30
CB3A	144.8	50	120	7	1	30
CB4B	144.8	50	120	7	0.5	30
CB5B	235.2	50	120	7	2	30
CB6A	235.2	50	120	7	1	30
CB7A	235.2	50	120	7	0.5	30

TABLE 5-3 THIRD SET OF ABRASIVE WATER JET CUTTING CONDITIONS FOR SILICON WAFER

CUT NUMBER	ABRASIVE FLOW RATE (GPM)	PRESSURE (KSI)	ABRASIVE NUMBER	NOZZLE NUMBER	TRAVERSE SPEED (IN/MIN)	CARBIDE NUMBER
CC1B	56	30	220	10	2	30
CC2B	56	30	220	10	1	30
CC3B	56	30	220	10	0.5	30
CC4A	56	50	220	10	2	30
CC5B	56	50	220	10	1	30
CC6A	56	50	220	10	0.5	30

Some of the silicon cuts were analyzed for microstructural characteristics by use of a scanning electron microscope. This was done in order to determine the effects of the water jet stream on the surface microstructure of the sample.

Due to limitations on the size of the sample that can fit into the SEM, the cut wafers had to be cut down to a smaller size in order to fit into the vacuum chamber of the microscope. Samples had to be placed into the chamber individually to be analyzed.

The Videometrix analysis of the cuts consisted of using the TOPO program in order to get roughness measurements of the cuts. These measurements were compared in an attempt to determine the best cutting conditions for obtaining smooth cuts with the abrasive water jet cutter.

Sample preparation for the videometrix microscope amounted to removing the small pieces of the wafer that contained the individual cuts and mounting them on their edges so that the videometrix would be analyzing the surface of the edge. The samples had to be mounted so that their surfaces were situated parallel to the stage. Z-axis measurements were taken over a .25 inch length of the edge with 50 data points being taken for each edge length. These measurements quantify the variation in the surface height from point to point. From this data, roughness measurements were determined.

The roughness is defined as the average surface deviation above and below the center line.

The roughness measurements were analyzed and compared in order to determine the trends in roughness vs. cutting conditions as well as to determine the conditions for the best cut that was obtained.

CHAPTER 6

EXPERIMENTAL RESULTS

The results for the abrasive water jet cuts of the silicon wafer are broken down into different categories. These categories are microstructure and roughness. The results for microstructure are shown in the form of SEM micrographs of some of the different cuts. The results for roughness are shown in the form of tables of Matrix Videometrix compiled data points for each cut, along with final results for roughness and comparisons between roughness values for different cutting conditions.

6.1 Microstructural Characteristics of the Cuts

Figures 6-1 through 6-22 in appendix A are SEM micrographs of the initial set of cuts. They show the surface of some of the cuts at 50x and either 500x or 200x magnifications. All of the micrographs, regardless of the cutting conditions, appear to exhibit similar surface characteristics for the silicon material.

The SEM micrographs in figures 6-1 and 6-2 seem to be fairly representative of all of the micrographs, so they will be used to explain the effects of waterjet cutting on the surface microstructure. They show the first cut with 229 grams/minute abrasive flow rate, 50 KSI water pressure, and 5 inches/minute cutting speed at 50x and 500x respectively.

These micrographs illustrate that the erosion of the workpiece takes place through the process of chipping and cracking of the material. Figure 6-1 seems to show that the material was removed by breaking sample pieces off along crystal planes. The cracking of the material appears to have taken place parallel to the surface of the wafer.

There was some speculation among those involved in the project that there was some plastic flow of the silicon that took place along the cut. Although some of the micrographs give this appearance, it is highly unlikely that plastic flow will take place at such low cutting temperatures in the brittle silicon material.

It seems more likely that the material is fracturing and chipping off along the crystal planes, thereby creating a layered appearance in the micrographs that could be mistaken for plastic flow.

There are two types of cracks that occur in abrasive water jet machining of brittle materials. They are radial cracks that are normal to the surface that cause strength degradation, and lateral cracks that form on planes parallel to the surface that relate to material removal. These cracks and material removal take place through the bombardment of the surface with multiple particles moving at high speeds. As these particles contact the surface of the target material, they are decelerated and a transfer of energy from the moving particles to the surface takes place. This energy transfer causes the surface of the target material to move.

If this force exceeds the bond strength of the molecules, the bonds will break and the material will fracture (47). Multiple fractures that intersect will cause particles of the material to loosen and separate from the target body.

This is consistent with abrasive water jet cutting theory. Lateral cracking in the material is the main cause of material removal in abrasive water jet cutting. Because of the single crystal structure of silicon, most of the lateral cracking should take place along crystal planes. It takes less energy to fracture the crystal along these planes than it does to fracture it across planes. This means that the most natural way for the crystal to fracture is along the crystal planes. This fracturing along these planes appears to be what is taking place in these samples.

The surface roughness corresponds to the radial cracking and material removal. Because the cracking that occurs perpendicular to the wafer surface is not taking place along crystal planes, the resultant surface is not as smooth as if it takes place along flat crystal planes.

The cuts themselves appear to be square edged due to the masking of the sample surface with plastic tape. There is some chipping that occurs at the edges, making them less square than is ideally desirable.

There is also another point that is not shown in the micrographs that should be mentioned. The edge of the cuts on the back side of the wafer where the water jet stream exits the material is not smooth around the cuts. It appears as if the force from the cutting jet stream is chipping large chunks of material off of the back of the wafer as it exits the sample. This may be due to poor support of the substrate during cutting. If a better backing is created that could give better support to the back of the substrate, this problem could be minimized. This is a major problem that will have to be dealt with if abrasive water jet cutting is going to become a viable method for the large scale machining of electronic substrates.

In the micrographs, it can also be seen that there are some defects that take place away from the actual cutting surfaces. This occurs because of the imperfection of the cutting jet stream. Some stray particles are projected out of the nozzle at a wider angles than are desired, causing them to strike the sample surface at points away from the cutting area. This is seen most clearly in the 50x micrographs.

The clear plastic tape masking was used to try to prevent this. However, as the cutting takes place, two things may occur. The first is that the tape may slide or come loose from the surface under the force of the cutting stream. The second is that the jetstream itself may penetrate and erode the mask, leaving the sample surface exposed, and allowing it to be damaged by the jet stream.

6.2 Roughness Characteristics

The results for the roughness of the cuts were obtained by using the Matrix Videometrix Econoscope. The results for each cut are shown in table 6-1 through table 6-25. Table 6-26 shows a summary of the final roughness values along with the cutting conditions for each cut. These can be found in appendix C.

The results for the roughness of the different cuts were analyzed in an attempt to find a correlation between cutting conditions and roughness. Graphs of the results were made for roughness vs. cutting speed at the different cutting conditions of abrasive flow rate and water pressure. Graphs were also made for roughness vs. water pressure for varying conditions of cutting speed and abrasive flow rate. Additional graphs were made for roughness vs. abrasive flow rate for various conditions of cutting speed and water pressure.

All of the graphs for the roughness values are shown in Figures 6-23 through 6-45. These are located in appendix B.

Figures 6-23 through 6-30 show graphs of the results of the cutting speed vs. roughness.

Figure 6-23 (abrasive flow rate 56 GPM, water pressure 50 KSI) shows the best roughness to be at a 2 in./minute cutting speed. Figure 6-24 (abrasive flow rate 144 GPM, water pressure 50 KSI) shows the best roughness to be at 1 in./minute cutting speed. Figure 6-25 (abrasive flow rate 185 GPM, water pressure 50 KSI) shows the best roughness to be at 3 in./ minute. Figure 6-26 (abrasive flow rate 229 GPM, water pressure 50 KSI) shows the best roughness to be at 5 in./ minute. Figure 6-27 (abrasive flow rate 235 GPM, water pressure 50 KSI) shows the best roughness to be at a cutting speed of 1 in./minute.

Figure 6-28 (abrasive flow rate 56 GPM, water pressure 30 KSI) shows the best roughness to be at a 1 in/ minute cutting speed. Figure 6-29 (abrasive flow rate 185 GPM, water pressure 33) shows the best roughness to be at a 2 in./minute cutting speed. Figure 6-30 (abrasive flow rate 229 GPM, water pressure 33 KSI) shows the best roughness to be at a 3 in./minute cutting speed.

The general trend for roughness vs. cutting speed at 50 KSI water pressure has the best roughness at either a 1 in./minute or a 2 in./minute cutting speed. This tends to show that higher traverse speeds result in better roughness values. A similar trend is seen in the 30 KSI results.

A comparison of different water pressures on roughness was made using varying conditions of cutting speed and abrasive flow rate. The results can be seen in figures 6-31 through 6-38.

Figures 6-31 through 6-34 are for abrasive flow rates of 56 GPM.

Figure 6-31 (abrasive flow rate 56 GPM, speed .5) shows the roughness for the 50 KSI water pressure to be better than the roughness for the 30 KSI water pressure. Figure 6-32 (abrasive flow rate 56 GPM, cutting speed 1 in./min.) shows the 30 KSI water pressure to yield better results than the 50 KSI water pressure. Figure 6-33 (abrasive flow rate 56 GPM, cutting speed 2 in./min.) shows the roughness for the 50 KSI cut to be better than the roughness for the 30 KSI cut.

Figures 6-34 through 6-36 illustrate the affect of the different pressures on roughness at an abrasive flow rate of 185 grams/minute. Figure 6-34 (abrasive flow rate 185 GPM, speed 1 in./min.), figure 6-35 (abrasive flow rate 185 GPM, speed 2 in./min.), and figure 6-36 (abrasive flow rate 185, speed 3) all show the roughness for 30 KSI water pressure to be better than the roughness at 50 KSI for the same conditions of abrasive flow rate and cutting speed.

Figures 6-37 and 6-38 compare the roughnesses for the 33 KSI and 50 KSI water pressures for an abrasive flow rate of 229 grams/ minute. At this abrasive flow rate, both figures 6-37 (abrasive flow rate 229 GPM, speed 1 in/minute) and 6-38 (abrasive flow rate 229 GPM, speed 3 in/minute) show the roughnesses for the 33 KSI cuts to be better than the roughnesses for the 50 KSI cuts.

In general, the 30 KSI pressure seems to get better results than the 50 KSI pressure. However, at the 56 gram/ minute flow rate, the best roughness was achieved at the 50 KSI pressure.

An analysis of the effect of abrasive flow rate on roughness was also done. The results are shown in figures 6-39 through 6-45. Figures 6-39 through 6-42 show the effect of abrasive flow rate at 50 KSI at various cutting speeds from .5 in./minute to 3 in./minute. Figure 6-39 (pressure 50

KSI, speed .5 in./minute) shows better roughness values for lower abrasive flow rates as do figures 6-43 (30 KSI, speed 1 in./minute) and 6-44 (pressure 30 KSI, speed 2 in./minute) and figure 6-41 (pressure 50 KSI, speed 2 in./minute). Figure 6-42 (pressure 50 KSI, speed 3 in./minute) and figure 6-45 (pressure 30 KSI, speed 3 in./minute) show the opposite trend with better roughness values coming at higher abrasive flow rates. Figure 6-40 (pressure 50 KSI, speed 1 in./minute) shows an intersesting trend with the best roughness values to be at both the high abrasive flow rates and the low abrasive flow rates, with the worst roughness values falling in the middle.

In general, at 50 KSI, a lower abrasive flow rate results in better roughness values. At 30 KSI, a lower abrasive flow rate also results in better roughness values.

CHAPTER 7

CONCLUSIONS

Abrasive water jet cutting could be a viable non-traditional machining method for the cutting of ceramic substrates.

The SEM micrographs illustrate tht effects of abrasive water jet machining on the substrate. They show that the brittle silicon material is removed in layers and breaks off parallel to the surface of the wafer, along the flat crystal planes. This is consistent with crystalline fracture in that the bond strength between atoms running parallel to a crystal plane is greater than the bond strength between atoms runnning across crytal planes.

The roughness trends for the abrasive water jet cutting conditions are as follows. The roughness values range from 170 microinches to 644 microinches. The 170 microinch result comes at the cutting conditions of: abrasive flow rate of 56 grams per minute, 30 KSI water pressure, nozzle #10, and a traverse speed of 1 inch per minute.

When roughness is plotted vs. water pressure under constant conditions of abrasive flow rate and cutting speed, the overwhelming trend is that the 30 KSI pressure achieves better roughness values than the 50 KSI pressure.

When roughness is plotted vs. abrasive flow rate under constant conditions of water pressure and traverse speed, low abrasive flow rates result in the best roughness values for both 30KSI and 50KSI water pressures.

A plot of roughness vs. traverse speed under constant conditions of water pressure and abrasive flow rate shows the optimum cutting speed to be between 1 and 2 inches per minute.

These cutting conditions and roughnesses will have to be studied in further detail to determine whether or not abrasive water jet cutting can be adjusted to get at least as good a result in terms of roughness as the traditional cutting methods that are currently employed, while having a minimal effect in terms of impurities and other microstructural deformities on the substrates.

APPENDIX A

SEM MICROGRAPHS OF MACHINED SURFACES

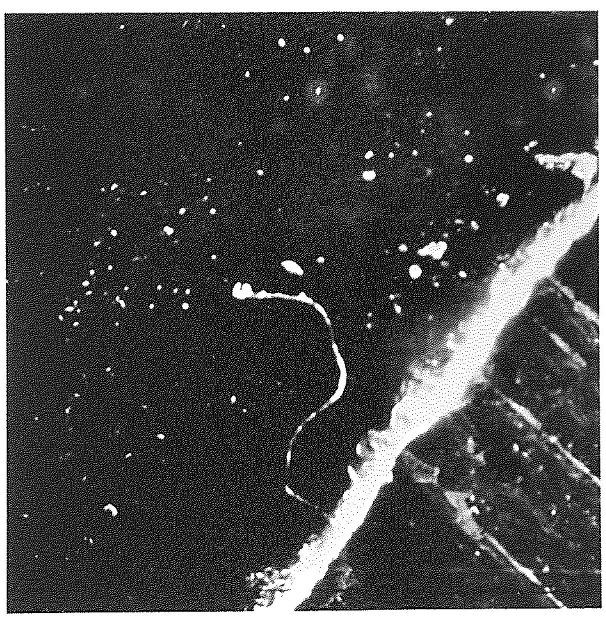

FIGURE 6-1 50X MICROGRAPH OF CUT CA01A
CUTTING CONDITIONS: AFR: 229 GPM
50 KSI WATER PRESSURE
NOZZLE #10
TRAVERSE SPEED: 5 IN./MIN.
20 KEV

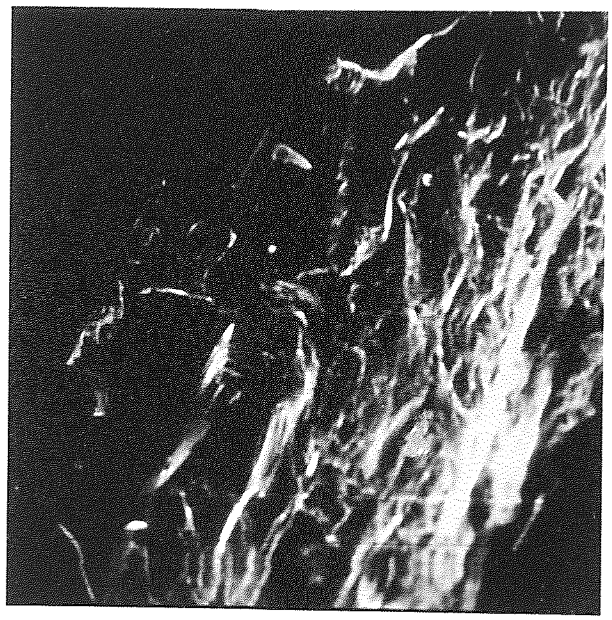

FIGURE 6-2 500X MICROGRAPH OF CUT CA01A
CUTTING CONDITIONS: AFR: 229 GPM
50 KSI WATER PRESSURE
NOZZLE #10
TRAVERSE SPEED: 5 IN./MIN.
20 KEV

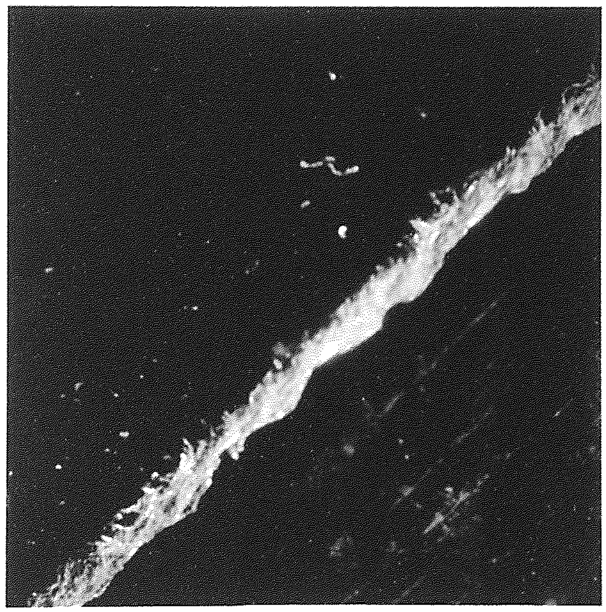

FIGURE 6-3 50X MICROGRAPH OF CUT CA03A
CUTTING CONDITIONS: AFR: 229 GPM
50 KSI WATER PRESSURE
NOZZLE #10
TRAVERSE SPEED: 2 IN./MIN.
20 KEV

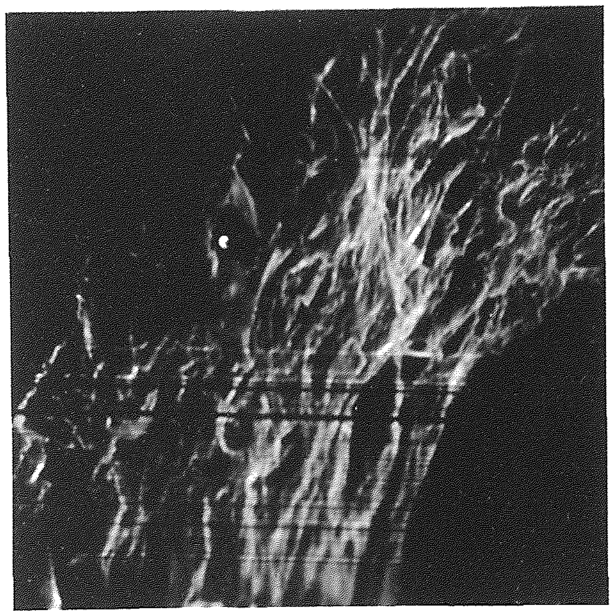

FIGURE 6-4 500X MICROGRAPH OF CUT CA03A
CUTTING CONDITIONS: AFR: 229 GPM
50 KSI WATER PRESSURE
NOZZLE #10
TRAVERSE SPEED: 2 IN./MIN.
20 KEV

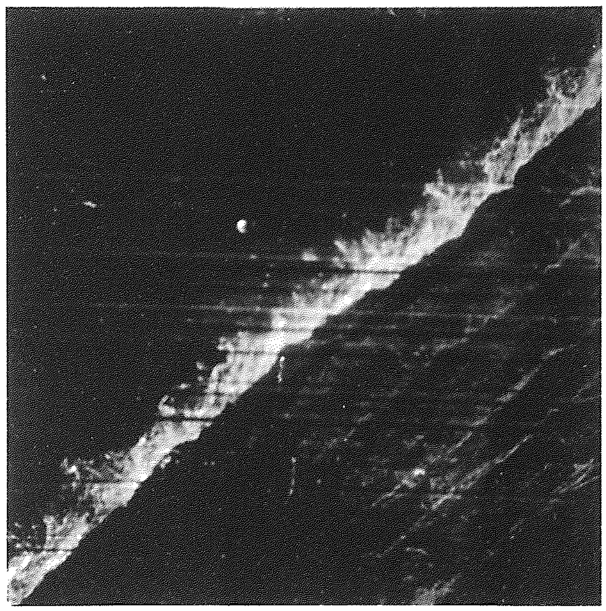

FIGURE 6-5 50X MICROGRAPH OF CUT CA04A
CUTTING CONDITIONS: AFR: 229 GPM
50 KSI WATER PRESSURE
NOZZLE #10
TRAVERSE SPEED: 1 IN./MIN.
20 KEV

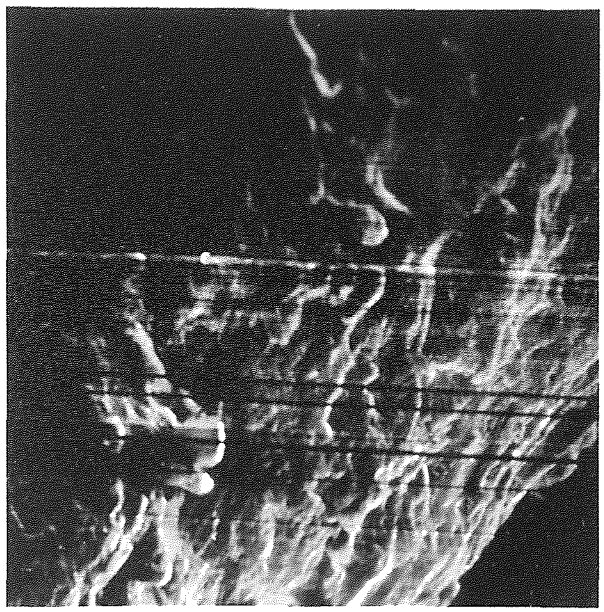

FIGURE 6-6 500X MICROGRAPH OF CUT CA04A
CUTTING CONDITIONS: AFR: 229 GPM
50 KSI WATER PRESSURE
NOZZLE #10
TRAVERSE SPEED: 1 IN./MIN.
20 KEV

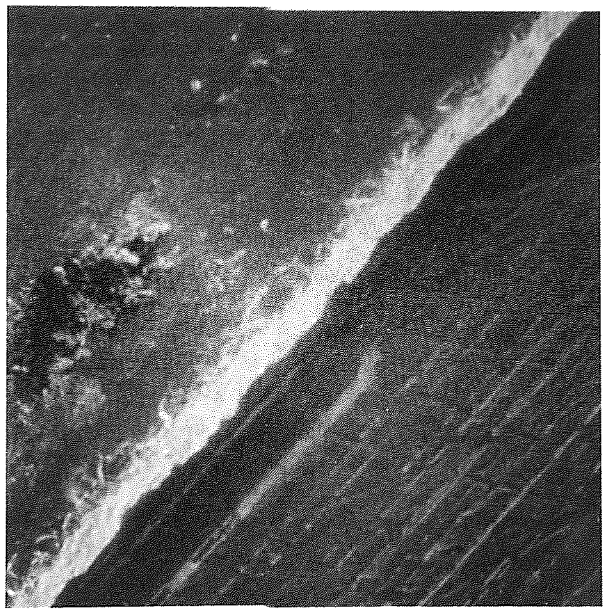

FIGURE 6-7 50X MICROGRAPH OF CUT CA05A
CUTTING CONDITIONS: AFR: 229 GPM
33 KSI WATER PRESSURE
NOZZLE #10
TRAVERSE SPEED: 3 IN./MIN.
20 KEV

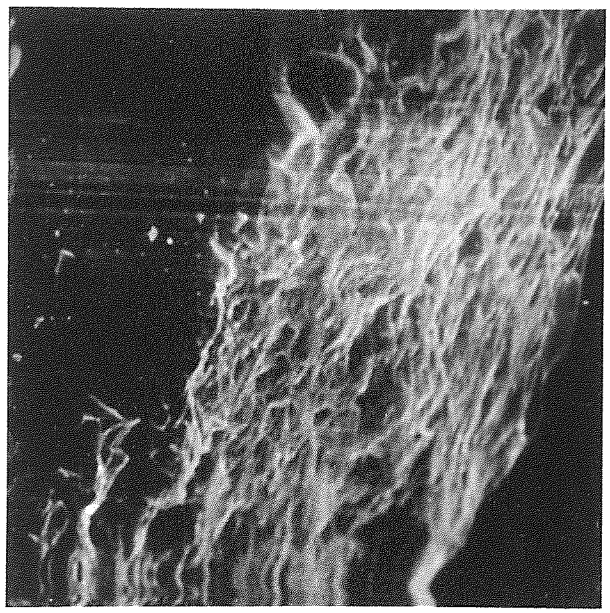

FIGURE 6-8 500X MICROGRAPH OF CUT CA05A
CUTTING CONDITIONS: AFR: 229 GPM
33 KSI WATER PRESSURE
NOZZLE #10
TRAVERSE SPEED: 3 IN./MIN.
20 KEV

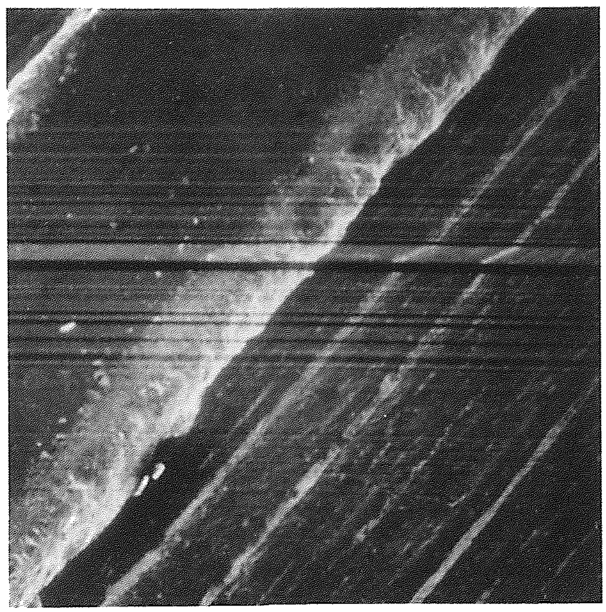

FIGURE 6-9 50X MICROGRAPH OF CUT CA08A
CUTTING CONDITIONS: AFR: 185 GPM
33 KSI WATER PRESSURE
NOZZLE #10
TRAVERSE SPEED: 1 IN./MIN.
20 KEV

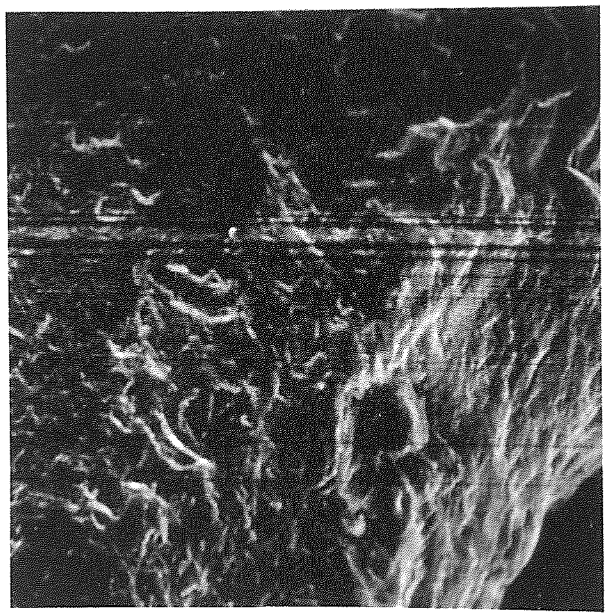

FIGURE 6-10 500X MICROGRAPH OF CUT CA08A
CUTTING CONDITIONS: AFR: 185 GPM
33 KSI WATER PRESSURE
NOZZLE #10
TRAVERSE SPEED: 1 IN./MIN.
20 KEV

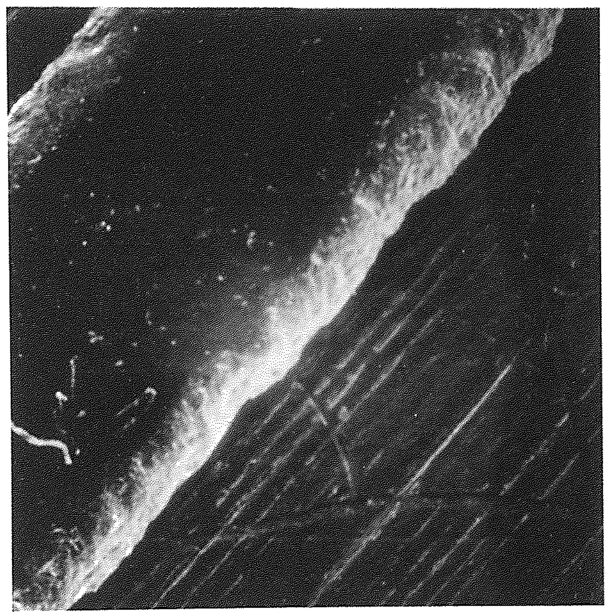

FIGURE 6-11 50X MICROGRAPH OF CUT CA09A
CUTTING CONDITIONS: AFR: 185 GPM
33 KSI WATER PRESSURE
NOZZLE #10
TRAVERSE SPEED: 2 IN./MIN.
20 KEV

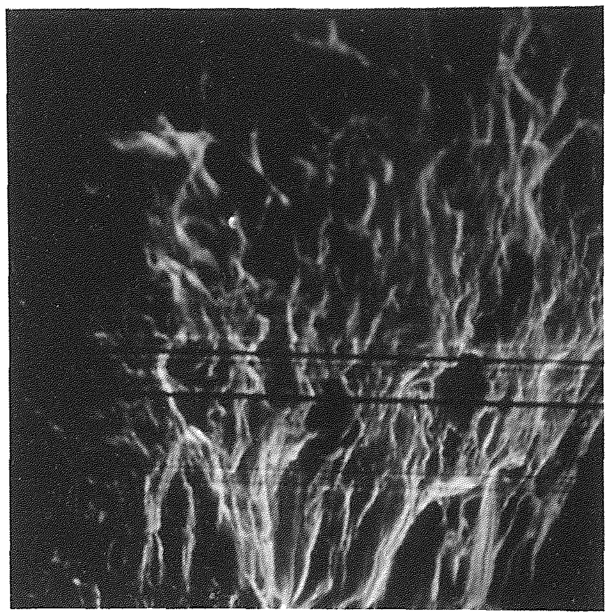

FIGURE 6-12 500X MICROGRAPH OF CUT CA09A
CUTTING CONDITIONS: AFR: 185 GPM
33 KSI WATER PRESSURE
NOZZLE #10
TRAVERSE SPEED: 2 IN./MIN.
20 KEV

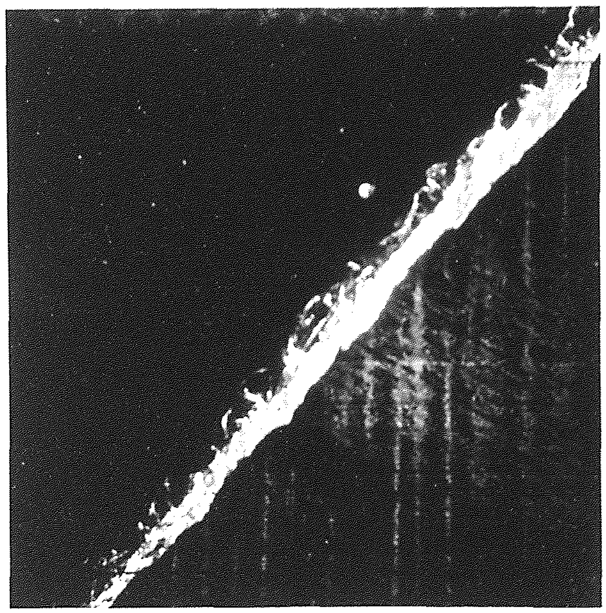

FIGURE 6-13 50X MICROGRAPH OF CUT CA10A
CUTTING CONDITIONS: AFR: 185 GPM
33 KSI WATER PRESSURE
NOZZLE #10
TRAVERSE SPEED: 3 IN./MIN.
20 KEV

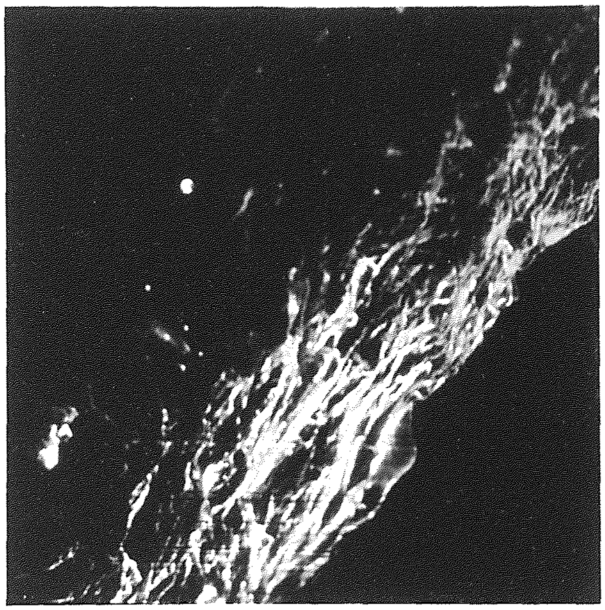

FIGURE 6-14 200X MICROGRAPH OF CUT CÂ10A
CUTTING CONDITIONS: AFR: 185 GPM
33 KSI WATER PRESSURE
NOZZLE #10
TRAVERSE SPEED: 3 IN./MIN.
20 KEV

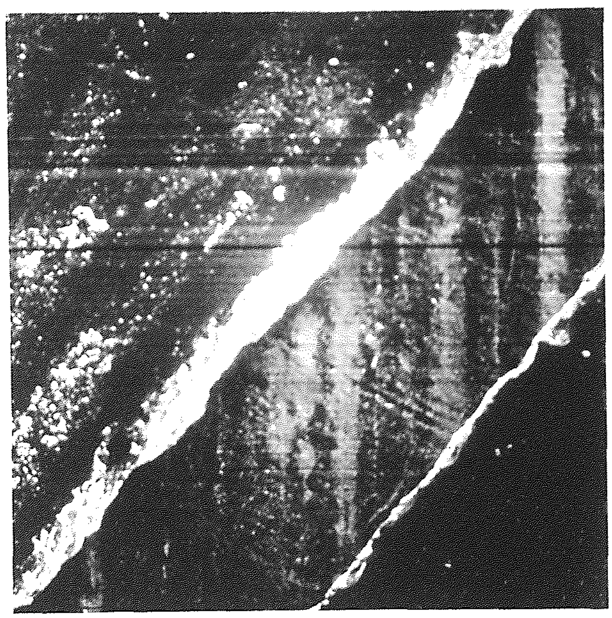

FIGURE 6-15 50X MICROGRAPH OF CUT CA11H
CUTTING CONDITIONS: AFR: 185 GPM
50 KSI WATER PRESSURE
NOZZLE #10
TRAVERSE SPEED: 3 IN./MIN.
20 KEV

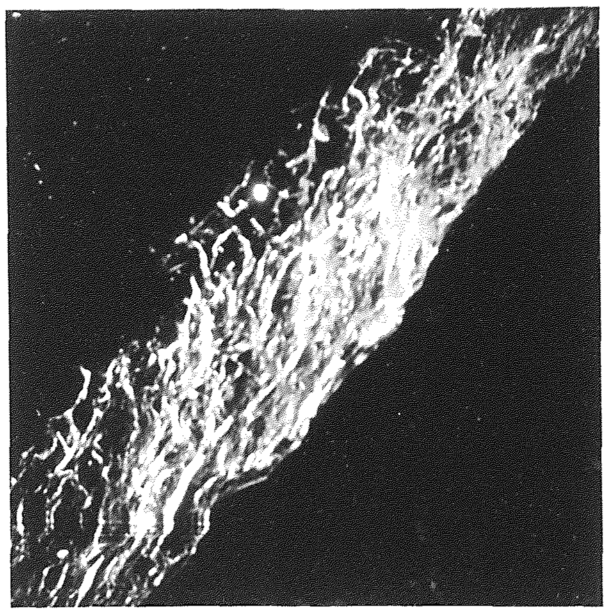

FIGURE 6-16 200X MICROGRAPH OF CUT CA11H
CUTTING CONDITIONS: AFR: 185 GPM
50 KSI WATER PRESSURE
NOZZLE #10
TRAVERSE SPEED: 3 IN./MIN.
20 KEV

FIGURE 6-17 50X MICROGRAPH OF CUT CA12A
CUTTING CONDITIONS: AFR: 185 GPM
50 KSI WATER PRESSURE
NOZZLE #10
TRAVERSE SPEED: 2 IN./MIN.
20 KEV

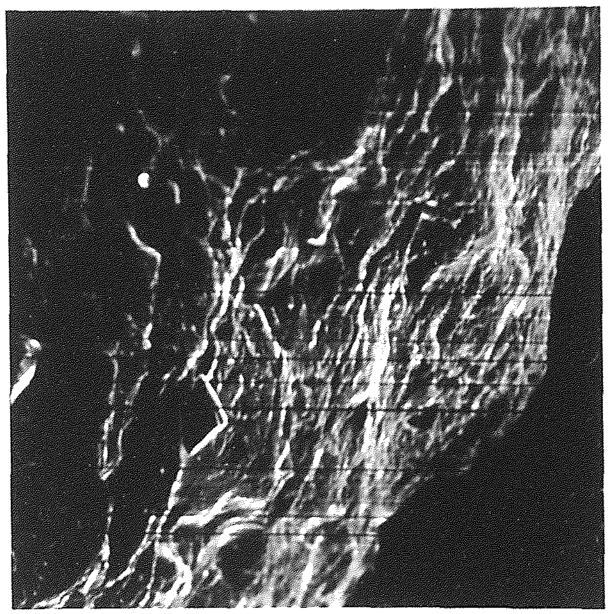

FIGURE 6-18 500X MICROGRAPH OF CUT CA12A
CUTTING CONDITIONS: AFR: 185 GPM
50 KSI WATER PRESSURE
NOZZLE #10
TRAVERSE SPEED: 2 IN./MIN.
20 KEV

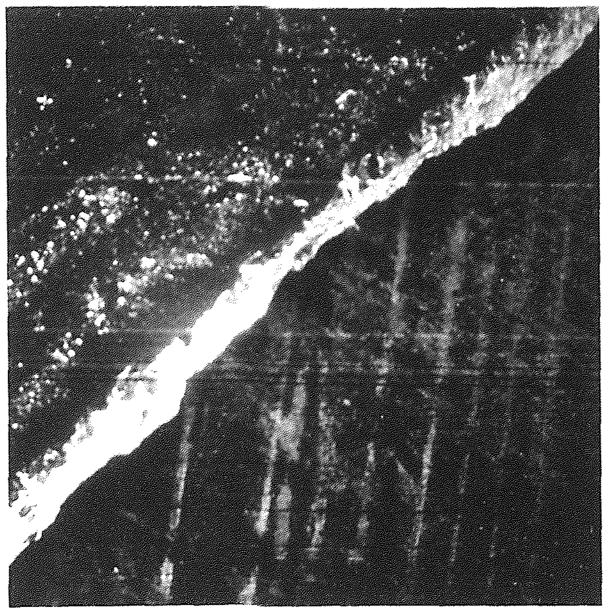

FIGURE 6-19 50X MICROGRAPH OF CUT CA13A
CUTTING CONDITIONS: AFR: 185 GPM
50 KSI WATER PRESSURE
NOZZLE #10
TRAVERSE SPEED: 1 IN./MIN.
20 KEV

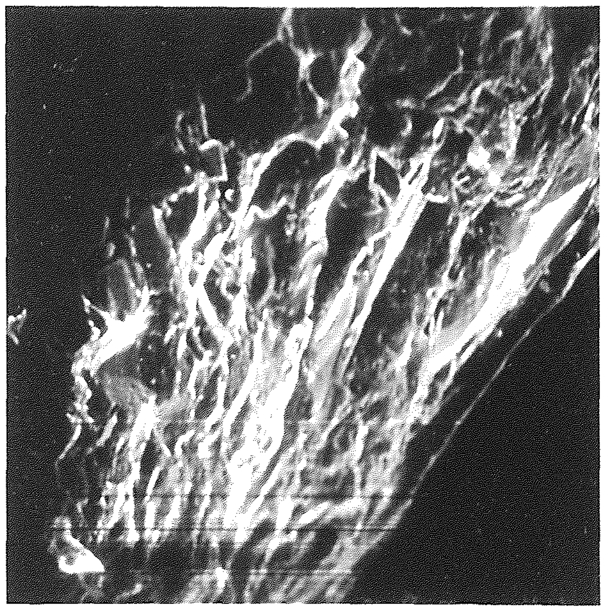

FIGURE 6-20 500X MICROGRAPH OF CUT CA13A
CUTTING CONDITIONS: AFR: 185 GPM
50 KSI WATER PRESSURE
NOZZLE #10
TRAVERSE SPEED: 1 IN./MIN.
20 KEV

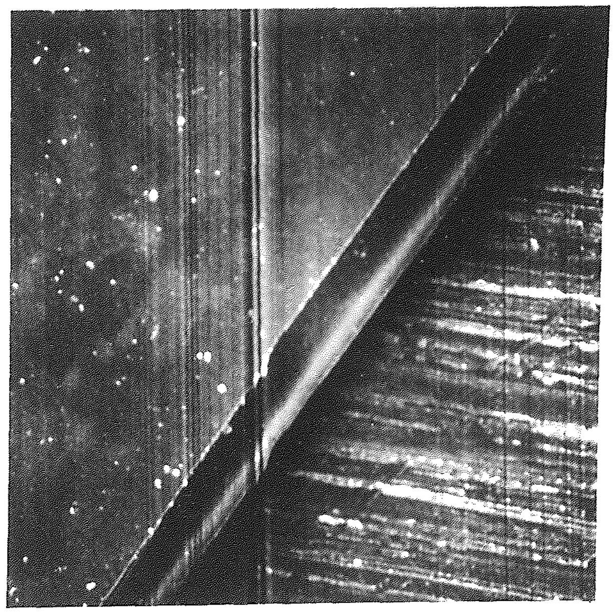

FIGURE 6-21 50X MICROGRAPH OF A CLEAVED SURFACE
20 KEV

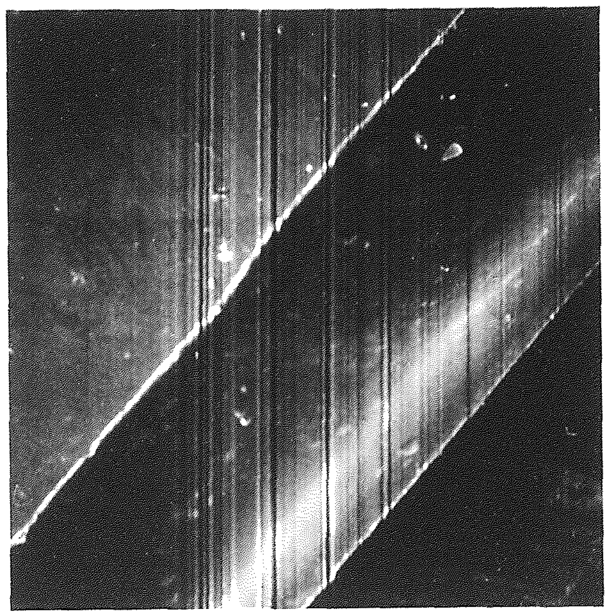

FIGURE 6-22 200X MICROGRAPH OF A CLEAVED SURFACE
20 KEV

APPENDIX B

GRAPHS OF ROUGHNESS VALUES FOR DIFFERENT CUTTING CONDITIONS

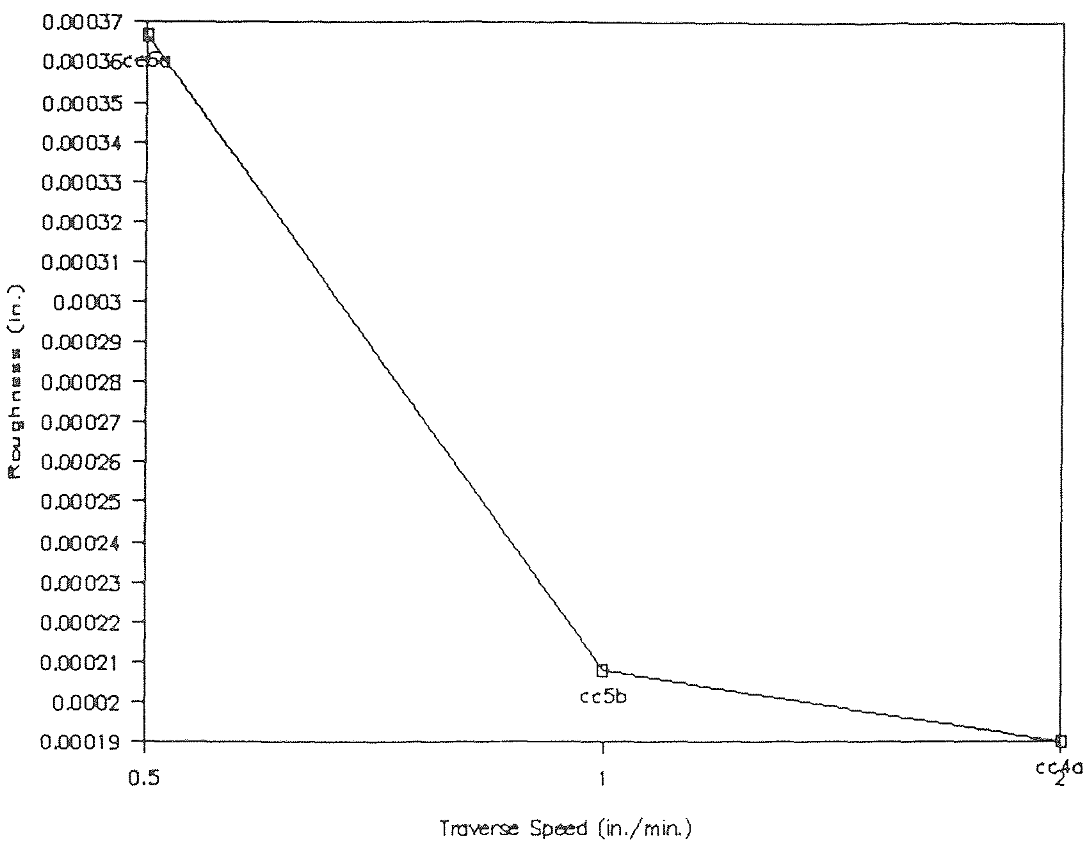

FIGURE 6-23 GRAPH OF ROUGHNESS VS. TRAVERSE SPEED
AFR: 56 GPM
50 KSI
NOZZLE #10
CARBIDE #30

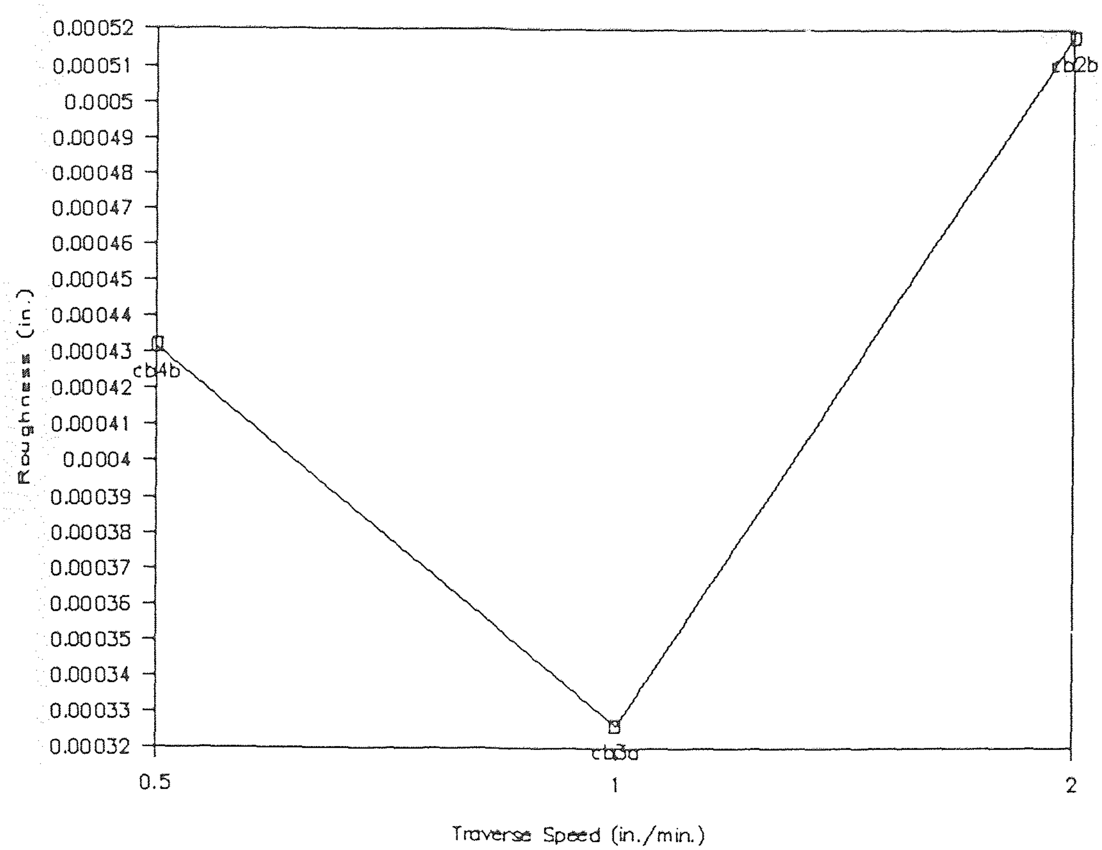

FIGURE 6-24 GRAPH OF ROUGHNESS VS. TRAVERSE SPEED
AFR: 144 GPM
50 KSI
NOZZLE #7
CARBIDE #30

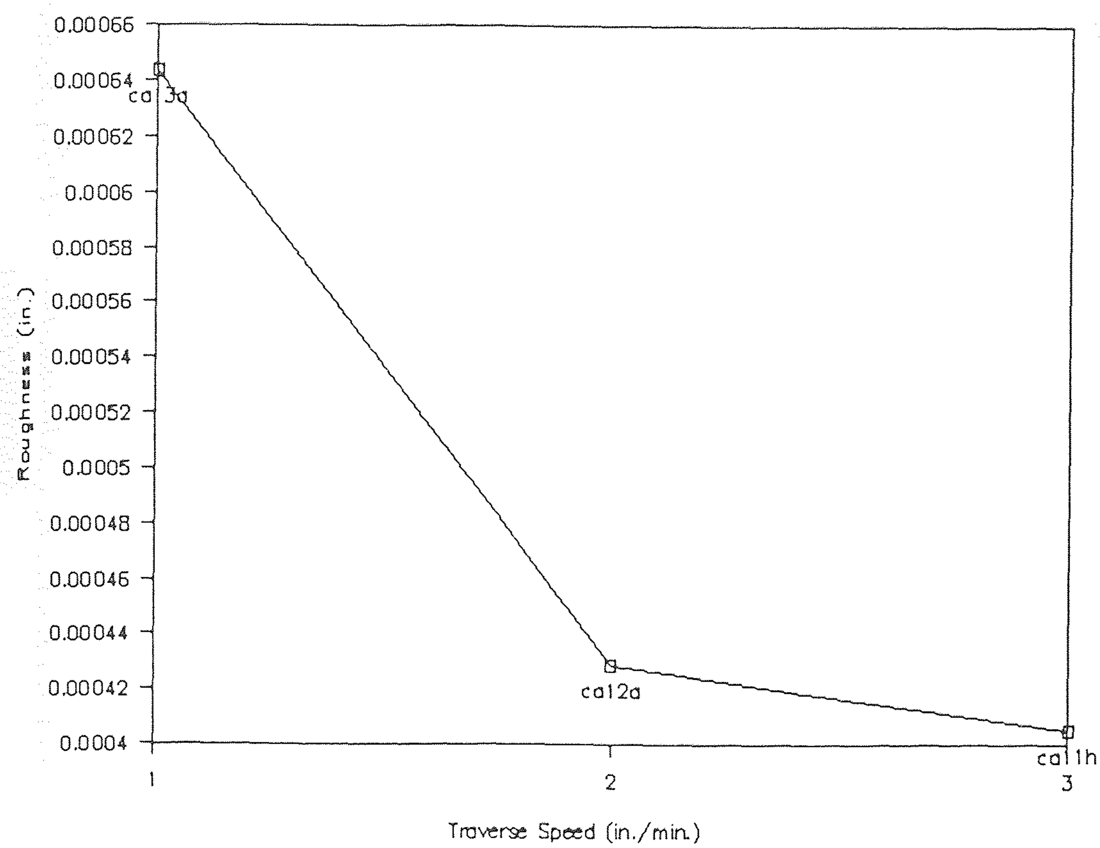

FIGURE 6-25 GRAPH OF ROUGHNESS VS. TRAVERSE SPEED
AFR: 185 GPM
50 KSI
NOZZLE #10
CARBIDE #30

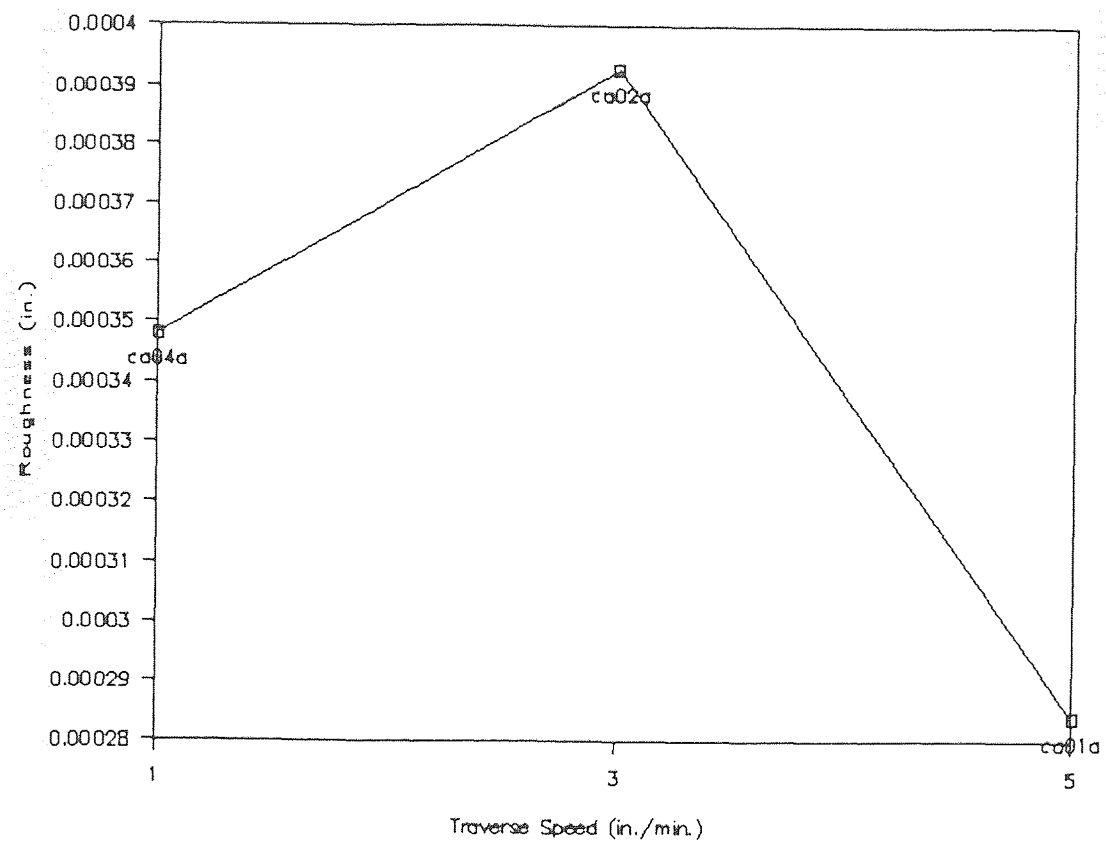

FIGURE 6-26 GRAPH OF ROUGHNESS VS. TRAVERSE SPEED
AFR: 229 GPM
50 KSI
NOZZLE #10
CARBIDE #30

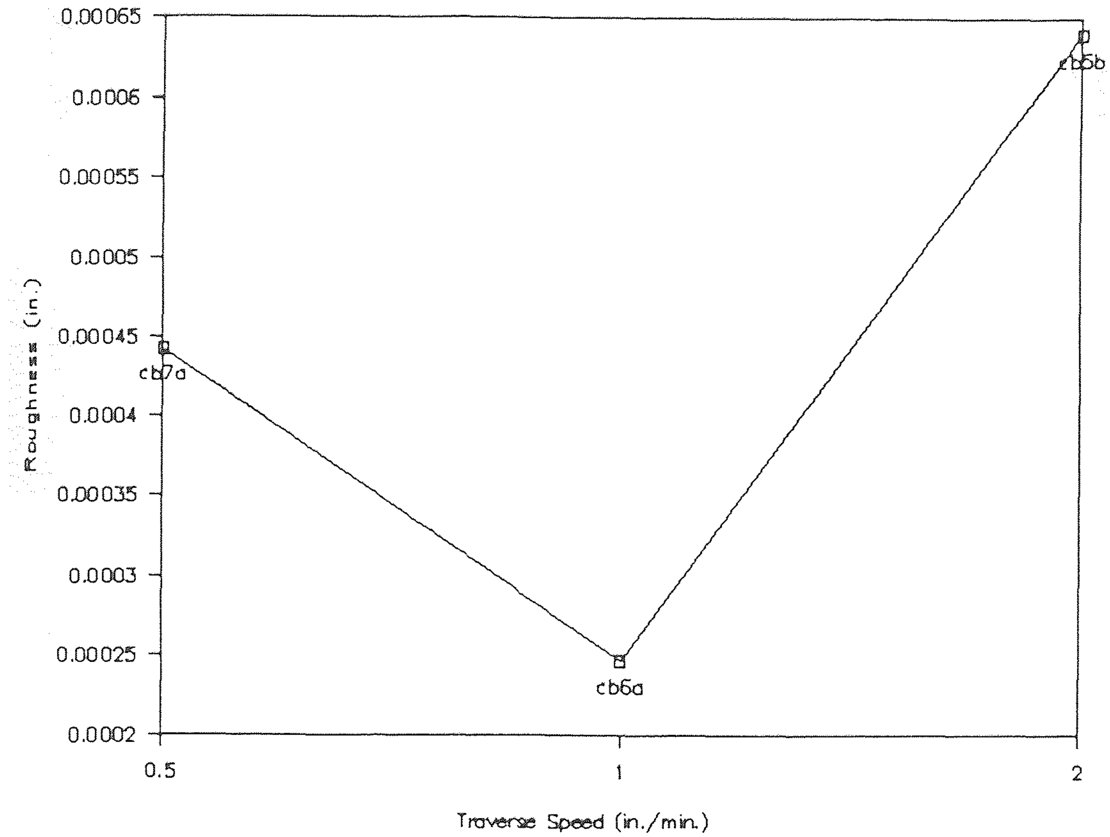

FIGURE 6-27 GRAPH OF ROUGHNESS VS. TRAVERSE SPEED
AFR: 235 GPM
50 KSI
NOZZLE #7
CARBIDE #30

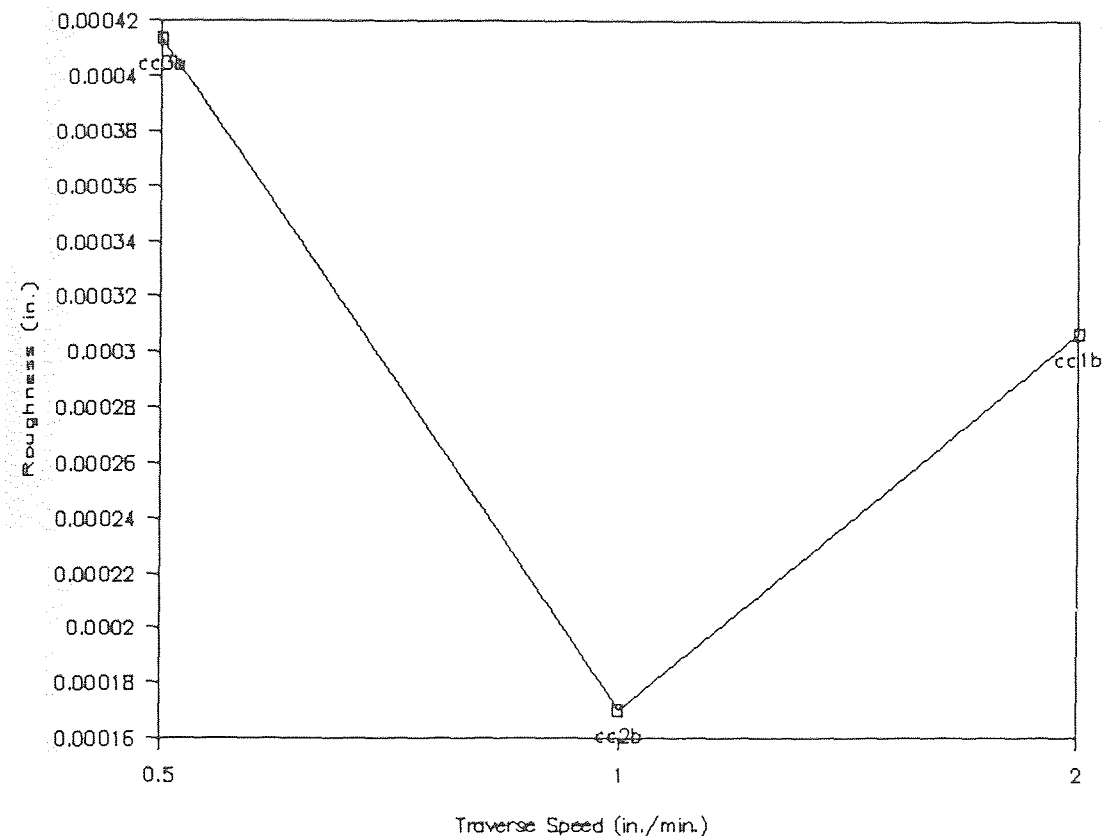

FIGURE 6-28 GRAPH OF ROUGHNESS VS. TRAVERSE SPEED
AFR: 56 GPM
30 KSI
NOZZLE #10
CARBIDE #30

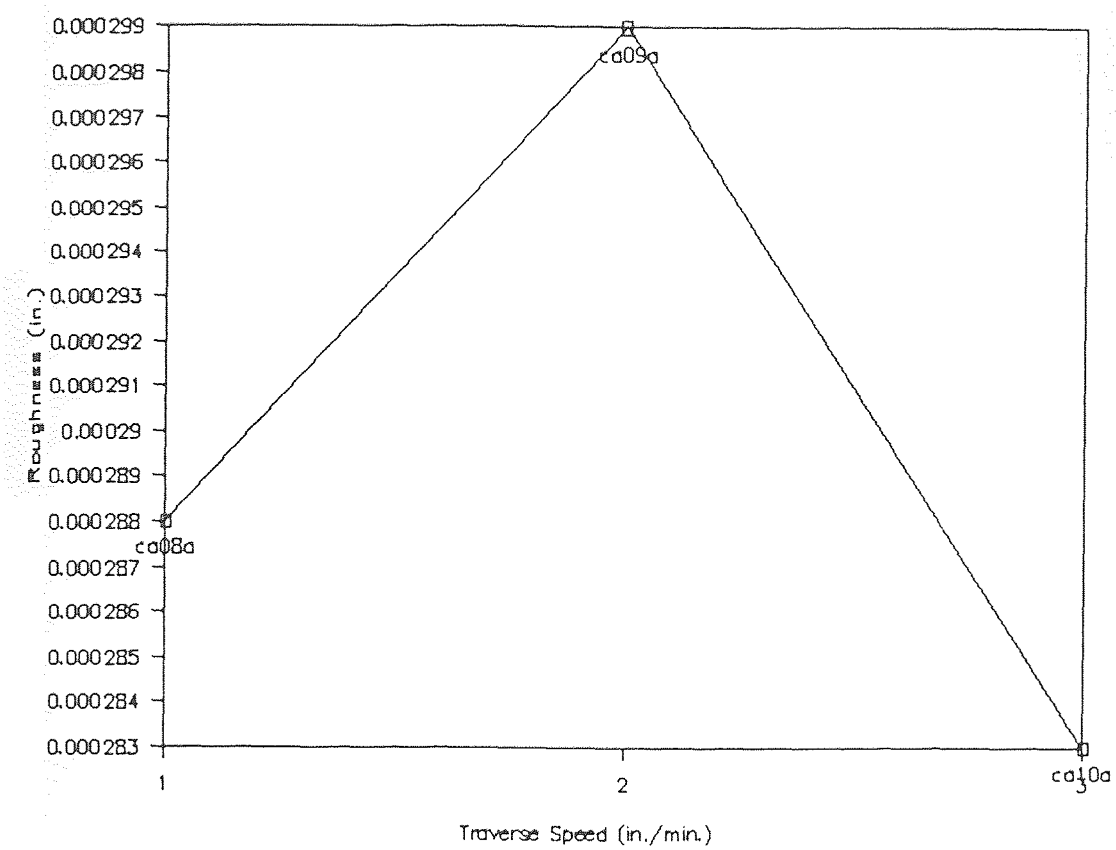

FIGURE 6-29 GRAPH OF ROUGHNESS VS. TRAVERSE SPEED
AFR: 185 GPM
33 KSI
NOZZLE #10
CARBIDE #30

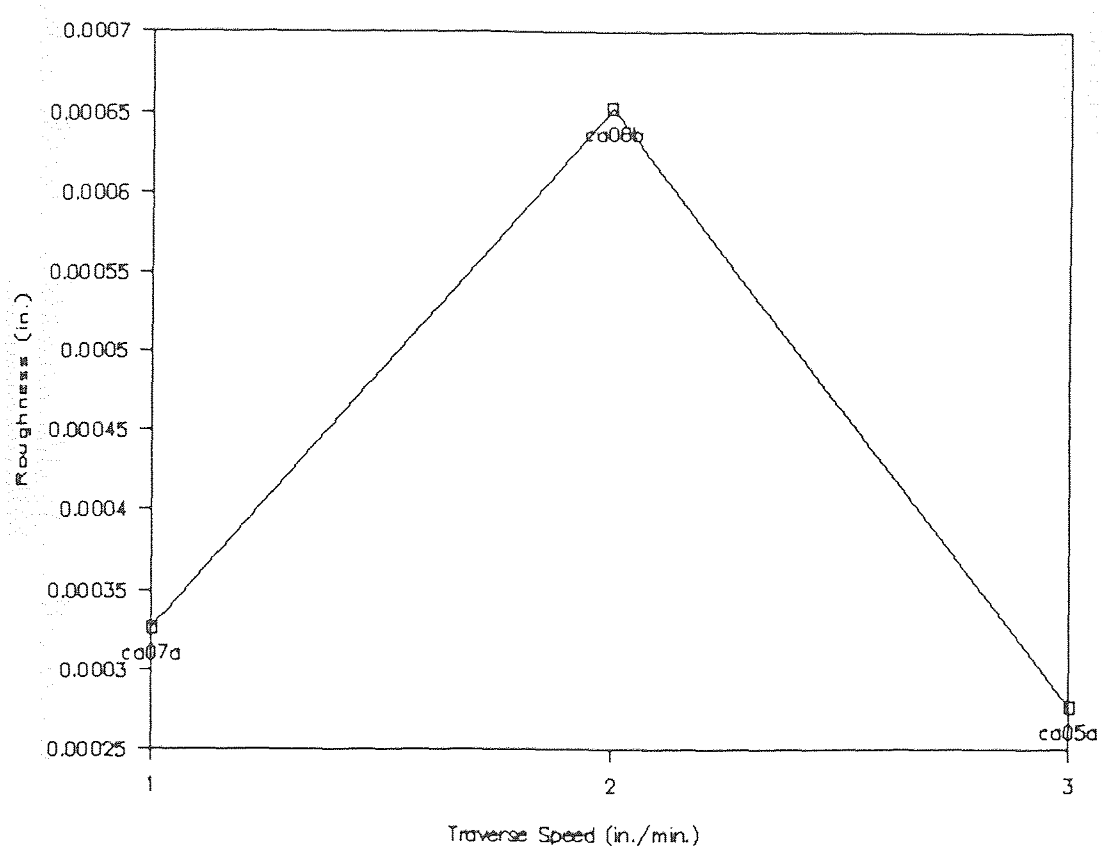

FIGURE 6-30 GRAPH OF ROUGHNESS VS. TRAVERSE SPEED
AFR: 229 GPM
33 KSI
NOZZLE #10
CARBIDE #30

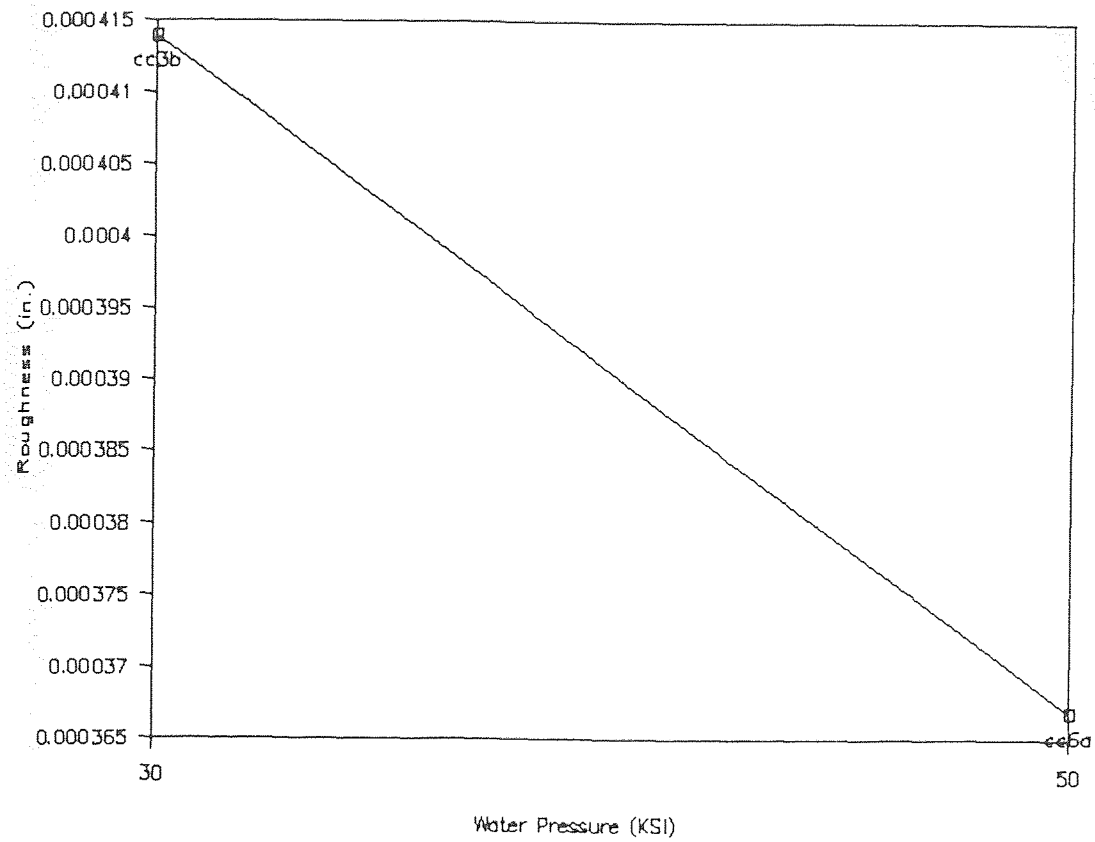

FIGURE 6-31 GRAPH OF ROUGHNESS VS. PRESSURE
AFR: 56 GPM
CARBIDE #30
SPEED: .5 IN/MIN.

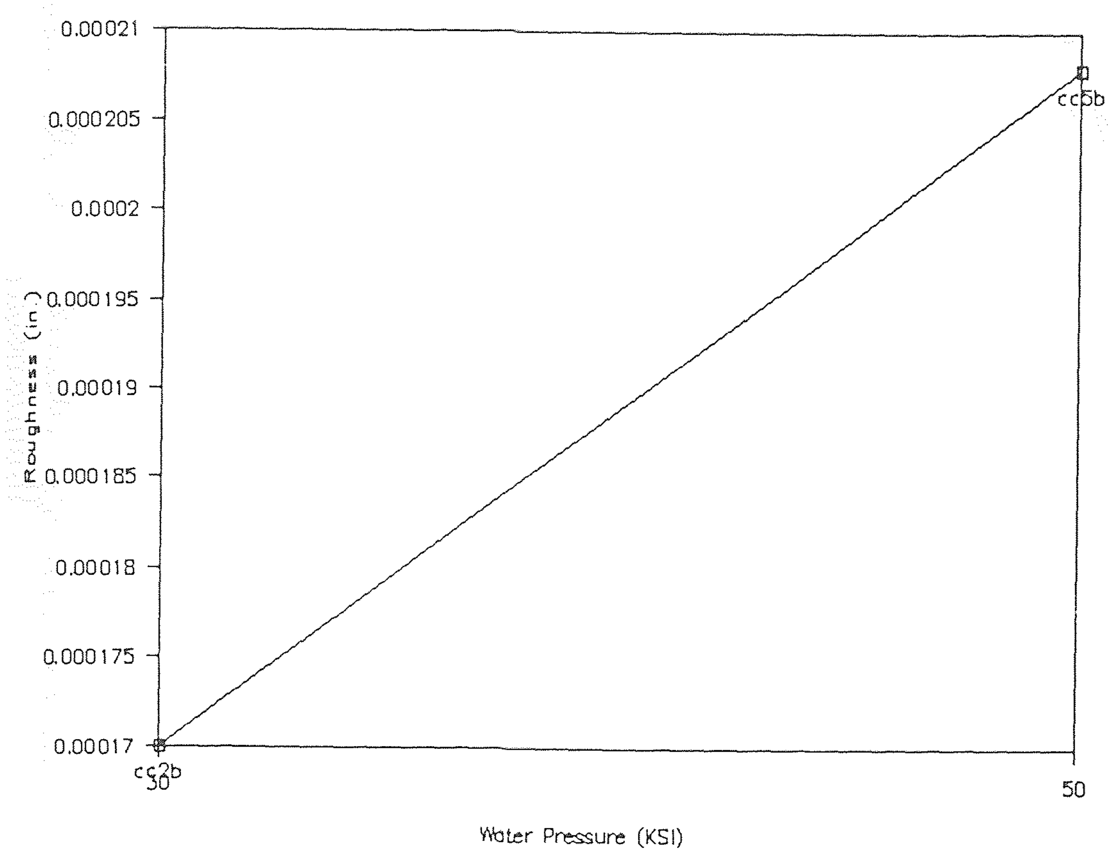

FIGURE 6-32 GRAPH OF ROUGHNESS VS. PRESSURE
AFR: 56 GPM
CARBIDE #30
SPEED: 1 IN/MIN.

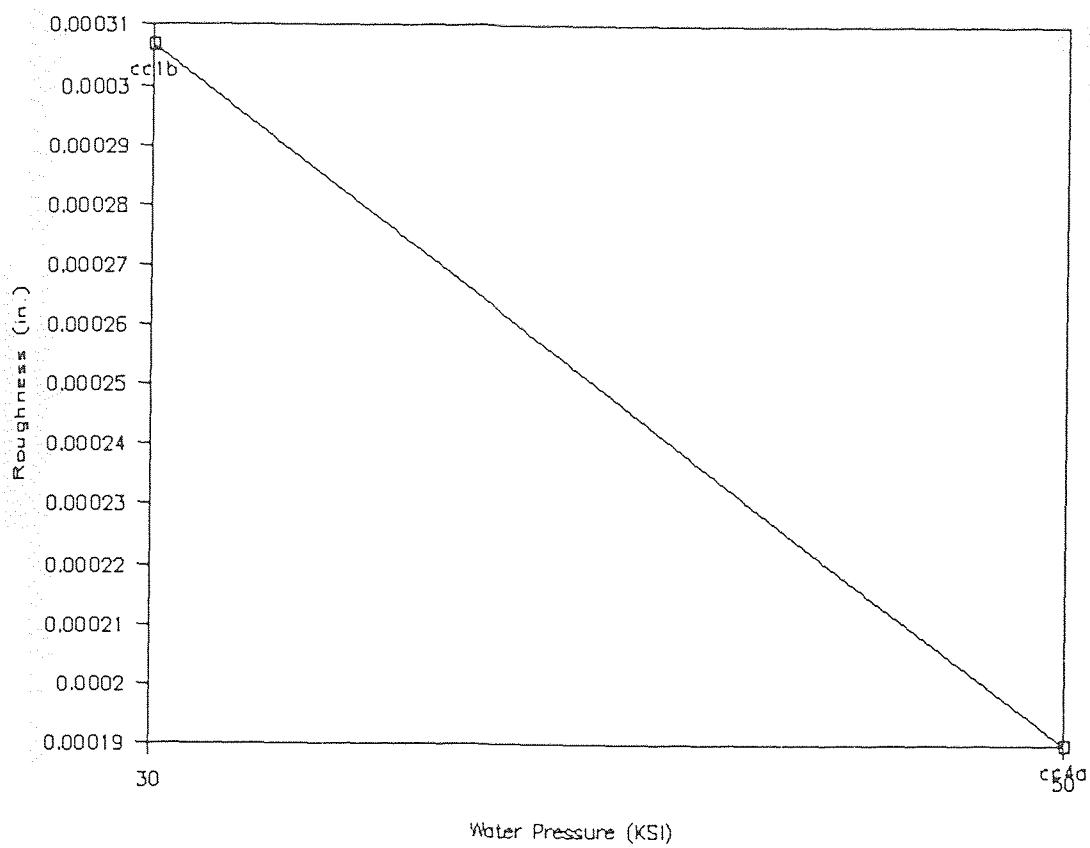

FIGURE 6-33 GRAPH OF ROUGHNESS VS. PRESSURE
AFR: 56 GPM
CARBIDE #30
SPEED: 2 IN/MIN.

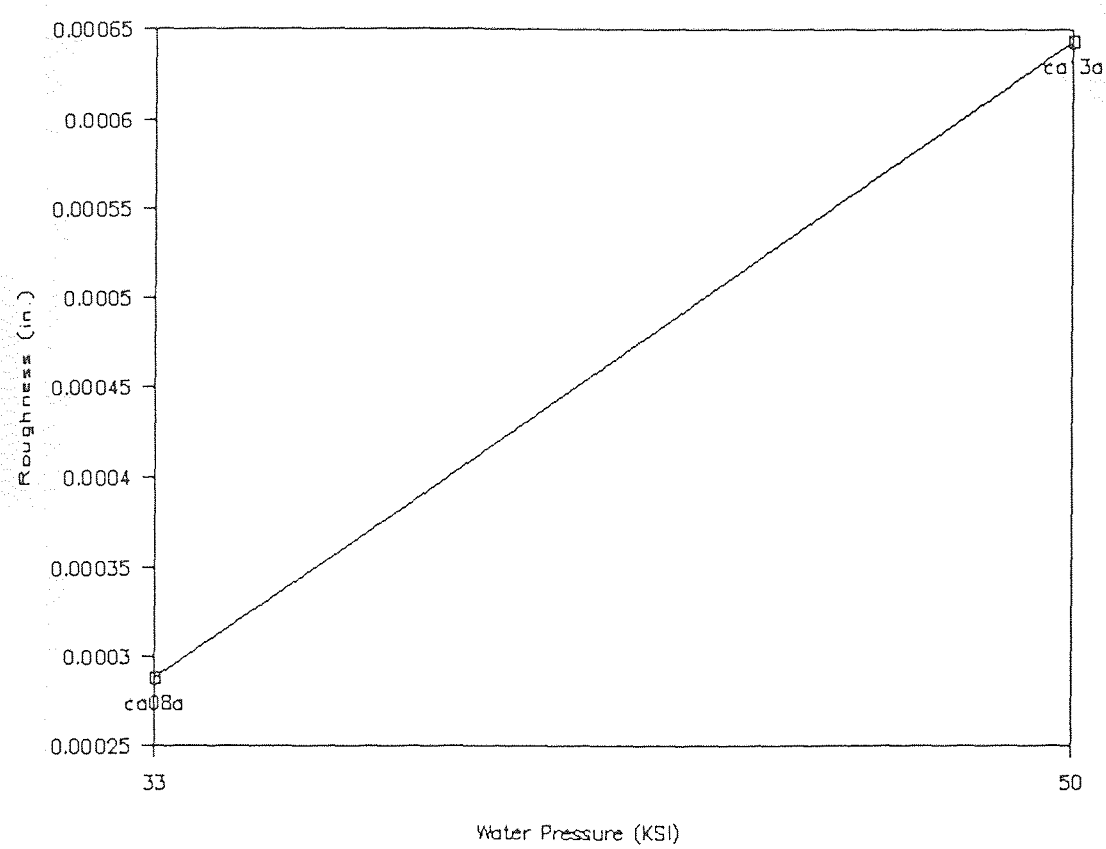

FIGURE 6-34 GRAPH OF ROUGHNESS VS. PRESSURE
AFR: 56 GPM
CARBIDE #30
SPEED: 2 IN/MIN.

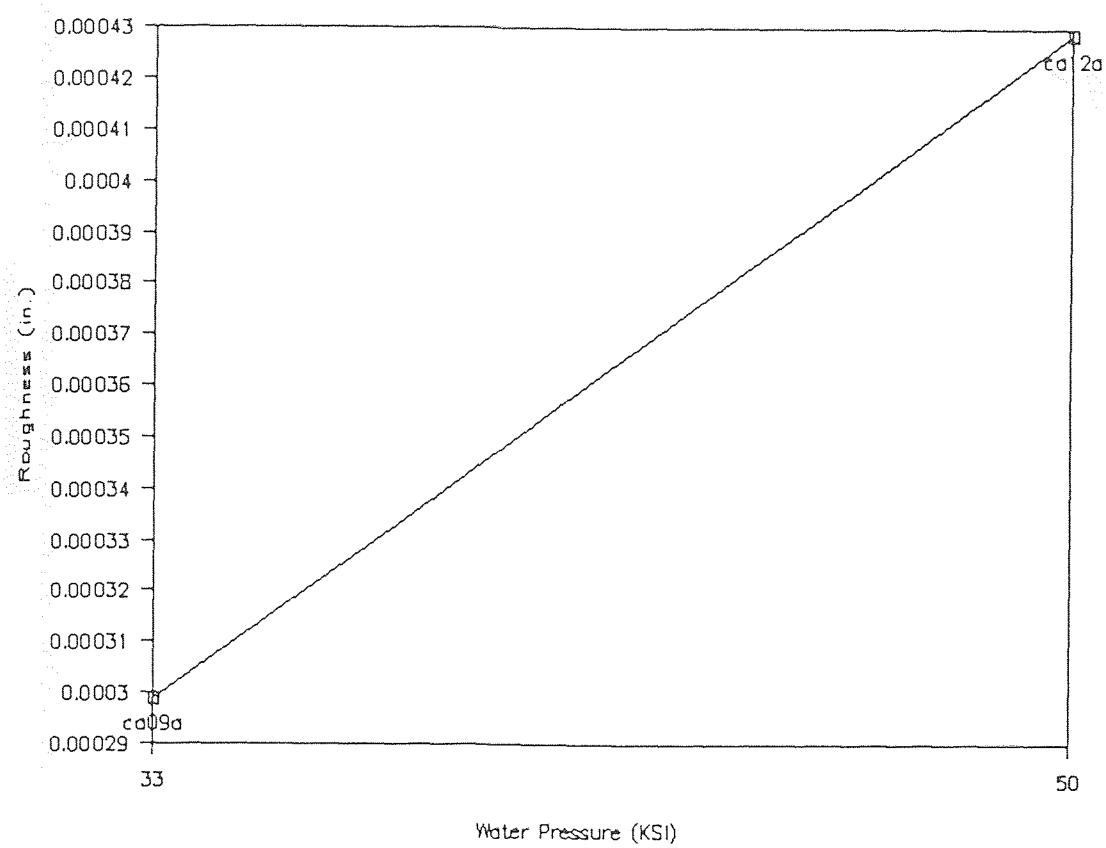

FIGURE 6-35 GRAPH OF ROUGHNESS VS. PRESSURE
AFR: 185 GPM
CARBIDE #30
SPEED: 2 IN/MIN.

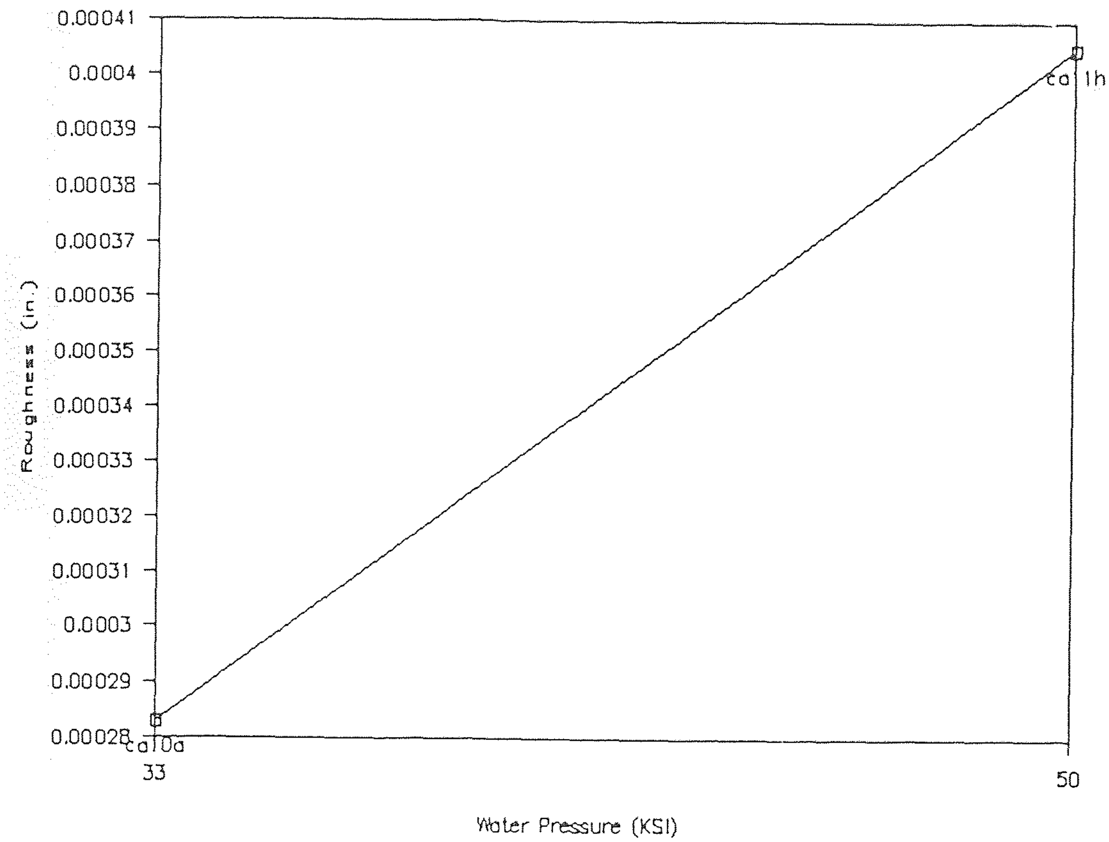

FIGURE 6-36 GRAPH OF ROUGHNESS VS. PRESSURE
AFR: 185 GPM
CARBIDE #30
SPEED: 3 IN/MIN.

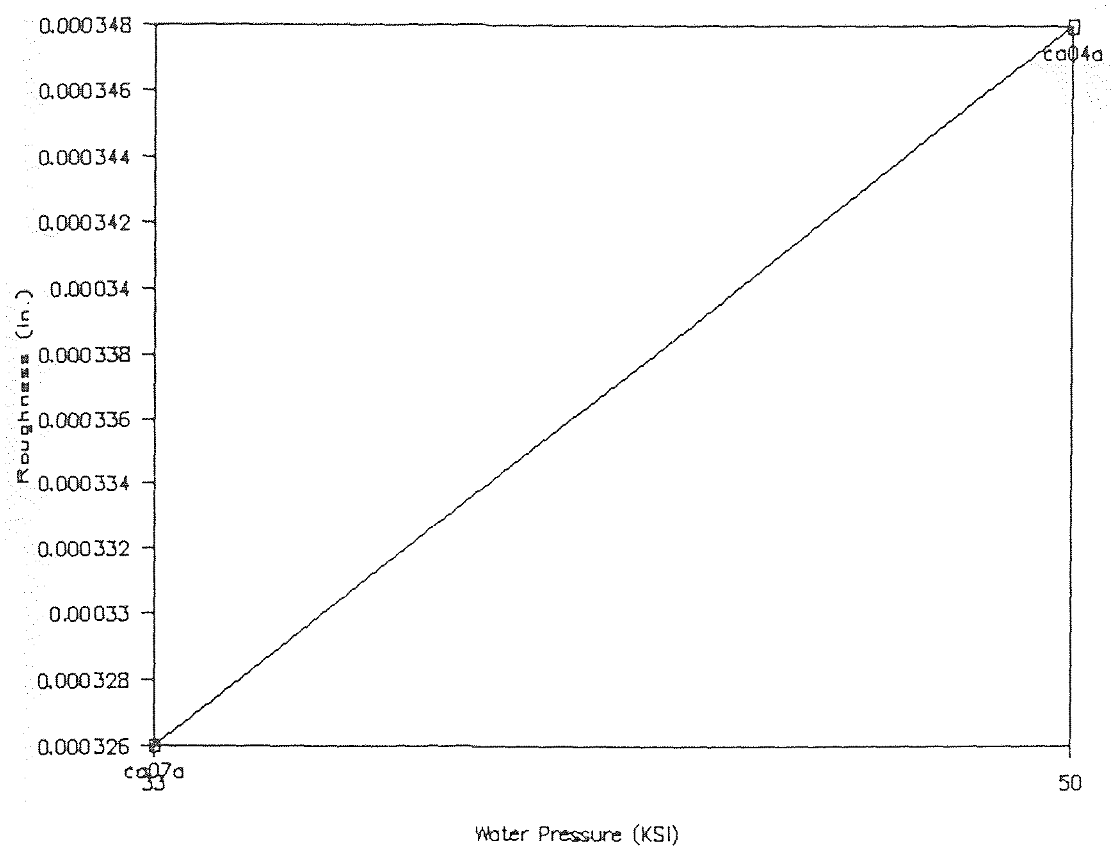

FIGURE 6-37 GRAPH OF ROUGHNESS VS. PRESSURE
AFR: 229 GPM
CARBIDE #30
SPEED: 1 IN/MIN.

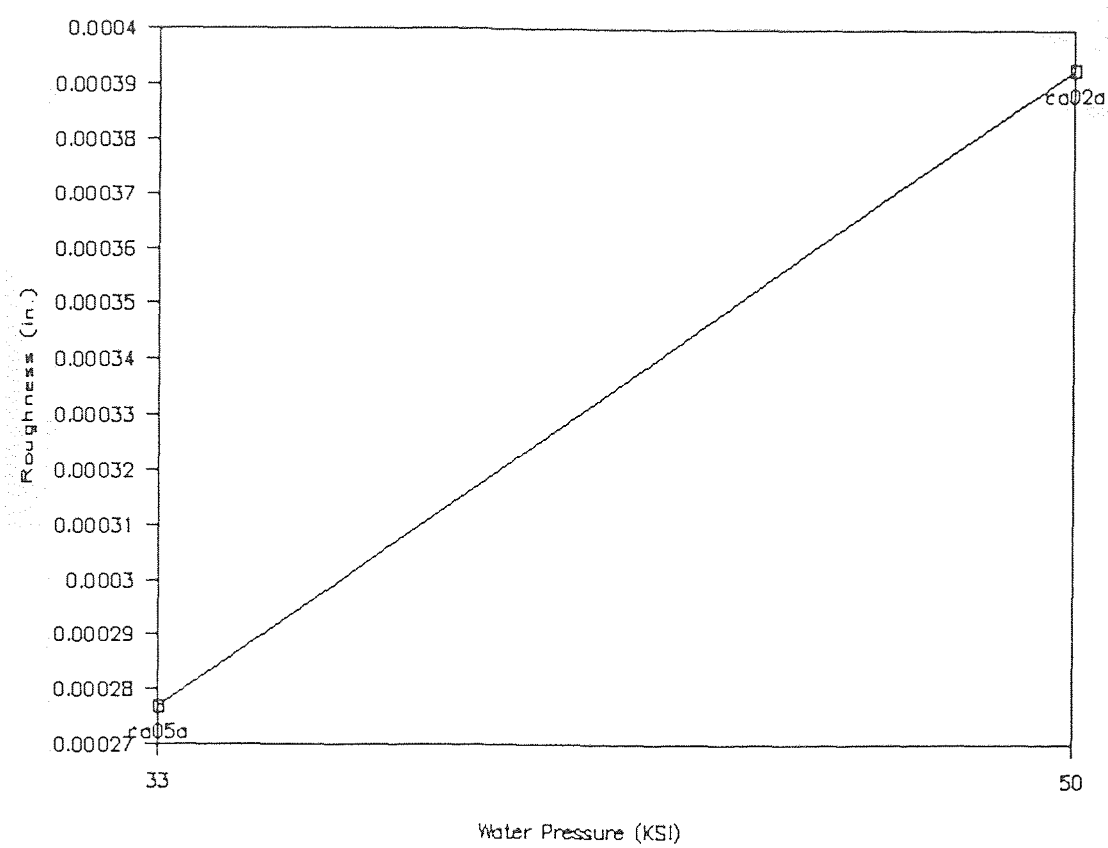

FIGURE 6-38 GRAPH OF ROUGHNESS VS. PRESSURE
AFR: 229 GPM
CARBIDE #30
SPEED: 3 IN/MIN.

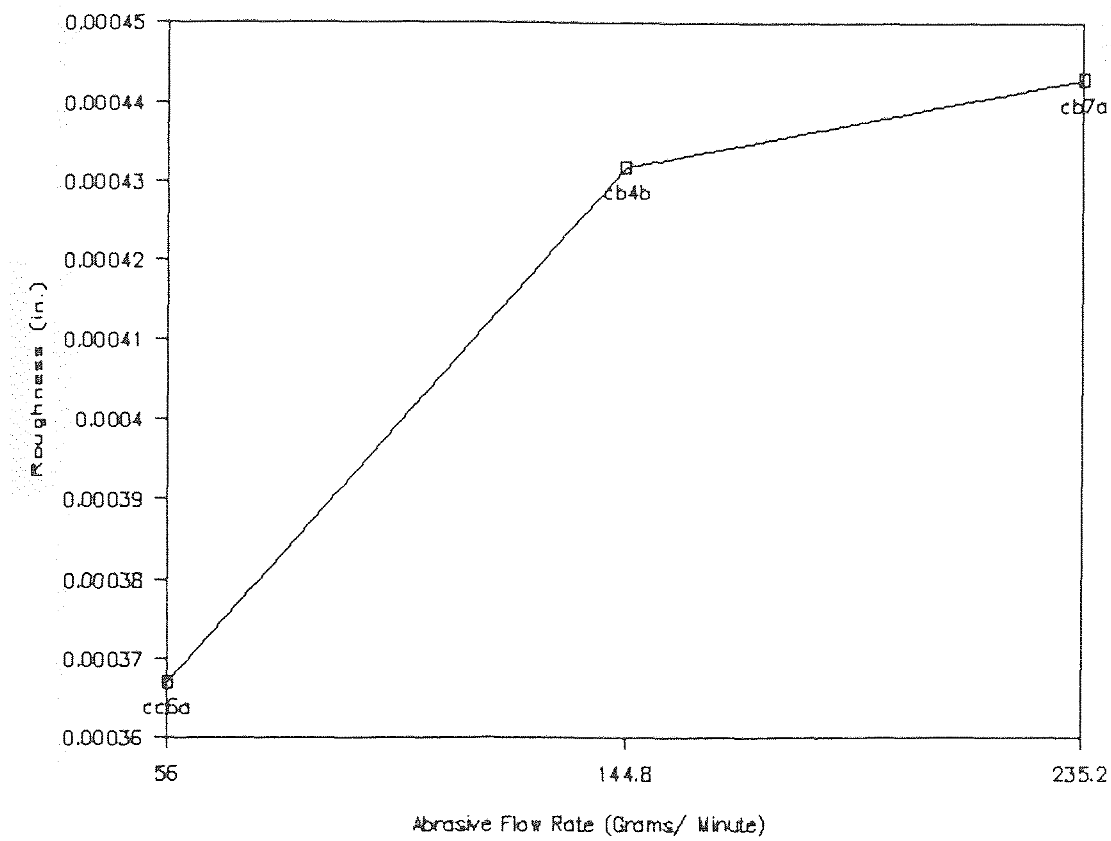

FIGURE 6-39 GRAPH OF ROUGHNESS VS. ABRASIVE FLOW RATE
PRESSURE: 50 KSI
CARBIDE #30
SPEED: .5 IN/MIN.

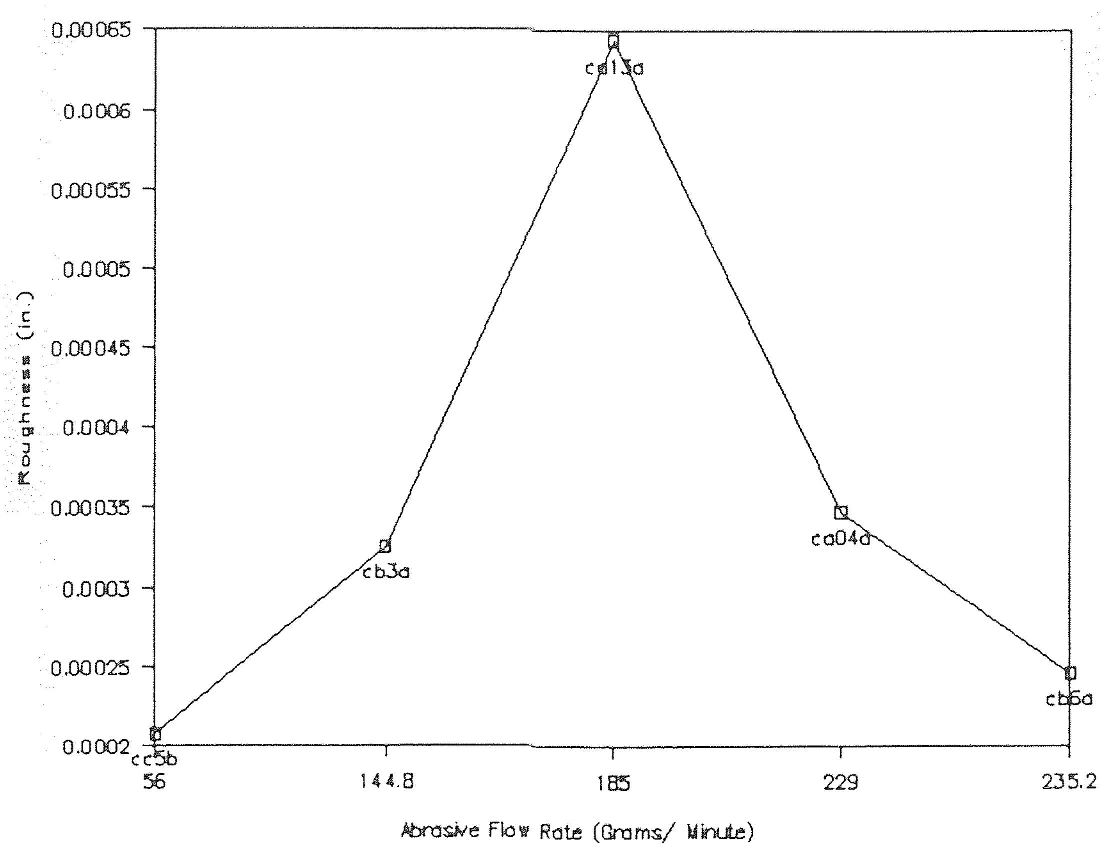

FIGURE 6-40 GRAPH OF ROUGHNESS VS. ABRASIVE FLOW RATE
PRESSURE: 50 KSI
CARBIDE #30
SPEED: 1 IN/MIN.

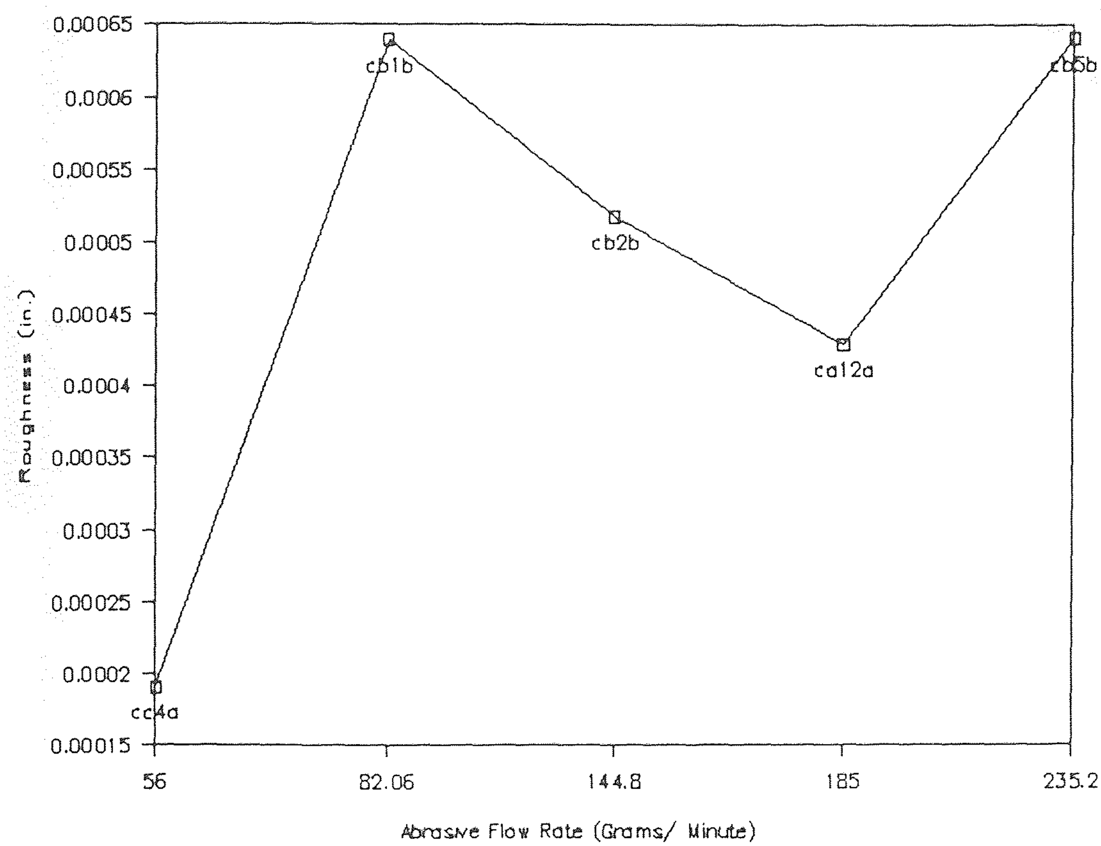

FIGURE 6-41 GRAPH OF ROUGHNESS VS. ABRASIVE FLOW RATE
PRESSURE: 50 KSI
CARBIDE #30
SPEED: 2 IN/MIN.

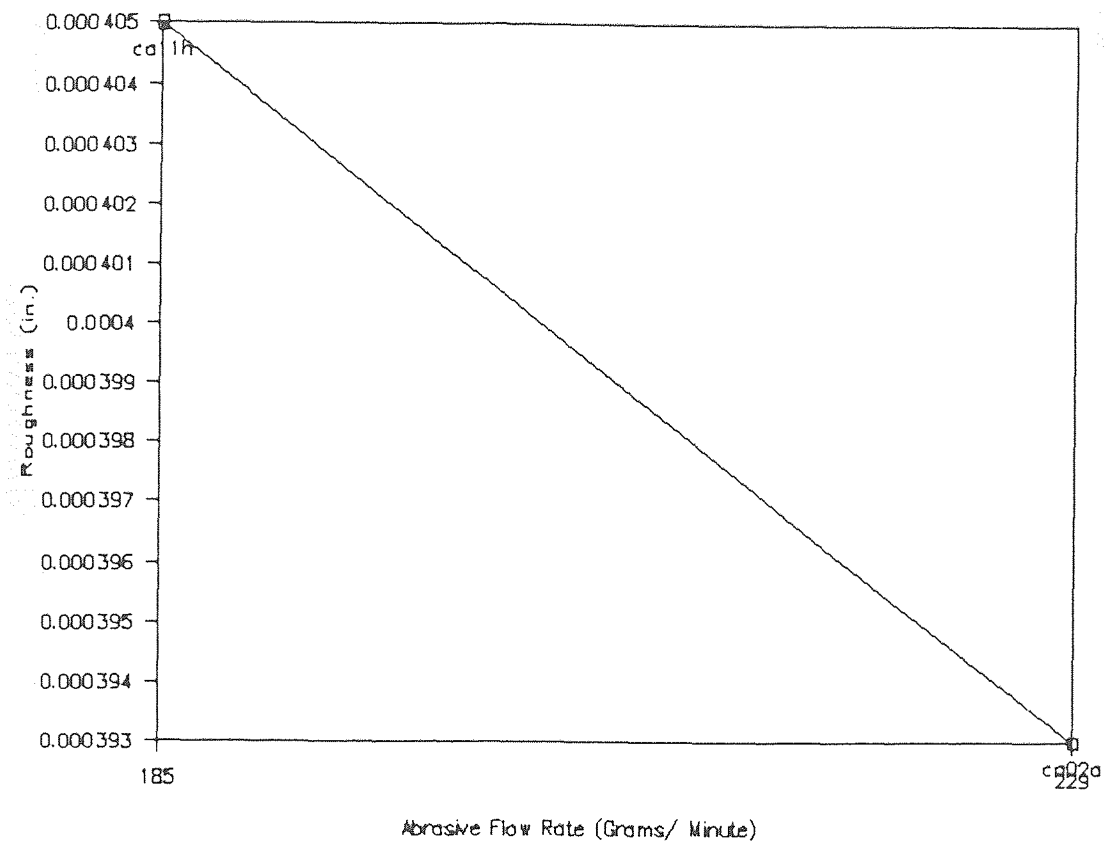

FIGURE 6-42 GRAPH OF ROUGHNESS VS. ABRASIVE FLOW RATE
PRESSURE: 50 KSI
CARBIDE #30
SPEED: 3 IN/MIN.

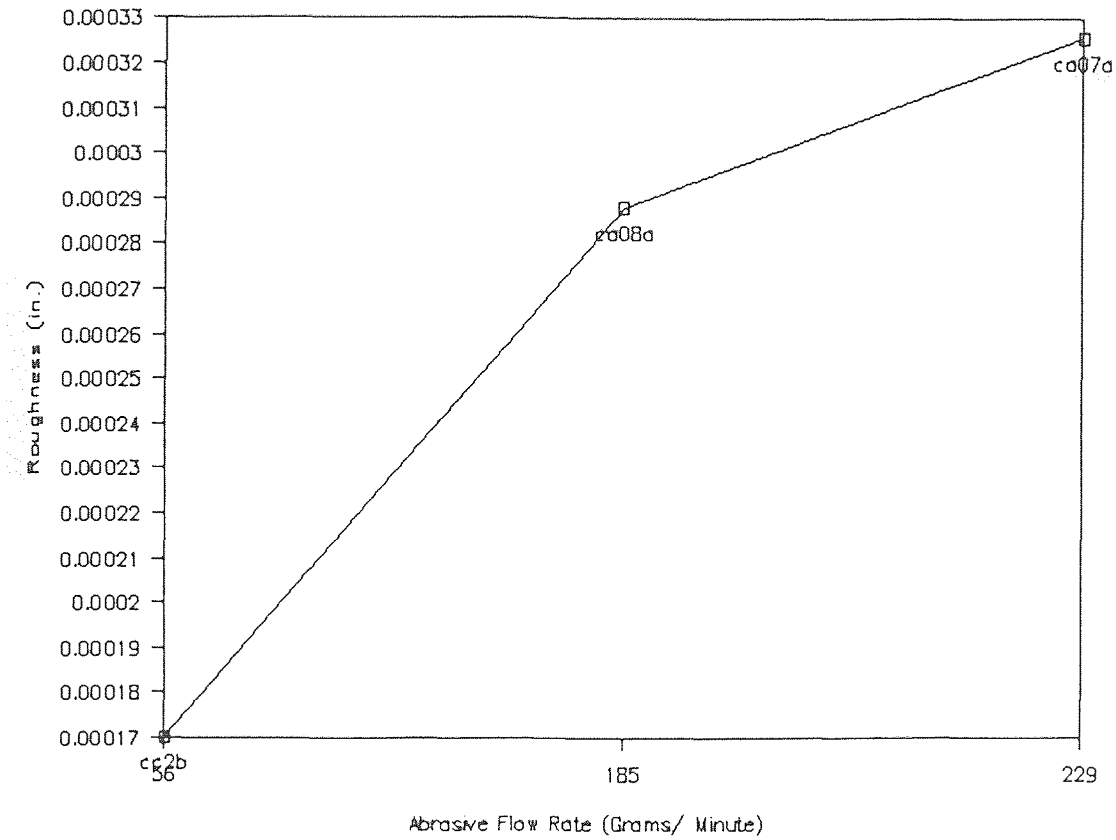

FIGURE 6-43 GRAPH OF ROUGHNESS VS. ABRASIVE FLOW RATE
PRESSURE: 30 KSI
CARBIDE #30
SPEED: 1 IN/MIN.

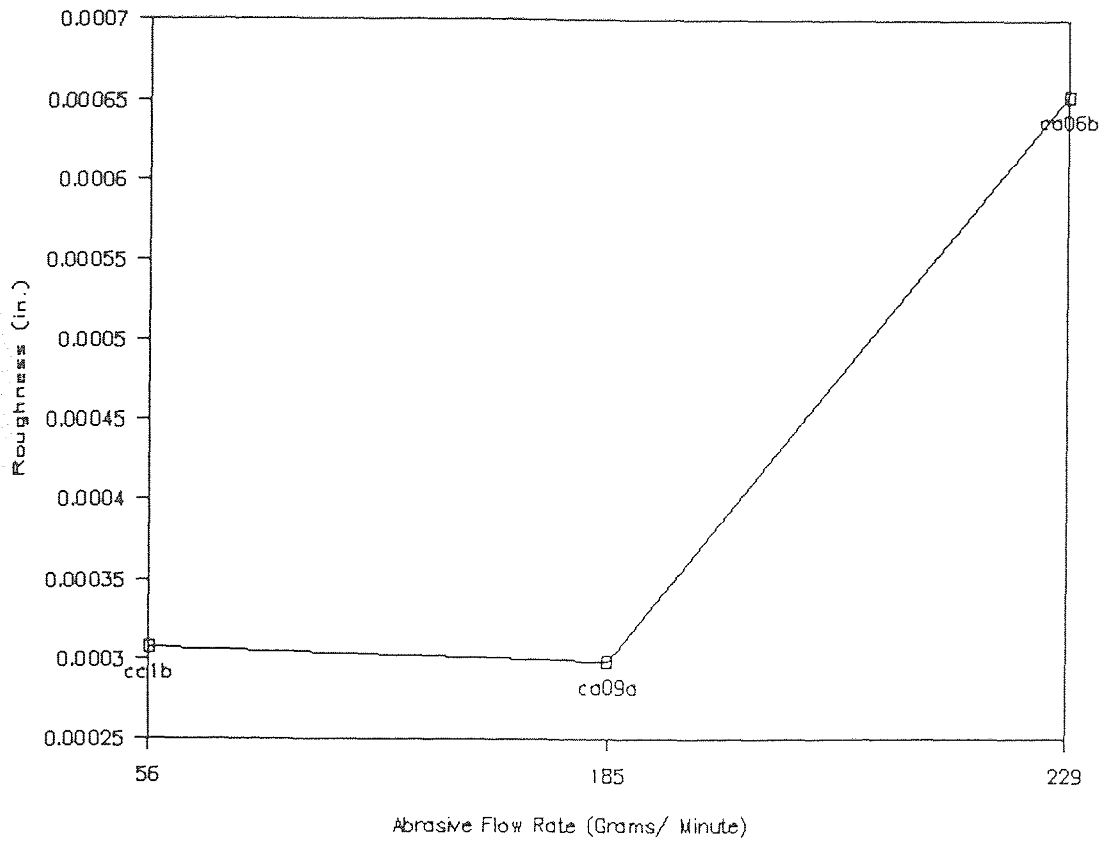

FIGURE 6-44 GRAPH OF ROUGHNESS VS. ABRASIVE FLOW RATE
PRESSURE: 30 KSI
CARBIDE #30
SPEED: 2 IN/MIN.

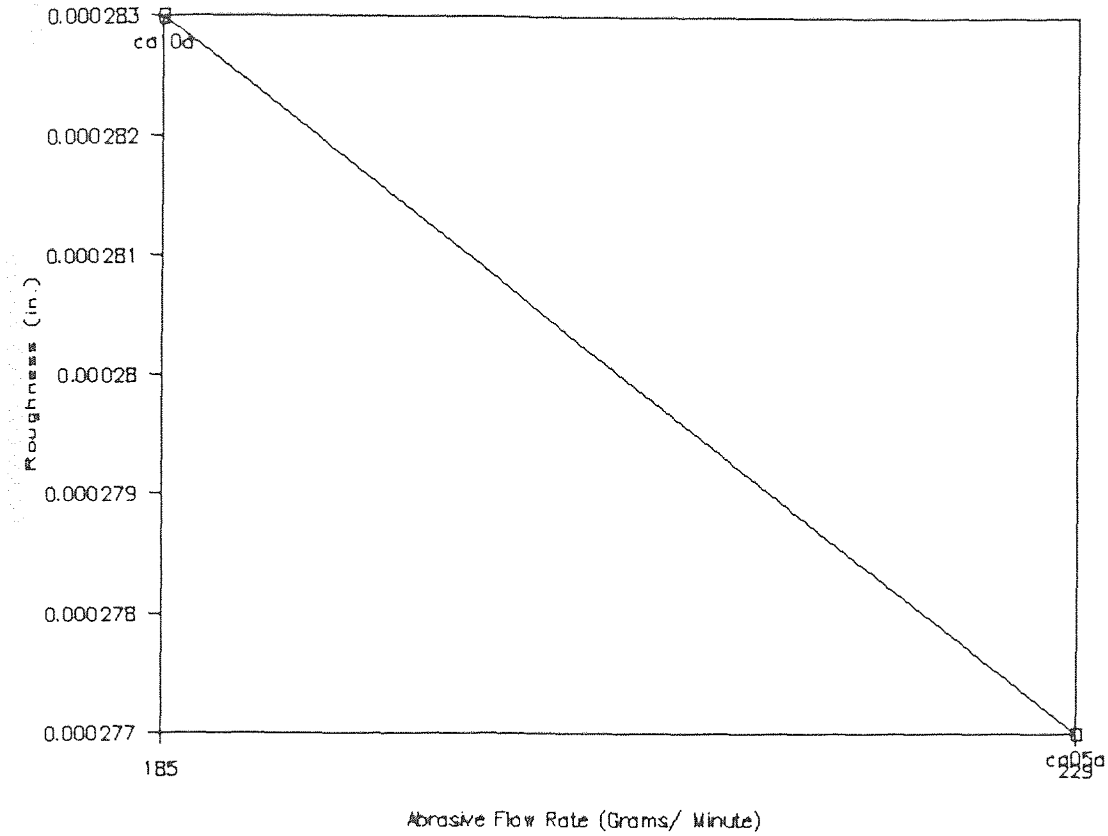

FIGURE 6-45 GRAPH OF ROUGHNESS VS. ABRASIVE FLOW RATE
PRESSURE: 30 KSI
CARBIDE #30
SPEED: 3 IN/MIN.

APPENDIX C

TABLES OF ROUGHNESS MEASUREMENT DATA FROM VIDEOMETRIX ECONOSCOPE

TABLE 6-1 ROUGHNESS MEASUREMENT DATA FOR CUT CA01A

MATRIX VIDEOMETRIX

TOPO TM

Measurement Data

X POSITION	Y POSITION	Z POSITION	ROW	COLUMN
0.00000	0.00000	0.00000	0	0
0.00000	0.00510	0.00022	1	0
0.00000	0.01020	0.00005	2	0
0.00000	0.01531	0.00009	3	0
0.00000	0.02041	0.00003	4	0
0.00000	0.02551	-0.00012	5	0
0.00000	0.03061	0.00016	6	0
0.00000	0.03571	-0.00001	7	0
0.00000	0.04082	0.00036	8	0
0.00000	0.04592	0.00027	9	0
0.00000	0.05102	0.00001	10	0
0.00000	0.05612	-0.00019	11	0
0.00000	0.06122	-0.00012	12	0
0.00000	0.06633	-0.00005	13	0
0.00000	0.07143	-0.00083	14	0
0.00000	0.07653	-0.00094	15	0
0.00000	0.08163	-0.00031	16	0
0.00000	0.08673	0.00006	17	0
0.00000	0.09184	0.00012	18	0
0.00000	0.09694	-0.00013	19	0
0.00000	0.10204	0.00003	20	0
0.00000	0.10714	0.00018	21	0
0.00000	0.11224	-0.00011	22	0
0.00000	0.11735	0.00014	23	0
0.00000	0.12245	0.00014	24	0
0.00000	0.12755	-0.00004	25	0
0.00000	0.13265	0.00000	26	0
0.00000	0.13776	-0.00014	27	0
0.00000	0.14286	0.00001	28	0

TABLE 6-1 ROUGHNESS MEASUREMENT DATA FOR CUT CA01A (CONTINUED)

X POSITION	Y POSITION	Z POSITION	ROW	COLUMN
0.00000	0.14796	0.00005	29	0
0.00000	0.15306	-0.00023	30	0
0.00000	0.15816	-0.00014	31	0
0.00000	0.16327	-0.00044	32	0
0.00000	0.16837	-0.00084	33	0
0.00000	0.17347	-0.00016	34	0
0.00000	0.17857	-0.00030	35	0
0.00000	0.18367	-0.00069	36	0
0.00000	0.18878	-0.00062	37	0
0.00000	0.19388	-0.00056	38	0
0.00000	0.19898	-0.00009	39	0
0.00000	0.20408	-0.00036	40	0
0.00000	0.20918	-0.00034	41	0
0.00000	0.21429	-0.00075	42	0
0.00000	0.21939	-0.00032	43	0
0.00000	0.22449	-0.00113	44	0
0.00000	0.22959	-0.00061	45	0
0.00000	0.23469	-0.00076	46	0
0.00000	0.23980	-0.00045	47	0
0.00000	0.24490	-0.00064	48	0
0.00000	0.25000	-0.00006	49	0

TABLE 6-1 SUMMARY

	X	Y	Z
Total Axis Travel:	.00100	.25000	
# of Focus Points:	1.00000	50.00000	
Step Increments :	.00100	.00510	
Z pioint (MIN) :	-0.00059	.22453	-.00113
(MAX) :	-0.00003	.04082	.00036
(MEAN) :			-.00021

TABLE 6-2 ROUGHNESS MEASUREMENT DATA FOR CUT CA02A

MATRIX VIDEOMETRIX

TOPO TM

Measurement Data

X POSITION	Y POSITION	Z POSITION	ROW	COLUMN
0.00000	0.00000	0.00000	0	0
0.00000	0.00510	0.00001	1	0
0.00000	0.01020	-0.00023	2	0
0.00000	0.01531	0.00041	3	0
0.00000	0.02041	0.00074	4	0
0.00000	0.02551	0.00084	5	0
0.00000	0.03061	0.00067	6	0
0.00000	0.03571	0.00091	7	0
0.00000	0.04082	0.00102	8	0
0.00000	0.04592	0.00089	9	0
0.00000	0.05102	0.00096	10	0
0.00000	0.05612	0.00089	11	0
0.00000	0.06122	0.00041	12	0
0.00000	0.06633	0.00037	13	0
0.00000	0.07143	-0.00023	14	0
0.00000	0.07653	-0.00048	15	0
0.00000	0.08163	-0.00068	16	0
0.00000	0.08673	-0.00052	17	0
0.00000	0.09184	-0.00040	18	0
0.00000	0.09694	-0.00039	19	0
0.00000	0.10204	0.00014	20	0
0.00000	0.10714	0.00046	21	0
0.00000	0.11224	0.00077	22	0
0.00000	0.11735	0.00047	23	0
0.00000	0.12245	0.00046	24	0
0.00000	0.12755	0.00010	25	0
0.00000	0.13265	-0.00025	26	0
0.00000	0.13776	0.00026	27	0
0.00000	0.14286	0.00047	28	0
0.00000	0.14796	0.00041	29	0
0.00000	0.15306	0.00059	30	0
0.00000	0.15816	0.00018	31	0
0.00000	0.16327	-0.00003	32	0
0.00000	0.16837	0.00017	33	0
0.00000	0.17347	0.00026	34	0
0.00000	0.17857	0.00009	35	0
0.00000	0.18367	0.00000	36	0
0.00000	0.18878	-0.00012	37	0

TABLE 6-2 ROUGHNESS MEASUREMENT DATA FOR CUT CA02A (CONTINUED)

X POSITION	Y POSITION	Z POSITION	ROW	COLUMN
0.00000	0.19388	0.00027	38	0
0.00000	0.19898	0.00109	39	0
0.00000	0.20408	0.00100	40	0
0.00000	0.20918	0.00094	41	0
0.00000	0.21429	0.00073	42	0
0.00000	0.21939	0.00008	43	0
0.00000	0.22449	0.00023	44	0
0.00000	0.22959	-0.00010	45	0
0.00000	0.23469	-0.00027	46	0
0.00000	0.23980	-0.00061	47	0
0.00000	0.24490	-0.00011	48	0
0.00000	0.25000	0.00002	49	0

TABLE 6-2 SUMMARY

	X	Y	Z
Total Axis Travel:	.00100	.25000	
# of Focus Points:	1.00000	50.00000	
Step Increments :	.00100	.00510	
Z pioint (MIN) :	-0.00002	.08163	-.00068
(MAX) :	-0.00020	.19901	.00109
(MEAN) :			.00026

TABLE 6-3 ROUGHNESS MEASUREMENT DATA FOR CUT CA04A

MATRIX VIDEOMETRIX

TOPO TM

Measurement Data

X POSITION	Y POSITION	Z POSITION	ROW	COLUMN
0.00000	0.00000	0.00000	0	0
0.00000	0.00510	0.00026	1	0
0.00000	0.01020	0.00058	2	0
0.00000	0.01531	0.00037	3	0
0.00000	0.02041	0.00110	4	0
0.00000	0.02551	0.00136	5	0
0.00000	0.03061	0.00076	6	0
0.00000	0.03571	0.00074	7	0
0.00000	0.04082	0.00075	8	0
0.00000	0.04592	0.00056	9	0
0.00000	0.05102	0.00053	10	0
0.00000	0.05612	-0.00193	11	0
0.00000	0.06122	0.00056	12	0
0.00000	0.06633	0.00113	13	0
0.00000	0.07143	0.00087	14	0
0.00000	0.07653	0.00129	15	0
0.00000	0.08163	0.00113	16	0
0.00000	0.08673	0.00060	17	0
0.00000	0.09184	0.00074	18	0
0.00000	0.09694	0.00065	19	0
0.00000	0.10204	0.00040	20	0
0.00000	0.10714	0.00031	21	0
0.00000	0.11224	0.00050	22	0
0.00000	0.11735	0.00065	23	0
0.00000	0.12245	0.00068	24	0
0.00000	0.12755	0.00068	25	0
0.00000	0.13265	0.00058	26	0
0.00000	0.13776	0.00110	27	0
0.00000	0.14286	0.00095	28	0
0.00000	0.14796	0.00013	29	0
0.00000	0.15306	0.00035	30	0
0.00000	0.15816	0.00040	31	0
0.00000	0.16327	0.00000	32	0
0.00000	0.16837	0.00026	33	0
0.00000	0.17347	0.00063	34	0
0.00000	0.17857	0.00120	35	0
0.00000	0.18367	0.00130	36	0
0.00000	0.18878	0.00131	37	0

TABLE 6-3 ROUGHNESS MEASUREMENT DATA FOR CUT CA04A
(CONTINUED)

X POSITION	Y POSITION	Z POSITION	ROW	COLUMN
0.00000	0.19388	0.00043	38	0
0.00000	0.19898	0.00059	39	0
0.00000	0.20408	0.00096	40	0
0.00000	0.20918	0.00127	41	0
0.00000	0.21429	0.00112	42	0
0.00000	0.21939	0.00087	43	0
0.00000	0.22449	0.00089	44	0
0.00000	0.22959	0.00102	45	0
0.00000	0.23469	0.00109	46	0
0.00000	0.23980	0.00058	47	0
0.00000	0.24490	0.00051	48	0
0.00000	0.25000	-0.00033	49	0

TABLE 6-3 SUMMARY

	X	Y	Z
Total Axis Travel:	.00100	.25000	
# of Focus Points:	1.00000	50.00000	
Step Increments :	.00100	.00510	
Z pioint (MIN) :	-0.00106	.05613	-.00193
(MAX) :	0.00000	.02551	.00136
(MEAN) :			.00065

TABLE 6-4 ROUGHNESS MEASUREMENT DATA FOR CUT CA05A

MATRIX VIDEOMETRIX

TOPO TM

Measurement Data

X POSITION	Y POSITION	Z POSITION	ROW	COLUMN
0.00000	0.00000	0.00000	0	0
0.00000	0.00510	0.00053	1	0
0.00000	0.01020	0.00000	2	0
0.00000	0.01531	0.00001	3	0
0.00000	0.02041	0.00002	4	0
0.00000	0.02551	0.00003	5	0
0.00000	0.03061	0.00046	6	0
0.00000	0.03571	0.00029	7	0
0.00000	0.04082	0.00030	8	0
0.00000	0.04592	0.00073	9	0
0.00000	0.05102	0.00047	10	0
0.00000	0.05612	0.00030	11	0
0.00000	0.06122	0.00019	12	0
0.00000	0.06633	-0.00008	13	0
0.00000	0.07143	-0.00012	14	0
0.00000	0.07653	0.00017	15	0
0.00000	0.08163	0.00023	16	0
0.00000	0.08673	0.00045	17	0
0.00000	0.09184	0.00054	18	0
0.00000	0.09694	-0.00008	19	0
0.00000	0.10204	0.00013	20	0
0.00000	0.10714	0.00016	21	0
0.00000	0.11224	-0.00016	22	0
0.00000	0.11735	0.00015	23	0
0.00000	0.12245	-0.00018	24	0
0.00000	0.12755	-0.00059	25	0
0.00000	0.13265	-0.00045	26	0
0.00000	0.13776	-0.00129	27	0
0.00000	0.14286	-0.00155	28	0
0.00000	0.14796	-0.00010	29	0
0.00000	0.15306	-0.00005	30	0
0.00000	0.15816	-0.00007	31	0
0.00000	0.16327	0.00004	32	0
0.00000	0.16837	-0.00018	33	0
0.00000	0.17347	-0.00077	34	0
0.00000	0.17857	-0.00038	35	0
0.00000	0.18367	-0.00039	36	0
0.00000	0.18878	-0.00029	37	0

TABLE 6-4 ROUGHNESS MEASUREMENT DATA FOR CUT CA05A (CONTINUED)

X POSITION	Y POSITION	Z POSITION	ROW	COLUMN
0.00000	0.19388	-0.00013	38	0
0.00000	0.19898	-0.00009	39	0
0.00000	0.20408	-0.00008	40	0
0.00000	0.20918	0.00036	41	0
0.00000	0.21429	-0.00002	42	0
0.00000	0.21939	0.00000	43	0
0.00000	0.22449	0.00022	44	0
0.00000	0.22959	0.00028	45	0
0.00000	0.23469	0.00009	46	0
0.00000	0.23980	-0.00018	47	0
0.00000	0.24490	-0.00017	48	0
0.00000	0.25000	0.00026	49	0

TABLE 6-4 SUMMARY

	X	Y	Z
Total Axis Travel:	.00100	.25000	
# of Focus Points:	1.00000	50.00000	
Step Increments :	.00100	.00510	
Z pioint (MIN) :	-0.00207	.14286	-.00155
(MAX) :	0.00075	.04592	.00073
(MEAN) :			-.00002

TABLE 6-5 ROUGHNESS MEASUREMENT DATA FOR CUT CA06B

MATRIX VIDEOMETRIX

TOPO TM

Measurement Data

X POSITION	Y POSITION	Z POSITION	ROW	COLUMN
0.00000	0.00000	0.00000	0	0
0.00000	0.00510	-0.00008	1	0
0.00000	0.01020	-0.00038	2	0
0.00000	0.01531	-0.00061	3	0
0.00000	0.02041	-0.00028	4	0
0.00000	0.02551	-0.00003	5	0
0.00000	0.03061	-0.00068	6	0
0.00000	0.03571	-0.00078	7	0
0.00000	0.04082	-0.00047	8	0
0.00000	0.04592	-0.00042	9	0
0.00000	0.05102	-0.00075	10	0
0.00000	0.05612	-0.00052	11	0
0.00000	0.06122	-0.00099	12	0
0.00000	0.06633	-0.00155	13	0
0.00000	0.07143	-0.00083	14	0
0.00000	0.07653	-0.00083	15	0
0.00000	0.08163	-0.00129	16	0
0.00000	0.08673	-0.00145	17	0
0.00000	0.09184	-0.00176	18	0
0.00000	0.09694	-0.00195	19	0
0.00000	0.10204	-0.00161	20	0
0.00000	0.10714	-0.00132	21	0
0.00000	0.11224	-0.00122	22	0
0.00000	0.11735	-0.00126	23	0
0.00000	0.12245	-0.00180	24	0
0.00000	0.12755	-0.00143	25	0
0.00000	0.13265	-0.00167	26	0
0.00000	0.13776	-0.00135	27	0
0.00000	0.14286	-0.00159	28	0
0.00000	0.14796	-0.00184	29	0
0.00000	0.15306	-0.00209	30	0
0.00000	0.15816	-0.00168	31	0
0.00000	0.16327	-0.00151	32	0
0.00000	0.16837	-0.00145	33	0
0.00000	0.17347	-0.00155	34	0
0.00000	0.17857	-0.00163	35	0
0.00000	0.18367	-0.00222	36	0
0.00000	0.18878	-0.00234	37	0

TABLE 6-5 ROUGHNESS MEASUREMENT DATA FOR CUT CA06B
(CONTINUED)

X POSITION	Y POSITION	Z POSITION	ROW	COLUMN
0.00000	0.19388	-0.00149	38	0
0.00000	0.19898	-0.00228	39	0
0.00000	0.20408	-0.00188	40	0
0.00000	0.20918	-0.00242	41	0
0.00000	0.21429	-0.00229	42	0
0.00000	0.21939	-0.00257	43	0
0.00000	0.22449	-0.00293	44	0
0.00000	0.22959	-0.00315	45	0
0.00000	0.23469	-0.00294	46	0
0.00000	0.23980	-0.00303	47	0
0.00000	0.24490	-0.00249	48	0
0.00000	0.25000	-0.00284	49	0

TABLE 6-5 SUMMARY

	X	Y	Z
Total Axis Travel:	.00100	.25000	
# of Focus Points:	1.00000	50.00000	
Step Increments :	.00100	.00510	
Z pioint (MIN) :	0.00000	.22957	-.00315
(MAX) :	0.00000	.00000	.00000
(MEAN) :			-.00151

TABLE 6-6 ROUGHNESS MEASUREMENT DATA FOR CUT CA07A

MATRIX VIDEOMETRIX

TOPO TM

Measurement Data

X POSITION	Y POSITION	Z POSITION	ROW	COLUMN
0.00000	0.00000	0.00000	0	0
0.00000	0.00510	-0.00153	1	0
0.00000	0.01020	-0.00133	2	0
0.00000	0.01531	-0.00157	3	0
0.00000	0.02041	-0.00135	4	0
0.00000	0.02551	-0.00133	5	0
0.00000	0.03061	-0.00158	6	0
0.00000	0.03571	-0.00133	7	0
0.00000	0.04082	-0.00127	8	0
0.00000	0.04592	-0.00148	9	0
0.00000	0.05102	-0.00148	10	0
0.00000	0.05612	-0.00127	11	0
0.00000	0.06122	-0.00150	12	0
0.00000	0.06633	-0.00197	13	0
0.00000	0.07143	-0.00169	14	0
0.00000	0.07653	-0.00159	15	0
0.00000	0.08163	-0.00167	16	0
0.00000	0.08673	-0.00113	17	0
0.00000	0.09184	-0.00113	18	0
0.00000	0.09694	-0.00167	19	0
0.00000	0.10204	-0.00167	20	0
0.00000	0.10714	-0.00194	21	0
0.00000	0.11224	-0.00180	22	0
0.00000	0.11735	-0.00236	23	0
0.00000	0.12245	-0.00137	24	0
0.00000	0.12755	-0.00188	25	0
0.00000	0.13265	-0.00180	26	0
0.00000	0.13776	-0.00231	27	0
0.00000	0.14286	-0.00211	28	0
0.00000	0.14796	-0.00211	29	0
0.00000	0.15306	-0.00141	30	0
0.00000	0.15816	-0.00142	31	0
0.00000	0.16327	-0.00151	32	0
0.00000	0.16837	-0.00167	33	0
0.00000	0.17347	-0.00143	34	0
0.00000	0.17857	-0.00179	35	0
0.00000	0.18367	-0.00177	36	0
0.00000	0.18878	-0.00197	37	0

TABLE 6-6 ROUGHNESS MEASUREMENT DATA FOR CUT CA07A (CONTINUED)

X POSITION	Y POSITION	Z POSITION	ROW	COLUMN
0.00000	0.19388	-0.00225	38	0
0.00000	0.19898	-0.00227	39	0
0.00000	0.20408	-0.00215	40	0
0.00000	0.20918	-0.00227	41	0
0.00000	0.21429	-0.00194	42	0
0.00000	0.21939	-0.00285	43	0
0.00000	0.22449	-0.00221	44	0
0.00000	0.22959	-0.00198	45	0
0.00000	0.23469	-0.00191	46	0
0.00000	0.23980	-0.00214	47	0
0.00000	0.24490	-0.00164	48	0
0.00000	0.25000	-0.00166	49	0

TABLE 6-6 SUMMARY

	X	Y	Z
Total Axis Travel:	.00100	.25000	
# of Focus Points:	1.00000	50.00000	
Step Increments :	.00100	.00510	
Z pioint (MIN) :	0.00000	.21939	-.00285
(MAX) :	0.00000	.01531	.00000
(MEAN) :			-.00171

TABLE 6-7 ROUGHNESS MEASUREMENT DATA FOR CUT CA08A

MATRIX VIDEOMETRIX

TOPO TM

Measurement Data

X POSITION	Y POSITION	Z POSITION	ROW	COLUMN
0.00000	0.00000	0.00000	0	0
0.00000	0.00510	-0.00000	1	0
0.00000	0.01020	0.00017	2	0
0.00000	0.01531	0.00030	3	0
0.00000	0.02041	0.00010	4	0
0.00000	0.02551	-0.00009	5	0
0.00000	0.03061	0.00025	6	0
0.00000	0.03571	0.00023	7	0
0.00000	0.04082	0.00042	8	0
0.00000	0.04592	0.00053	9	0
0.00000	0.05102	0.00050	10	0
0.00000	0.05612	0.00071	11	0
0.00000	0.06122	0.00063	12	0
0.00000	0.06633	0.00038	13	0
0.00000	0.07143	0.00017	14	0
0.00000	0.07653	0.00004	15	0
0.00000	0.08163	-0.00027	16	0
0.00000	0.08673	-0.00043	17	0
0.00000	0.09184	-0.00067	18	0
0.00000	0.09694	-0.00084	19	0
0.00000	0.10204	-0.00047	20	0
0.00000	0.10714	-0.00046	21	0
0.00000	0.11224	-0.00017	22	0
0.00000	0.11735	0.00022	23	0
0.00000	0.12245	0.00020	24	0
0.00000	0.12755	0.00015	25	0
0.00000	0.13265	-0.00005	26	0
0.00000	0.13776	-0.00021	27	0
0.00000	0.14286	-0.00039	28	0
0.00000	0.14796	-0.00042	29	0
0.00000	0.15306	-0.00015	30	0
0.00000	0.15816	-0.00041	31	0
0.00000	0.16327	-0.00049	32	0
0.00000	0.16837	-0.00045	33	0
0.00000	0.17347	0.00000	34	0
0.00000	0.17857	0.00003	35	0
0.00000	0.18367	-0.00021	36	0
0.00000	0.18878	-0.00040	37	0

TABLE 6-7 ROUGHNESS MEASUREMENT DATA FOR CUT CA08A (CONTINUED)

X POSITION	Y POSITION	Z POSITION	ROW	COLUMN
0.00000	0.19388	-0.00053	38	0
0.00000	0.19898	-0.00028	39	0
0.00000	0.20408	-0.00026	40	0
0.00000	0.20918	-0.00029	41	0
0.00000	0.21429	-0.00013	42	0
0.00000	0.21939	-0.00015	43	0
0.00000	0.22449	-0.00009	44	0
0.00000	0.22959	-0.00034	45	0
0.00000	0.23469	-0.00059	46	0
0.00000	0.23980	-0.00017	47	0
0.00000	0.24490	-0.00044	48	0
0.00000	0.25000	-0.00043	49	0

TABLE 6-7 SUMMARY

	X	Y	Z
Total Axis Travel:	.00100	.25000	
# of Focus Points:	1.00000	50.00000	
Step Increments :	.00100	.00510	
Z pioint (MIN) :	-0.00003	.09695	-.00084
(MAX) :	-0.00004	.05616	.00071
(MEAN) :			-.00010

TABLE 6-8 ROUGHNESS MEASUREMENT DATA FOR CUT CA09A

MATRIX VIDEOMETRIX

TOPO TM

Measurement Data

X POSITION	Y POSITION	Z POSITION	ROW	COLUMN
0.00000	0.00000	0.00000	0	0
0.00000	0.00510	-0.00023	1	0
0.00000	0.01020	-0.00012	2	0
0.00000	0.01531	-0.00030	3	0
0.00000	0.02041	-0.00007	4	0
0.00000	0.02551	-0.00022	5	0
0.00000	0.03061	-0.00038	6	0
0.00000	0.03571	0.00025	7	0
0.00000	0.04082	-0.00015	8	0
0.00000	0.04592	-0.00003	9	0
0.00000	0.05102	-0.00005	10	0
0.00000	0.05612	-0.00032	11	0
0.00000	0.06122	-0.00001	12	0
0.00000	0.06633	-0.00037	13	0
0.00000	0.07143	-0.00007	14	0
0.00000	0.07653	-0.00025	15	0
0.00000	0.08163	-0.00008	16	0
0.00000	0.08673	0.00002	17	0
0.00000	0.09184	-0.00048	18	0
0.00000	0.09694	-0.00029	19	0
0.00000	0.10204	0.00035	20	0
0.00000	0.10714	-0.00048	21	0
0.00000	0.11224	0.00004	22	0
0.00000	0.11735	0.00032	23	0
0.00000	0.12245	0.00019	24	0
0.00000	0.12755	-0.00008	25	0
0.00000	0.13265	0.00003	26	0
0.00000	0.13776	0.00033	27	0
0.00000	0.14286	-0.00017	28	0
0.00000	0.14796	-0.00035	29	0
0.00000	0.15306	0.00030	30	0
0.00000	0.15816	-0.00013	31	0
0.00000	0.16327	-0.00046	32	0
0.00000	0.16837	-0.00017	33	0
0.00000	0.17347	0.00013	34	0
0.00000	0.17857	-0.00002	35	0
0.00000	0.18367	-0.00037	36	0
0.00000	0.18878	0.00032	37	0

TABLE 6-8 ROUGHNESS MEASUREMENT DATA FOR CUT CA09A (CONTINUED)

X POSITION	Y POSITION	Z POSITION	ROW	COLUMN
0.00000	0.19388	0.00038	38	0
0.00000	0.19898	0.00041	39	0
0.00000	0.20408	0.00014	40	0
0.00000	0.20918	-0.00006	41	0
0.00000	0.21429	0.00288	42	0
0.00000	0.21939	0.00046	43	0
0.00000	0.22449	0.00022	44	0
0.00000	0.22959	-0.00039	45	0
0.00000	0.23469	0.00027	46	0
0.00000	0.23980	0.00031	47	0
0.00000	0.24490	0.00066	48	0
0.00000	0.25000	0.00041	49	0

TABLE 6-8 SUMMARY

	X	Y	Z
Total Axis Travel:	.00100	.25000	
# of Focus Points:	1.00000	50.00000	
Step Increments :	.00100	.00510	
Z pioint (MIN) :	0.00007	.10714	-.00048
(MAX) :	-0.00084	.21429	.00288
(MEAN) :			-.00005

TABLE 6-9 ROUGHNESS MEASUREMENT DATA FOR CUT CA10A

MATRIX VIDEOMETRIX

TOPO TM

Measurement Data

X POSITION	Y POSITION	Z POSITION	ROW	COLUMN
0.00000	0.00000	0.00000	0	0
0.00000	0.00510	-0.00024	1	0
0.00000	0.01020	-0.00002	2	0
0.00000	0.01531	-0.00014	3	0
0.00000	0.02041	0.00021	4	0
0.00000	0.02551	0.00020	5	0
0.00000	0.03061	-0.00004	6	0
0.00000	0.03571	0.00013	7	0
0.00000	0.04082	-0.00049	8	0
0.00000	0.04592	-0.00167	9	0
0.00000	0.05102	-0.00169	10	0
0.00000	0.05612	-0.00020	11	0
0.00000	0.06122	-0.00060	12	0
0.00000	0.06633	0.00032	13	0
0.00000	0.07143	-0.00010	14	0
0.00000	0.07653	0.00064	15	0
0.00000	0.08163	-0.00010	16	0
0.00000	0.08673	0.00008	17	0
0.00000	0.09184	0.00043	18	0
0.00000	0.09694	0.00028	19	0
0.00000	0.10204	0.00026	20	0
0.00000	0.10714	0.00040	21	0
0.00000	0.11224	0.00045	22	0
0.00000	0.11735	0.00031	23	0
0.00000	0.12245	0.00033	24	0
0.00000	0.12755	-0.00020	25	0
0.00000	0.13265	0.00003	26	0
0.00000	0.13776	0.00001	27	0
0.00000	0.14286	-0.00016	28	0
0.00000	0.14796	0.00007	29	0
0.00000	0.15306	-0.00031	30	0
0.00000	0.15816	-0.00057	31	0
0.00000	0.16327	-0.00039	32	0
0.00000	0.16837	-0.00004	33	0
0.00000	0.17347	0.00013	34	0
0.00000	0.17857	-0.00025	35	0
0.00000	0.18367	0.00006	36	0
0.00000	0.18878	0.00007	37	0

TABLE 6-9 ROUGHNESS MEASUREMENT DATA FOR CUT CA10A
(CONTINUED)

X POSITION	Y POSITION	Z POSITION	ROW	COLUMN
0.00000	0.19388	0.00016	38	0
0.00000	0.19898	0.00004	39	0
0.00000	0.20408	0.00014	40	0
0.00000	0.20918	-0.00030	41	0
0.00000	0.21429	-0.00000	42	0
0.00000	0.21939	-0.00003	43	0
0.00000	0.22449	0.00018	44	0
0.00000	0.22959	0.00032	45	0
0.00000	0.23469	0.00043	46	0
0.00000	0.23980	0.00027	47	0
0.00000	0.24490	-0.00011	48	0
0.00000	0.25000	0.00037	49	0

TABLE 6-9 SUMMARY

	X	Y	Z
Total Axis Travel:	.00100	.25000	
# of Focus Points:	1.00000	50.00000	
Step Increments :	.00100	.00510	
Z pioint (MIN) :	0.00006	.05101	-.00169
(MAX) :	0.00005	.07654	.00064
(MEAN) :			-.00003

TABLE 6-10 ROUGHNESS MEASUREMENT DATA FOR CUT CA11H

MATRIX VIDEOMETRIX

TOPO TM

Measurement Data

X POSITION	Y POSITION	Z POSITION	ROW	COLUMN
0.00000	0.00000	0.00000	0	0
0.00000	0.00510	-0.00005	1	0
0.00000	0.01020	-0.00003	2	0
0.00000	0.01531	-0.00111	3	0
0.00000	0.02041	-0.00042	4	0
0.00000	0.02551	-0.00016	5	0
0.00000	0.03061	-0.00062	6	0
0.00000	0.03571	-0.00072	7	0
0.00000	0.04082	-0.00026	8	0
0.00000	0.04592	-0.00074	9	0
0.00000	0.05102	-0.00072	10	0
0.00000	0.05612	-0.00108	11	0
0.00000	0.06122	-0.00154	12	0
0.00000	0.06633	-0.00155	13	0
0.00000	0.07143	-0.00109	14	0
0.00000	0.07653	-0.00051	15	0
0.00000	0.08163	-0.00086	16	0
0.00000	0.08673	-0.00133	17	0
0.00000	0.09184	-0.00184	18	0
0.00000	0.09694	-0.00070	19	0
0.00000	0.10204	-0.00050	20	0
0.00000	0.10714	-0.00049	21	0
0.00000	0.11224	-0.00047	22	0
0.00000	0.11735	-0.00089	23	0
0.00000	0.12245	-0.00021	24	0
0.00000	0.12755	-0.00059	25	0
0.00000	0.13265	-0.00063	26	0
0.00000	0.13776	-0.00047	27	0
0.00000	0.14286	0.00008	28	0
0.00000	0.14796	-0.00131	29	0
0.00000	0.15306	-0.00076	30	0
0.00000	0.15816	-0.00030	31	0
0.00000	0.16327	-0.00023	32	0
0.00000	0.16837	-0.00065	33	0
0.00000	0.17347	-0.00063	34	0
0.00000	0.17857	-0.00024	35	0
0.00000	0.18367	-0.00018	36	0
0.00000	0.18878	-0.00066	37	0

TABLE 6-10 ROUGHNESS MEASUREMENT DATA FOR CUT CA11H (CONTINUED)

X POSITION	Y POSITION	Z POSITION	ROW	COLUMN
0.00000	0.19388	-0.00003	38	0
0.00000	0.19898	0.00083	39	0
0.00000	0.20408	0.00060	40	0
0.00000	0.20918	0.00002	41	0
0.00000	0.21429	-0.00066	42	0
0.00000	0.21939	-0.00094	43	0
0.00000	0.22449	-0.00129	44	0
0.00000	0.22959	-0.00115	45	0
0.00000	0.23469	-0.00036	46	0
0.00000	0.23980	-0.00088	47	0
0.00000	0.24490	-0.00022	48	0
0.00000	0.25000	0.00006	49	0

TABLE 6-10 SUMMARY

	X	Y	Z
Total Axis Travel:	.00100	.25000	
# of Focus Points:	1.00000	50.00000	
Step Increments :	.00100	.00510	
Z pioint (MIN) :	0.00000	.09184	-.00184
(MAX) :	0.00000	.19898	.00083
(MEAN) :			-.00057

TABLE 6-11 ROUGHNESS MEASUREMENT DATA FOR CUT CA12A

MATRIX VIDEOMETRIX

TOPO TM

Measurement Data

X POSITION	Y POSITION	Z POSITION	ROW	COLUMN
0.00000	0.00000	0.00000	0	0
0.00000	0.00510	-0.00063	1	0
0.00000	0.01020	-0.00006	2	0
0.00000	0.01531	0.00026	3	0
0.00000	0.02041	0.00028	4	0
0.00000	0.02551	-0.00004	5	0
0.00000	0.03061	0.00010	6	0
0.00000	0.03571	-0.00080	7	0
0.00000	0.04082	-0.00017	8	0
0.00000	0.04592	-0.00008	9	0
0.00000	0.05102	0.00094	10	0
0.00000	0.05612	-0.00050	11	0
0.00000	0.06122	0.00030	12	0
0.00000	0.06633	-0.00083	13	0
0.00000	0.07143	-0.00159	14	0
0.00000	0.07653	-0.00044	15	0
0.00000	0.08163	-0.00036	16	0
0.00000	0.08673	-0.00077	17	0
0.00000	0.09184	-0.00072	18	0
0.00000	0.09694	-0.00048	19	0
0.00000	0.10204	-0.00033	20	0
0.00000	0.10714	-0.00061	21	0
0.00000	0.11224	-0.00050	22	0
0.00000	0.11735	-0.00098	23	0
0.00000	0.12245	-0.00070	24	0
0.00000	0.12755	-0.00034	25	0
0.00000	0.13265	-0.00058	26	0
0.00000	0.13776	-0.00101	27	0
0.00000	0.14286	-0.00091	28	0
0.00000	0.14796	-0.00165	29	0
0.00000	0.15306	-0.00108	30	0
0.00000	0.15816	-0.00088	31	0
0.00000	0.16327	-0.00103	32	0
0.00000	0.16837	-0.00085	33	0
0.00000	0.17347	-0.00053	34	0
0.00000	0.17857	-0.00049	35	0
0.00000	0.18367	-0.00047	36	0
0.00000	0.18878	-0.00050	37	0

TABLE 6-11 ROUGHNESS MEASUREMENT DATA FOR CUT CA12A (CONTINUED)

X POSITION	Y POSITION	Z POSITION	ROW	COLUMN
0.00000	0.19388	-0.00160	38	0
0.00000	0.19898	-0.00099	39	0
0.00000	0.20408	0.00007	40	0
0.00000	0.20918	0.00039	41	0
0.00000	0.21429	-0.00071	42	0
0.00000	0.21939	0.00014	43	0
0.00000	0.22449	0.00026	44	0
0.00000	0.22959	-0.00037	45	0
0.00000	0.23469	-0.00042	46	0
0.00000	0.23980	0.00012	47	0
0.00000	0.24490	0.00022	48	0
0.00000	0.25000	0.00033	49	0

TABLE 6-11 SUMMARY

	X	Y	Z
Total Axis Travel:	.00100	.25000	
# of Focus Points:	1.00000	50.00000	
Step Increments :	.00100	.00510	
Z pioint (MIN) :	0.00000	.14795	-.00165
(MAX) :	0.00001	.05104	.00094
(MEAN) :			-.00043

TABLE 6-12 ROUGHNESS MEASUREMENT DATA FOR CUT CA13A

MATRIX VIDEOMETRIX

TOPO TM

Measurement Data

X POSITION	Y POSITION	Z POSITION	ROW	COLUMN
0.00000	0.00000	0.00000	0	0
0.00000	0.00510	-0.00056	1	0
0.00000	0.01020	-0.00084	2	0
0.00000	0.01531	-0.00033	3	0
0.00000	0.02041	-0.00014	4	0
0.00000	0.02551	0.00027	5	0
0.00000	0.03061	0.00022	6	0
0.00000	0.03571	0.00030	7	0
0.00000	0.04082	-0.00082	8	0
0.00000	0.04592	0.00035	9	0
0.00000	0.05102	0.00029	10	0
0.00000	0.05612	0.00016	11	0
0.00000	0.06122	-0.00010	12	0
0.00000	0.06633	0.00022	13	0
0.00000	0.07143	0.00015	14	0
0.00000	0.07653	-0.00029	15	0
0.00000	0.08163	-0.00071	16	0
0.00000	0.08673	-0.00032	17	0
0.00000	0.09184	0.00008	18	0
0.00000	0.09694	-0.00085	19	0
0.00000	0.10204	-0.00073	20	0
0.00000	0.10714	-0.00000	21	0
0.00000	0.11224	-0.00049	22	0
0.00000	0.11735	0.00004	23	0
0.00000	0.12245	0.00012	24	0
0.00000	0.12755	-0.00061	25	0
0.00000	0.13265	-0.00051	26	0
0.00000	0.13776	-0.00084	27	0
0.00000	0.14286	-0.00122	28	0
0.00000	0.14796	-0.00116	29	0
0.00000	0.15306	-0.00116	30	0
0.00000	0.15816	-0.00094	31	0
0.00000	0.16327	-0.00054	32	0
0.00000	0.16837	-0.00148	33	0
0.00000	0.17347	-0.00193	34	0
0.00000	0.17857	-0.00060	35	0
0.00000	0.18367	-0.00172	36	0
0.00000	0.18878	-0.00129	37	0

TABLE 6-12 ROUGHNESS MEASUREMENT DATA FOR CUT CA13A
(CONTINUED)

X POSITION	Y POSITION	Z POSITION	ROW	COLUMN
0.00000	0.19388	-0.00154	38	0
0.00000	0.19898	-0.00112	39	0
0.00000	0.20408	-0.00195	40	0
0.00000	0.20918	-0.00348	41	0
0.00000	0.21429	-0.00220	42	0
0.00000	0.21939	-0.00210	43	0
0.00000	0.22449	-0.00182	44	0
0.00000	0.22959	-0.00178	45	0
0.00000	0.23469	-0.00070	46	0
0.00000	0.23980	-0.00108	47	0
0.00000	0.24490	-0.00013	48	0
0.00000	0.25000	0.00001	49	0

TABLE 6-12 SUMMARY

	X	Y	Z
Total Axis Travel:	.00100	.25000	
# of Focus Points:	1.00000	50.00000	
Step Increments :	.00100	.00510	
Z pioint (MIN) :	-0.00033	.20917	-.00348
(MAX) :	0.00000	.04592	.00036
(MEAN) :			-.00072

TABLE 6-13 ROUGHNESS MEASUREMENT DATA FOR CUT CB1B

MATRIX VIDEOMETRIX

TOPO TM

Measurement Data

X POSITION	Y POSITION	Z POSITION	ROW	COLUMN
0.00000	0.00000	0.00000	0	0
0.00000	0.00510	-0.00056	1	0
0.00000	0.01020	-0.00037	2	0
0.00000	0.01531	0.00066	3	0
0.00000	0.02041	0.00039	4	0
0.00000	0.02551	0.00076	5	0
0.00000	0.03061	0.00014	6	0
0.00000	0.03571	-0.00003	7	0
0.00000	0.04082	-0.00018	8	0
0.00000	0.04592	-0.00020	9	0
0.00000	0.05102	-0.00012	10	0
0.00000	0.05612	-0.00025	11	0
0.00000	0.06122	-0.00080	12	0
0.00000	0.06633	-0.00092	13	0
0.00000	0.07143	-0.00081	14	0
0.00000	0.07653	-0.00072	15	0
0.00000	0.08163	-0.00073	16	0
0.00000	0.08673	-0.00138	17	0
0.00000	0.09184	-0.00125	18	0
0.00000	0.09694	-0.00002	19	0
0.00000	0.10204	-0.00048	20	0
0.00000	0.10714	0.00014	21	0
0.00000	0.11224	-0.00091	22	0
0.00000	0.11735	-0.00131	23	0
0.00000	0.12245	-0.00025	24	0
0.00000	0.12755	0.00038	25	0
0.00000	0.13265	0.00035	26	0
0.00000	0.13776	-0.00002	27	0
0.00000	0.14286	-0.00033	28	0
0.00000	0.14796	0.00029	29	0
0.00000	0.15306	0.00037	30	0
0.00000	0.15816	0.00032	31	0
0.00000	0.16327	-0.00018	32	0
0.00000	0.16837	-0.00091	33	0
0.00000	0.17347	-0.00114	34	0
0.00000	0.17857	-0.00057	35	0
0.00000	0.18367	-0.00067	36	0
0.00000	0.18878	-0.00037	37	0

TABLE 6-13 ROUGHNESS MEASUREMENT DATA FOR CUT CB1B
(CONTINUED)

X POSITION	Y POSITION	Z POSITION	ROW	COLUMN
0.00000	0.19388	0.00008	38	0
0.00000	0.19898	0.00043	39	0
0.00000	0.20408	0.00056	40	0
0.00000	0.20918	-0.00026	41	0
0.00000	0.21429	-0.00056	42	0
0.00000	0.21939	-0.00081	43	0
0.00000	0.22449	-0.00128	44	0
0.00000	0.22959	-0.00090	45	0
0.00000	0.23469	-0.00047	46	0
0.00000	0.23980	-0.00058	47	0
0.00000	0.24490	-0.00063	48	0
0.00000	0.25000	-0.00051	49	0

TABLE 6-13 SUMMARY

	X	Y	Z
Total Axis Travel:	.00100	.25000	
# of Focus Points:	1.00000	50.00000	
Step Increments :	.00100	.00510	
Z pioint (MIN) :	0.00000	.08673	-.00138
(MAX) :	0.00000	.01531	.00076
(MEAN) :			-.00033

TABLE 6-14 ROUGHNESS MEASUREMENT DATA FOR CUT CB2B

MATRIX VIDEOMETRIX

TOPO TM

Measurement Data

X POSITION	Y POSITION	Z POSITION	ROW	COLUMN
0.00000	0.00000	0.00000	0	0
0.00000	0.00510	-0.00027	1	0
0.00000	0.01020	-0.00023	2	0
0.00000	0.01531	-0.00101	3	0
0.00000	0.02041	-0.00155	4	0
0.00000	0.02551	-0.00107	5	0
0.00000	0.03061	-0.00097	6	0
0.00000	0.03571	-0.00090	7	0
0.00000	0.04082	-0.00056	8	0
0.00000	0.04592	-0.00038	9	0
0.00000	0.05102	-0.00087	10	0
0.00000	0.05612	-0.00055	11	0
0.00000	0.06122	-0.00060	12	0
0.00000	0.06633	-0.00124	13	0
0.00000	0.07143	-0.00085	14	0
0.00000	0.07653	-0.00140	15	0
0.00000	0.08163	-0.00153	16	0
0.00000	0.08673	-0.00087	17	0
0.00000	0.09184	-0.00053	18	0
0.00000	0.09694	-0.00036	19	0
0.00000	0.10204	-0.00004	20	0
0.00000	0.10714	-0.00096	21	0
0.00000	0.11224	-0.00174	22	0
0.00000	0.11735	-0.00230	23	0
0.00000	0.12245	-0.00241	24	0
0.00000	0.12755	-0.00241	25	0
0.00000	0.13265	-0.00171	26	0
0.00000	0.13776	-0.00221	27	0
0.00000	0.14286	-0.00163	28	0
0.00000	0.14796	-0.00139	29	0
0.00000	0.15306	-0.00165	30	0
0.00000	0.15816	-0.00101	31	0
0.00000	0.16327	-0.00043	32	0
0.00000	0.16837	-0.00065	33	0
0.00000	0.17347	-0.00200	34	0
0.00000	0.17857	-0.00159	35	0
0.00000	0.18367	-0.00033	36	0
0.00000	0.18878	-0.00041	37	0

TABLE 6-14 ROUGHNESS MEASUREMENT DATA FOR CUT CB2B (CONTINUED)

X POSITION	Y POSITION	Z POSITION	ROW	COLUMN
0.00000	0.19388	-0.00078	38	0
0.00000	0.19898	-0.00114	39	0
0.00000	0.20408	-0.00044	40	0
0.00000	0.20918	-0.00047	41	0
0.00000	0.21429	-0.00061	42	0
0.00000	0.21939	-0.00078	43	0
0.00000	0.22449	-0.00080	44	0
0.00000	0.22959	-0.00135	45	0
0.00000	0.23469	-0.00135	46	0
0.00000	0.23980	-0.00062	47	0
0.00000	0.24490	-0.00036	48	0
0.00000	0.25000	-0.00003	49	0

TABLE 6-14 SUMMARY

	X	Y	Z
Total Axis Travel:	.00100	.25000	
# of Focus Points:	1.00000	50.00000	
Step Increments :	.00100	.00510	
Z pioint (MIN) :	0.00000	.12245	-.00241
(MAX) :	0.00000	.00000	.00000
(MEAN) :			-.00097

TABLE 6-15 ROUGHNESS MEASUREMENT DATA FOR CUT CB3A

MATRIX VIDEOMETRIX

TOPO TM

Measurement Data

X POSITION	Y POSITION	Z POSITION	ROW	COLUMN
0.00000	0.00000	0.00000	0	0
0.00000	0.00510	-0.00038	1	0
0.00000	0.01020	-0.00056	2	0
0.00000	0.01531	-0.00006	3	0
0.00000	0.02041	-0.00038	4	0
0.00000	0.02551	-0.00052	5	0
0.00000	0.03061	-0.00046	6	0
0.00000	0.03571	0.00018	7	0
0.00000	0.04082	-0.00013	8	0
0.00000	0.04592	-0.00033	9	0
0.00000	0.05102	-0.00079	10	0
0.00000	0.05612	-0.00056	11	0
0.00000	0.06122	-0.00043	12	0
0.00000	0.06633	0.00044	13	0
0.00000	0.07143	-0.00002	14	0
0.00000	0.07653	0.00016	15	0
0.00000	0.08163	0.00003	16	0
0.00000	0.08673	0.00005	17	0
0.00000	0.09184	0.00077	18	0
0.00000	0.09694	0.00073	19	0
0.00000	0.10204	0.00019	20	0
0.00000	0.10714	0.00030	21	0
0.00000	0.11224	0.00024	22	0
0.00000	0.11735	-0.00039	23	0
0.00000	0.12245	-0.00013	24	0
0.00000	0.12755	-0.00055	25	0
0.00000	0.13265	-0.00122	26	0
0.00000	0.13776	-0.00174	27	0
0.00000	0.14286	-0.00087	28	0
0.00000	0.14796	-0.00064	29	0
0.00000	0.15306	-0.00014	30	0
0.00000	0.15816	0.00002	31	0
0.00000	0.16327	-0.00035	32	0
0.00000	0.16837	-0.00035	33	0
0.00000	0.17347	-0.00045	34	0
0.00000	0.17857	-0.00038	35	0
0.00000	0.18367	-0.00048	36	0
0.00000	0.18878	-0.00083	37	0

TABLE 6-15 ROUGHNESS MEASUREMENT DATA FOR CUT CB3A (CONTINUED)

X POSITION	Y POSITION	Z POSITION	ROW	COLUMN
0.00000	0.19388	-0.00013	38	0
0.00000	0.19898	-0.00013	39	0
0.00000	0.20408	-0.00049	40	0
0.00000	0.20918	-0.00049	41	0
0.00000	0.21429	-0.00019	42	0
0.00000	0.21939	-0.00036	43	0
0.00000	0.22449	-0.00011	44	0
0.00000	0.22959	-0.00012	45	0
0.00000	0.23469	-0.00031	46	0
0.00000	0.23980	-0.00023	47	0
0.00000	0.24490	-0.00050	48	0
0.00000	0.25000	0.00014	49	0

TABLE 6-15 SUMMARY

	X	Y	Z
Total Axis Travel:	.00100	.25000	
# of Focus Points:	1.00000	50.00000	
Step Increments :	.00100	.00510	
Z pioint (MIN) :	0.00000	.13776	-.00174
(MAX) :	0.00000	.09184	.00077
(MEAN) :			-.00026

TABLE 6-16 ROUGHNESS MEASUREMENT DATA FOR CUT CB4B

MATRIX VIDEOMETRIX

TOPO TM

Measurement-Data

X POSITION	Y POSITION	Z POSITION	ROW	COLUMN
0.00000	0.00000	0.00000	0	0
0.00000	0.00510	-0.00060	1	0
0.00000	0.01020	-0.00062	2	0
0.00000	0.01531	-0.00057	3	0
0.00000	0.02041	-0.00012	4	0
0.00000	0.02551	-0.00013	5	0
0.00000	0.03061	0.00060	6	0
0.00000	0.03571	0.00036	7	0
0.00000	0.04082	0.00076	8	0
0.00000	0.04592	0.00012	9	0
0.00000	0.05102	-0.00018	10	0
0.00000	0.05612	0.00037	11	0
0.00000	0.06122	-0.00001	12	0
0.00000	0.06633	-0.00040	13	0
0.00000	0.07143	-0.00023	14	0
0.00000	0.07653	0.00017	15	0
0.00000	0.08163	0.00011	16	0
0.00000	0.08673	-0.00072	17	0
0.00000	0.09184	-0.00106	18	0
0.00000	0.09694	-0.00104	19	0
0.00000	0.10204	-0.00069	20	0
0.00000	0.10714	-0.00050	21	0
0.00000	0.11224	-0.00014	22	0
0.00000	0.11735	-0.00003	23	0
0.00000	0.12245	-0.00021	24	0
0.00000	0.12755	-0.00015	25	0
0.00000	0.13265	-0.00040	26	0
0.00000	0.13776	-0.00046	27	0
0.00000	0.14286	-0.00077	28	0
0.00000	0.14796	-0.00042	29	0
0.00000	0.15306	-0.00022	30	0
0.00000	0.15816	-0.00012	31	0
0.00000	0.16327	0.00004	32	0
0.00000	0.16837	-0.00022	33	0
0.00000	0.17347	-0.00014	34	0
0.00000	0.17857	0.00014	35	0
0.00000	0.18367	-0.00023	36	0
0.00000	0.18878	-0.00086	37	0

TABLE 6-16 ROUGHNESS MEASUREMENT DATA FOR CUT CB4B (CONTINUED)

X POSITION	Y POSITION	Z POSITION	ROW	COLUMN
0.00000	0.19388	-0.00100	38	0
0.00000	0.19898	-0.00129	39	0
0.00000	0.20408	-0.00070	40	0
0.00000	0.20918	-0.00070	41	0
0.00000	0.21429	-0.00091	42	0
0.00000	0.21939	-0.00070	43	0
0.00000	0.22449	-0.00065	44	0
0.00000	0.22959	-0.00097	45	0
0.00000	0.23469	-0.00118	46	0
0.00000	0.23980	-0.00133	47	0
0.00000	0.24490	-0.00147	48	0
0.00000	0.25000	-0.00181	49	0

TABLE 6-16 SUMMARY

	X	Y	Z
Total Axis Travel:	.00100	.25000	
# of Focus Points:	1.00000	50.00000	
Step Increments :	.00100	.00510	
Z pioint (MIN) :	0.00000	.25000	-.00181
(MAX) :	0.00000	.04082	.00076
(MEAN) :			-.00043

TABLE 6-17 ROUGHNESS MEASUREMENT DATA FOR CUT CB5B

MATRIX VIDEOMETRIX

TOPO TM

Measurement Data

X POSITION	Y POSITION	Z POSITION	ROW	COLUMN
0.00000	0.00000	0.00000	0	0
0.00000	0.00510	-0.00077	1	0
0.00000	0.01020	-0.00118	2	0
0.00000	0.01531	-0.00038	3	0
0.00000	0.02041	-0.00046	4	0
0.00000	0.02551	-0.00139	5	0
0.00000	0.03061	-0.00187	6	0
0.00000	0.03571	-0.00127	7	0
0.00000	0.04082	-0.00111	8	0
0.00000	0.04592	-0.00158	9	0
0.00000	0.05102	-0.00150	10	0
0.00000	0.05612	-0.00136	11	0
0.00000	0.06122	-0.00216	12	0
0.00000	0.06633	-0.00068	13	0
0.00000	0.07143	-0.00038	14	0
0.00000	0.07653	-0.00024	15	0
0.00000	0.08163	-0.00105	16	0
0.00000	0.08673	-0.00071	17	0
0.00000	0.09184	-0.00025	18	0
0.00000	0.09694	-0.00136	19	0
0.00000	0.10204	-0.00110	20	0
0.00000	0.10714	-0.00144	21	0
0.00000	0.11224	-0.00125	22	0
0.00000	0.11735	-0.00051	23	0
0.00000	0.12245	-0.00020	24	0
0.00000	0.12755	-0.00017	25	0
0.00000	0.13265	-0.00122	26	0
0.00000	0.13776	-0.00158	27	0
0.00000	0.14286	-0.00087	28	0
0.00000	0.14796	-0.00121	29	0
0.00000	0.15306	-0.00100	30	0
0.00000	0.15816	-0.00103	31	0
0.00000	0.16327	-0.00123	32	0
0.00000	0.16837	-0.00106	33	0
0.00000	0.17347	-0.00054	34	0
0.00000	0.17857	0.00002	35	0
0.00000	0.18367	0.00016	36	0
0.00000	0.18878	0.00034	37	0

TABLE 6-17 ROUGHNESS MEASUREMENT DATA FOR CUT CB5B (CONTINUED)

X POSITION	Y POSITION	Z POSITION	ROW	COLUMN
0.00000	0.19388	0.00048	38	0
0.00000	0.19898	-0.00080	39	0
0.00000	0.20408	0.00025	40	0
0.00000	0.20918	0.00050	41	0
0.00000	0.21429	-0.00018	42	0
0.00000	0.21939	0.00016	43	0
0.00000	0.22449	0.00011	44	0
0.00000	0.22959	0.00060	45	0
0.00000	0.23469	0.00062	46	0
0.00000	0.23980	0.00059	47	0
0.00000	0.24490	0.00052	48	0
0.00000	0.25000	0.00046	49	0

TABLE 6-17 SUMMARY

	X	Y	Z
Total Axis Travel:	.00100	.25000	
# of Focus Points:	1.00000	50.00000	
Step Increments :	.00100	.00510	
Z pioint (MIN) :	0.00000	.06122	-.00216
(MAX) :	0.00000	.23469	.00062
(MEAN) :			-.00061

TABLE 6-18 ROUGHNESS MEASUREMENT DATA FOR CUT CB6A

MATRIX VIDEOMETRIX

TOPO TM

Measurement Data

X POSITION	Y POSITION	Z POSITION	ROW	COLUMN
0.00000	0.00000	0.00000	0	0
0.00000	0.00510	0.00013	1	0
0.00000	0.01020	-0.00015	2	0
0.00000	0.01531	0.00013	3	0
0.00000	0.02041	-0.00008	4	0
0.00000	0.02551	-0.00041	5	0
0.00000	0.03061	-0.00016	6	0
0.00000	0.03571	-0.00045	7	0
0.00000	0.04082	0.00014	8	0
0.00000	0.04592	-0.00005	9	0
0.00000	0.05102	-0.00013	10	0
0.00000	0.05612	0.00028	11	0
0.00000	0.06122	0.00012	12	0
0.00000	0.06633	-0.00091	13	0
0.00000	0.07143	-0.00046	14	0
0.00000	0.07653	-0.00044	15	0
0.00000	0.08163	-0.00014	16	0
0.00000	0.08673	-0.00019	17	0
0.00000	0.09184	-0.00054	18	0
0.00000	0.09694	-0.00009	19	0
0.00000	0.10204	0.00044	20	0
0.00000	0.10714	0.00017	21	0
0.00000	0.11224	0.00017	22	0
0.00000	0.11735	-0.00061	23	0
0.00000	0.12245	-0.00032	24	0
0.00000	0.12755	0.00004	25	0
0.00000	0.13265	-0.00025	26	0
0.00000	0.13776	-0.00023	27	0
0.00000	0.14286	-0.00009	28	0
0.00000	0.14796	0.00003	29	0
0.00000	0.15306	-0.00000	30	0
0.00000	0.15816	-0.00027	31	0
0.00000	0.16327	0.00003	32	0
0.00000	0.16837	-0.00029	33	0
0.00000	0.17347	-0.00001	34	0
0.00000	0.17857	-0.00020	35	0
0.00000	0.18367	-0.00028	36	0
0.00000	0.18878	0.00028	37	0

TABLE 6-18 ROUGHNESS MEASUREMENT DATA FOR CUT CB6A (CONTINUED)

X POSITION	Y POSITION	Z POSITION	ROW	COLUMN
0.00000	0.19388	0.00009	38	0
0.00000	0.19898	-0.00002	39	0
0.00000	0.20408	-0.00041	40	0
0.00000	0.20918	0.00029	41	0
0.00000	0.21429	0.00056	42	0
0.00000	0.21939	0.00049	43	0
0.00000	0.22449	0.00042	44	0
0.00000	0.22959	0.00056	45	0
0.00000	0.23469	0.00038	46	0
0.00000	0.23980	-0.00016	47	0
0.00000	0.24490	-0.00028	48	0
0.00000	0.25000	-0.00023	49	0

TABLE 6-18 SUMMARY

	X	Y	Z
Total Axis Travel:	.00100	.25000	
# of Focus Points:	1.00000	50.00000	
Step Increments :	.00100	.00510	
Z pioint (MIN) :	0.00000	.06633	-.00091
(MAX) :	0.00000	.21429	.00056
(MEAN) :			-.00006

TABLE 6-19 ROUGHNESS MEASUREMENT DATA FOR CUT CB7A

MATRIX VIDEOMETRIX

TOPO TM

Measurement Data

X POSITION	Y POSITION	Z POSITION	ROW	COLUMN
0.00000	0.00000	0.00000	0	0
0.00000	0.00510	0.00015	1	0
0.00000	0.01020	-0.00002	2	0
0.00000	0.01531	0.00096	3	0
0.00000	0.02041	0.00019	4	0
0.00000	0.02551	0.00002	5	0
0.00000	0.03061	0.00025	6	0
0.00000	0.03571	0.00038	7	0
0.00000	0.04082	0.00048	8	0
0.00000	0.04592	0.00011	9	0
0.00000	0.05102	-0.00027	10	0
0.00000	0.05612	0.00003	11	0
0.00000	0.06122	-0.00011	12	0
0.00000	0.06633	-0.00001	13	0
0.00000	0.07143	-0.00012	14	0
0.00000	0.07653	0.00011	15	0
0.00000	0.08163	0.00026	16	0
0.00000	0.08673	-0.00020	17	0
0.00000	0.09184	0.00019	18	0
0.00000	0.09694	0.00010	19	0
0.00000	0.10204	-0.00005	20	0
0.00000	0.10714	-0.00018	21	0
0.00000	0.11224	-0.00050	22	0
0.00000	0.11735	-0.00048	23	0
0.00000	0.12245	-0.00079	24	0
0.00000	0.12755	-0.00082	25	0
0.00000	0.13265	-0.00110	26	0
0.00000	0.13776	-0.00073	27	0
0.00000	0.14286	-0.00063	28	0
0.00000	0.14796	-0.00026	29	0
0.00000	0.15306	-0.00089	30	0
0.00000	0.15816	-0.00059	31	0
0.00000	0.16327	-0.00092	32	0
0.00000	0.16837	-0.00161	33	0
0.00000	0.17347	-0.00130	34	0
0.00000	0.17857	-0.00101	35	0
0.00000	0.18367	-0.00081	36	0
0.00000	0.18878	-0.00057	37	0

TABLE 6-19 ROUGHNESS MEASUREMENT DATA FOR CUT CB7A
(CONTINUED)

X POSITION	Y POSITION	Z POSITION	ROW	COLUMN
0.00000	0.19388	-0.00094	38	0
0.00000	0.19898	-0.00042	39	0
0.00000	0.20408	-0.00075	40	0
0.00000	0.20918	-0.00078	41	0
0.00000	0.21429	-0.00072	42	0
0.00000	0.21939	-0.00055	43	0
0.00000	0.22449	-0.00081	44	0
0.00000	0.22959	-0.00087	45	0
0.00000	0.23469	-0.00115	46	0
0.00000	0.23980	-0.00046	47	0
0.00000	0.24490	-0.00072	48	0
0.00000	0.25000	-0.00084	49	0

TABLE 6-19 SUMMARY

	X	Y	Z
Total Axis Travel:	.00100	.25000	
# of Focus Points:	1.00000	50.00000	
Step Increments :	.00100	.00510	
Z pioint (MIN) :	0.00000	.16837	-.00161
(MAX) :	0.00000	.01531	.00096
(MEAN) :			-.00040

TABLE 6-20 ROUGHNESS MEASUREMENT DATA FOR CUT CC1B

MATRIX VIDEOMETRIX

TOPO TM

Measurement Data

X POSITION	Y POSITION	Z POSITION	ROW	COLUMN
0.00000	0.00000	0.00000	0	0
0.00000	0.00510	-0.00047	1	0
0.00000	0.01020	-0.00047	2	0
0.00000	0.01531	-0.00047	3	0
0.00000	0.02041	-0.00022	4	0
0.00000	0.02551	0.00009	5	0
0.00000	0.03061	-0.00022	6	0
0.00000	0.03571	-0.00028	7	0
0.00000	0.04082	-0.00034	8	0
0.00000	0.04592	-0.00020	9	0
0.00000	0.05102	-0.00061	10	0
0.00000	0.05612	-0.00026	11	0
0.00000	0.06122	-0.00026	12	0
0.00000	0.06633	-0.00001	13	0
0.00000	0.07143	0.00051	14	0
0.00000	0.07653	0.00017	15	0
0.00000	0.08163	-0.00023	16	0
0.00000	0.08673	-0.00042	17	0
0.00000	0.09184	-0.00024	18	0
0.00000	0.09694	0.00009	19	0
0.00000	0.10204	-0.00020	20	0
0.00000	0.10714	0.00002	21	0
0.00000	0.11224	0.00043	22	0
0.00000	0.11735	0.00050	23	0
0.00000	0.12245	0.00024	24	0
0.00000	0.12755	0.00030	25	0
0.00000	0.13265	0.00025	26	0
0.00000	0.13776	-0.00018	27	0
0.00000	0.14286	0.00010	28	0
0.00000	0.14796	0.00015	29	0
0.00000	0.15306	0.00007	30	0
0.00000	0.15816	0.00024	31	0
0.00000	0.16327	0.00013	32	0
0.00000	0.16837	0.00001	33	0
0.00000	0.17347	0.00028	34	0
0.00000	0.17857	0.00027	35	0
0.00000	0.18367	0.00037	36	0
0.00000	0.18878	0.00054	37	0

TABLE 6-20 ROUGHNESS MEASUREMENT DATA FOR CUT CC1B (CONTINUED)

X POSITION	Y POSITION	Z POSITION	ROW	COLUMN
0.00000	0.19388	0.00012	38	0
0.00000	0.19898	0.00013	39	0
0.00000	0.20408	0.00031	40	0
0.00000	0.20918	0.00020	41	0
0.00000	0.21429	-0.00012	42	0
0.00000	0.21939	0.00040	43	0
0.00000	0.22449	0.00068	44	0
0.00000	0.22959	0.00097	45	0
0.00000	0.23469	0.00073	46	0
0.00000	0.23980	0.00078	47	0
0.00000	0.24490	0.00099	48	0
0.00000	0.25000	0.00084	49	0

TABLE 6-20 SUMMARY

	X	Y	Z
Total Axis Travel:	.00100	.25000	
# of Focus Points:	1.00000	50.00000	
Step Increments :	.00100	.00510	
Z pioint (MIN) :	0.00000	.05102	-.00061
(MAX) :	0.00000	.24490	.00099
(MEAN) :			.00011

TABLE 6-21 ROUGHNESS MEASUREMENT DATA FOR CUT CC2B

MATRIX VIDEOMETRIX

TOPO TM

Measurement Data

X POSITION	Y POSITION	Z POSITION	ROW	COLUMN
0.00000	0.00000	0.00000	0	0
0.00000	0.00510	0.00030	1	0
0.00000	0.01020	0.00026	2	0
0.00000	0.01531	0.00058	3	0
0.00000	0.02041	0.00068	4	0
0.00000	0.02551	0.00004	5	0
0.00000	0.03061	0.00027	6	0
0.00000	0.03571	0.00019	7	0
0.00000	0.04082	0.00021	8	0
0.00000	0.04592	0.00042	9	0
0.00000	0.05102	0.00020	10	0
0.00000	0.05612	-0.00006	11	0
0.00000	0.06122	0.00043	12	0
0.00000	0.06633	-0.00001	13	0
0.00000	0.07143	0.00014	14	0
0.00000	0.07653	0.00072	15	0
0.00000	0.08163	0.00026	16	0
0.00000	0.08673	-0.00005	17	0
0.00000	0.09184	0.00031	18	0
0.00000	0.09694	0.00019	19	0
0.00000	0.10204	0.00028	20	0
0.00000	0.10714	0.00010	21	0
0.00000	0.11224	0.00005	22	0
0.00000	0.11735	0.00011	23	0
0.00000	0.12245	0.00033	24	0
0.00000	0.12755	0.00058	25	0
0.00000	0.13265	0.00069	26	0
0.00000	0.13776	0.00032	27	0
0.00000	0.14286	0.00052	28	0
0.00000	0.14796	0.00017	29	0
0.00000	0.15306	0.00006	30	0
0.00000	0.15816	0.00048	31	0
0.00000	0.16327	0.00031	32	0
0.00000	0.16837	0.00029	33	0
0.00000	0.17347	0.00023	34	0
0.00000	0.17857	0.00043	35	0
0.00000	0.18367	0.00038	36	0
0.00000	0.18878	0.00030	37	0

TABLE 6-21 ROUGHNESS MEASUREMENT DATA FOR CUT CC2B (CONTINUED)

X POSITION	Y POSITION	Z POSITION	ROW	COLUMN
0.00000	0.19388	0.00037	38	0
0.00000	0.19898	0.00054	39	0
0.00000	0.20408	0.00000	40	0
0.00000	0.20918	0.00022	41	0
0.00000	0.21429	-0.00009	42	0
0.00000	0.21939	-0.00010	43	0
0.00000	0.22449	-0.00023	44	0
0.00000	0.22959	0.00006	45	0
0.00000	0.23469	0.00027	46	0
0.00000	0.23980	0.00019	47	0
0.00000	0.24490	0.00035	48	0
0.00000	0.25000	0.00049	49	0

TABLE 6-21 SUMMARY

	X	Y	Z
Total Axis Travel:	.00100	.25000	
# of Focus Points:	1.00000	50.00000	
Step Increments :	.00100	.00510	
Z pioint (MIN) :	0.00000	.22449	-.00023
(MAX) :	0.00000	.07653	.00072
(MEAN) :			.00026

TABLE 6-22 ROUGHNESS MEASUREMENT DATA FOR CUT CC3B

MATRIX VIDEOMETRIX

TOPO TM

Measurement Data

X POSITION	Y POSITION	Z POSITION	ROW	COLUMN
0.00000	0.00000	0.00000	0	0
0.00000	0.00510	0.00021	1	0
0.00000	0.01020	0.00026	2	0
0.00000	0.01531	0.00065	3	0
0.00000	0.02041	0.00063	4	0
0.00000	0.02551	0.00023	5	0
0.00000	0.03061	0.00015	6	0
0.00000	0.03571	0.00028	7	0
0.00000	0.04082	0.00059	8	0
0.00000	0.04592	0.00042	9	0
0.00000	0.05102	0.00023	10	0
0.00000	0.05612	0.00077	11	0
0.00000	0.06122	0.00082	12	0
0.00000	0.06633	0.00097	13	0
0.00000	0.07143	0.00096	14	0
0.00000	0.07653	0.00100	15	0
0.00000	0.08163	0.00094	16	0
0.00000	0.08673	0.00080	17	0
0.00000	0.09184	0.00042	18	0
0.00000	0.09694	0.00057	19	0
0.00000	0.10204	0.00069	20	0
0.00000	0.10714	0.00052	21	0
0.00000	0.11224	0.00079	22	0
0.00000	0.11735	0.00112	23	0
0.00000	0.12245	0.00060	24	0
0.00000	0.12755	0.00092	25	0
0.00000	0.13265	0.00050	26	0
0.00000	0.13776	0.00058	27	0
0.00000	0.14286	0.00048	28	0
0.00000	0.14796	0.00077	29	0
0.00000	0.15306	0.00071	30	0
0.00000	0.15816	0.00040	31	0
0.00000	0.16327	0.00013	32	0
0.00000	0.16837	0.00019	33	0
0.00000	0.17347	-0.00010	34	0
0.00000	0.17857	0.00026	35	0
0.00000	0.18367	0.00029	36	0
0.00000	0.18878	0.00036	37	0

TABLE 6-22 ROUGHNESS MEASUREMENT DATA FOR CUT CC3B
(CONTINUED)

X POSITION	Y POSITION	Z POSITION	ROW	COLUMN
0.00000	0.19388	0.00030	38	0
0.00000	0.19898	0.00003	39	0
0.00000	0.20408	-0.00030	40	0
0.00000	0.20918	0.00004	41	0
0.00000	0.21429	0.00037	42	0
0.00000	0.21939	0.00100	43	0
0.00000	0.22449	0.00180	44	0
0.00000	0.22959	0.00194	45	0
0.00000	0.23469	0.00183	46	0
0.00000	0.23980	0.00175	47	0
0.00000	0.24490	0.00206	48	0
0.00000	0.25000	0.00176	49	0

TABLE 6-22 SUMMARY

	X	Y	Z
Total Axis Travel:	.00100	.25000	
# of Focus Points:	1.00000	50.00000	
Step Increments :	.00100	.00510	
Z point (MIN) :	0.00000	.20408	-.00030
(MAX) :	0.00000	.24490	.00206
(MEAN) :			.00065

TABLE 6-23 ROUGHNESS MEASUREMENT DATA FOR CUT CC4A

MATRIX VIDEOMETRIX

TOPO TM

Measurement Data

X POSITION	Y POSITION	Z POSITION	ROW	COLUMN
0.00000	0.00000	0.00000	0	0
0.00000	0.00510	0.00004	1	0
0.00000	0.01020	0.00036	2	0
0.00000	0.01531	0.00045	3	0
0.00000	0.02041	0.00020	4	0
0.00000	0.02551	0.00033	5	0
0.00000	0.03061	0.00005	6	0
0.00000	0.03571	0.00027	7	0
0.00000	0.04082	0.00004	8	0
0.00000	0.04592	-0.00000	9	0
0.00000	0.05102	-0.00000	10	0
0.00000	0.05612	0.00007	11	0
0.00000	0.06122	0.00019	12	0
0.00000	0.06633	0.00042	13	0
0.00000	0.07143	0.00022	14	0
0.00000	0.07653	0.00025	15	0
0.00000	0.08163	0.00027	16	0
0.00000	0.08673	-0.00006	17	0
0.00000	0.09184	0.00011	18	0
0.00000	0.09694	0.00033	19	0
0.00000	0.10204	0.00008	20	0
0.00000	0.10714	0.00008	21	0
0.00000	0.11224	0.00028	22	0
0.00000	0.11735	0.00008	23	0
0.00000	0.12245	-0.00004	24	0
0.00000	0.12755	-0.00021	25	0
0.00000	0.13265	0.00022	26	0
0.00000	0.13776	0.00019	27	0
0.00000	0.14286	0.00011	28	0
0.00000	0.14796	0.00033	29	0
0.00000	0.15306	0.00023	30	0
0.00000	0.15816	-0.00039	31	0
0.00000	0.16327	0.00028	32	0
0.00000	0.16837	0.00055	33	0
0.00000	0.17347	0.00035	34	0
0.00000	0.17857	-0.00007	35	0
0.00000	0.18367	0.00010	36	0
0.00000	0.18878	0.00034	37	0

TABLE 6-23 ROUGHNESS MEASUREMENT DATA FOR CUT CC4A (CONTINUED)

X POSITION	Y POSITION	Z POSITION	ROW	COLUMN
0.00000	0.19388	0.00036	38	0
0.00000	0.19898	0.00026	39	0
0.00000	0.20408	-0.00012	40	0
0.00000	0.20918	0.00051	41	0
0.00000	0.21429	0.00048	42	0
0.00000	0.21939	0.00065	43	0
0.00000	0.22449	0.00046	44	0
0.00000	0.22959	0.00060	45	0
0.00000	0.23469	0.00079	46	0
0.00000	0.23980	0.00063	47	0
0.00000	0.24490	0.00043	48	0
0.00000	0.25000	0.00067	49	0

TABLE 6-23 SUMMARY

	X	Y	Z
Total Axis Travel:	.00100	.25000	
# of Focus Points:	1.00000	50.00000	
Step Increments :	.00100	.00510	
Z pioint (MIN) :	0.00000	.15816	-.00039
(MAX) :	0.00000	.23469	.00079
(MEAN) :			.00024

TABLE 6-24 ROUGHNESS MEASUREMENT DATA FOR CUT CC5B

MATRIX VIDEOMETRIX

TOPO TM

Measurement Data

X POSITION	Y POSITION	Z POSITION	ROW	COLUMN
0.00000	0.00000	0.00000	0	0
0.00000	0.00510	0.00003	1	0
0.00000	0.01020	-0.00001	2	0
0.00000	0.01531	0.00034	3	0
0.00000	0.02041	0.00064	4	0
0.00000	0.02551	-0.00004	5	0
0.00000	0.03061	-0.00003	6	0
0.00000	0.03571	-0.00033	7	0
0.00000	0.04082	-0.00010	8	0
0.00000	0.04592	-0.00002	9	0
0.00000	0.05102	-0.00022	10	0
0.00000	0.05612	-0.00026	11	0
0.00000	0.06122	-0.00023	12	0
0.00000	0.06633	0.00051	13	0
0.00000	0.07143	0.00009	14	0
0.00000	0.07653	-0.00001	15	0
0.00000	0.08163	0.00014	16	0
0.00000	0.08673	0.00014	17	0
0.00000	0.09184	0.00007	18	0
0.00000	0.09694	-0.00025	19	0
0.00000	0.10204	-0.00017	20	0
0.00000	0.10714	-0.00022	21	0
0.00000	0.11224	-0.00005	22	0
0.00000	0.11735	-0.00010	23	0
0.00000	0.12245	-0.00018	24	0
0.00000	0.12755	-0.00006	25	0
0.00000	0.13265	-0.00005	26	0
0.00000	0.13776	0.00005	27	0
0.00000	0.14286	-0.00035	28	0
0.00000	0.14796	-0.00037	29	0
0.00000	0.15306	-0.00026	30	0
0.00000	0.15816	-0.00027	31	0
0.00000	0.16327	-0.00046	32	0
0.00000	0.16837	-0.00065	33	0
0.00000	0.17347	-0.00070	34	0
0.00000	0.17857	-0.00058	35	0
0.00000	0.18367	-0.00084	36	0
0.00000	0.18878	-0.00040	37	0

TABLE 6-24 ROUGHNESS MEASUREMENT DATA FOR CUT CC5B
(CONTINUED)

X POSITION	Y POSITION	Z POSITION	ROW	COLUMN
0.00000	0.19388	-0.00039	38	0
0.00000	0.19898	-0.00025	39	0
0.00000	0.20408	-0.00048	40	0
0.00000	0.20918	-0.00036	41	0
0.00000	0.21429	-0.00010	42	0
0.00000	0.21939	-0.00032	43	0
0.00000	0.22449	-0.00024	44	0
0.00000	0.22959	0.00017	45	0
0.00000	0.23469	0.00001	46	0
0.00000	0.23980	-0.00004	47	0
0.00000	0.24490	-0.00020	48	0
0.00000	0.25000	-0.00016	49	0

TABLE 6-24 SUMMARY

	X	Y	Z
Total Axis Travel:	.00100	.25000	
# of Focus Points:	1.00000	50.00000	
Step Increments :	.00100	.00510	
Z pioint (MIN) :	0.00000	.18367	-.00084
(MAX) :	0.00000	.02041	.00064
(MEAN) :			-.00015

TABLE 6-25 ROUGHNESS MEASUREMENT DATA FOR CUT CC6A

MATRIX VIDEOMETRIX

TOPO TM

Measurement Data

X POSITION	Y POSITION	Z POSITION	ROW	COLUMN
0.00000	0.00000	0.00000	0	0
0.00000	0.00510	0.00021	1	0
0.00000	0.01020	0.00028	2	0
0.00000	0.01531	-0.00019	3	0
0.00000	0.02041	-0.00004	4	0
0.00000	0.02551	0.00006	5	0
0.00000	0.03061	-0.00001	6	0
0.00000	0.03571	0.00002	7	0
0.00000	0.04082	0.00037	8	0
0.00000	0.04592	0.00057	9	0
0.00000	0.05102	0.00074	10	0
0.00000	0.05612	0.00055	11	0
0.00000	0.06122	0.00046	12	0
0.00000	0.06633	0.00011	13	0
0.00000	0.07143	-0.00029	14	0
0.00000	0.07653	-0.00010	15	0
0.00000	0.08163	0.00006	16	0
0.00000	0.08673	0.00008	17	0
0.00000	0.09184	0.00024	18	0
0.00000	0.09694	0.00017	19	0
0.00000	0.10204	-0.00027	20	0
0.00000	0.10714	-0.00002	21	0
0.00000	0.11224	-0.00033	22	0
0.00000	0.11735	-0.00023	23	0
0.00000	0.12245	-0.00046	24	0
0.00000	0.12755	-0.00075	25	0
0.00000	0.13265	-0.00061	26	0
0.00000	0.13776	-0.00001	27	0
0.00000	0.14286	-0.00043	28	0
0.00000	0.14796	-0.00058	29	0
0.00000	0.15306	-0.00055	30	0
0.00000	0.15816	-0.00050	31	0
0.00000	0.16327	-0.00044	32	0
0.00000	0.16837	-0.00056	33	0
0.00000	0.17347	-0.00058	34	0
0.00000	0.17857	-0.00078	35	0
0.00000	0.18367	-0.00054	36	0
0.00000	0.18878	-0.00037	37	0

TABLE 6-25 ROUGHNESS MEASUREMENT DATA FOR CUT CC6A (CONTINUED)

X POSITION	Y POSITION	Z POSITION	ROW	COLUMN
0.00000	0.19388	-0.00019	38	0
0.00000	0.19898	-0.00025	39	0
0.00000	0.20408	-0.00008	40	0
0.00000	0.20918	-0.00049	41	0
0.00000	0.21429	-0.00100	42	0
0.00000	0.21939	-0.00036	43	0
0.00000	0.22449	-0.00064	44	0
0.00000	0.22959	-0.00066	45	0
0.00000	0.23469	-0.00071	46	0
0.00000	0.23980	-0.00118	47	0
0.00000	0.24490	-0.00137	48	0
0.00000	0.25000	-0.00112	49	0

TABLE 6-25 SUMMARY

	X	Y	Z
Total Axis Travel:	.00100	.25000	
# of Focus Points:	1.00000	50.00000	
Step Increments :	.00100	.00510	
Z pioint (MIN) :	0.00000	.24490	-.00137
(MAX) :	0.00000	.05102	.00074
(MEAN) :			-.00026

TABLE 6-26 SUMMARY OF ROUGHNESS VALUES WITH CUTTING CONDITIONS FOR EACH CUT

CUT NUMBER	ABRASIVE FLOW RATE (GPM)	PRESS. (KSI)	ABRASIVE NUMBER	NOZZLE NUMBER	TRAVERSE SPEED (IN/MIN)	ROUGHNESS (INCHES)
CA01A	229	50	120	10	5	0.000284
CA02A	229	50	120	10	3	0.000393
CA04A	229	50	120	10	1	0.000348
CA05A	229	33	120	10	3	0.000277
CA06B	229	33	120	10	2	0.000653
CA07A	229	33	120	10	1	0.000326
CA08A	185	33	120	10	1	0.000288
CA09A	185	33	120	10	2	0.000299
CA10A	185	33	120	10	3	0.000283
CA11H	185	50	120	10	3	0.000405
CA12A	185	50	120	10	2	0.000429
CA13A	185	50	120	10	1	0.000644
CB1B	82.0	50	120	7	2	0.000640
CB2B	144.8	50	120	7	2	0.000518
CB3A	144.8	50	120	7	1	0.000326
CB4B	144.8	50	120	7	0.5	0.000432
CB5B	235.2	50	120	7	2	0.000641
CB6A	235.2	50	120	7	1	0.000246
CB7A	235.2	50	120	7	0.5	0.000443
CC1B	56	30	220	10	2	0.000307
CC2B	56	30	220	10	1	0.000170
CC3B	56	30	220	10	0.5	0.000414
CC4A	56	50	220	10	2	0.000190
CC5B	56	50	220	10	1	0.000208
CC6A	56	50	220	10	0.5	0.000367

REFERENCES

1. S.J. Schneider Jr., R.W. Rice, The Science of Ceramic Machining and Surface Finishing, pp. 2-7, 1970.

2. G.F. Benedict, Metals Handbook Volume 16 - Machining, 9th Edition, p. 510, 1989.

3. G.F. Benedict, Metals Handbook Volume 16 - Machining, 9th Edition, pp. 509-510, 1989.

4. G.E. Storck, Metals Handbook Volume 16 - Machining, 9th Edition, p. 511, 1989.

5. L.T. Rhoades, H.A. Clouser, Metals Handbook Volume 16 - Machining, 9th Edition, p. 514, 1989.

6. C.E. Johnston, Metals Handbook Volume 16 - Machining, 9th Edition, p. 520, 1989.

7. W.R. Tyrell, Metals Handbook Volume 16 - Machining, 9th Edition, p. 528, 1989.

8. T.L. Lievestro, Metals Handbook Volume 16 - Machining, 9th Edition, p. 533, 1989.

9. R.E. Phillips, Metals Handbook Volume 16 - Machining, 9th Edition, p. 542, 1989.

10. Metals Handbook Volume 16 - Machining, 9th Edition, p. 548, 1989.

11. A.M. Newton, Metals Handbook Volume 16 - Machining, 9th Edition, p. 551, 1989.

12. A.M. Newton, Metals Handbook Volume 16 - Machining, 9th Edition, p. 554, 1989.

13. J.E. Fuller, Metals Handbook Volume 16 - Machining, 9th Edition, p. 557, 1989.

14. Milton C. Shaw, Metal Cutting Principles, pp. 47-55, 1984.

15. H. Nogawa, Ceramics Processing - State of the Art of R&D in Japan, pp. 8.1-8.19, 1988.

16. Metals Handbook Volume 16 - Machining, 9th Edition, p. 560, 1989.

17. Metals Handbook Volume 16 - Machining, 9th Edition, p. 565, 1989.

REFERENCES
(CONTINUED)

18. R.W. Schneider, Metals Handbook Volume 16 - Machining, 9th Edition, p. 568, 1989.

19. D. Elza, G. White, Metals Handbook Volume 16 - Machining, 9th Edition, p. 572, 1989.

20. M. Ramulu, M. Hashish, Machining Characteristics of Advanced Materials MD-Vol. 16, 1989.

21. H. Nogawa, Ceramics Processing - State of the Art of R&D in Japan, pp. 7.1-7.24, 1988.

22. T. Fischer, Metals Handbook Volume 16 - Machining, 9th Edition, p. 577, 1989.

23. E.M. Langworthy, Metals Handbook Volume 16 - Machining, 9th Edition, p. 579, 1989.

24. H. Friedman, Metals Handbook Volume 16 - Machining, 9th Edition, p. 587, 1989.

25. Wei-Long Chen, Correlation Between Particles Velocities and Conditions of Abrasive Waterjet Formation, N.J.I.T. Doctoral Thesis, pp. 8-10, 1990.

26. E.S. Geskin, "Waterjet Cutting", Modern Manufacturing Systems, 1992.

27. Shy-Syan Chen, Investigation of Surface Formation in Abrasive Waterjet Cutting N.J.I.T. Masters Thesis, pp. 1-7, 1989.

28. R. Jordan, "Waterjets on the Cutting edge of Machining", Nontraditional Machining Conference Proceedings, 2-3 December, 1985, Cincinnati, Ohio, pp. 13-22, 1986.

29. R.J. Brook, Concise Encyclopedia of Advanced Ceramic Materials, p. 468, 1991.

30. E.S. Geskin, "Material Shaping by the Use of Waterjets", Modern Manufacturing Systems, 1992.

31. M. Hashish, "Turning with Abrasive Water Jets", Advances in Nontraditional Machining, p. 79, 1986.

32. T.J. Kim, J.G. Sylvia, L. Posner, "Piercing and Cutting of Ceramics by Abrasive Water Jet", Machining of Ceramic Materials and Components PED-Vol. 17, 1985.

REFERENCES (CONTINUED)

33. W.C. O'Mara, R.B. Herring, L.P. Hunt, Handbook of Semiconductor Silicon Technology, pp. 349-371, 1990.

34. Properties of Silicon, p. 8, 1988.

35. W.C. O'Mara, R.B. Herring, L.P. Hunt, Handbook of Semiconductor Silicon Technology, pp. 427-432, 1990.

36. S. Iyer, "Silicon Molecular Beam Epitaxy", Epitaxial Silicon Technology, pp. 150-154, 1989.

37. W.C. O'Mara, R.B. Herring, L.P. Hunt, Handbook of Semiconductor Silicon Technology, pp. 197-198, 1990.

38. J.I. Licari, L.R. Enlow, Hybrid Microcircuit Techology Handbook - Materials, Processes, Design, Testing and Production, pp. 25-26, 1988.

39. Properties of Silicon, p. 52, 1988.

40. A. Harper, Handbook of Materials and Processes for Electronics, pp. 7.90-7.99, 1970.

41. D.C. Guptor, Silicon Processing, 1983.

42. C.P. Gilmore, The Scanning Electron Microscope, p. 7, 1972.

43. P.R. Thornton, Scanning Electron Microscopy, Applications to Material and Device Science, pp. 13-45, 1968.

44. Matrix Videometrix Econoscope User's Manual.

45. D.C. Ray, P.K. Mishra, "Material Removal Rate in Abrasive Jet Machining: An Elasto-Plastic Model", Advances in Nontraditional Machining, pp. 111, 1986.

46. Allen Bradley Series B 8400 MP/ Bandit IV Revision F Firmware Controller Users Manual, 1988.

47. F. Shimura, Semiconductor Silicon Crystal Technology, pp. 22-78, 1989.